

Sparse Multivariate Linear Regression with Strongly Associated Response Variables

Daeyoung Ham^{1,*}, Bradley S. Price¹, Adam J. Rothman¹

Abstract

We propose new methods for multivariate linear regression when the regression coefficient matrix is sparse and the error covariance matrix is dense. We assume that the error covariance matrix has equicorrelation across the response variables. Two procedures are proposed: one is based on constant marginal response variance (compound symmetry), and the other is based on general varying marginal response variance. Two approximate procedures are also developed for high dimensions. We propose an approximation to the Gaussian validation likelihood for tuning parameter selection. Extensive numerical experiments illustrate when our procedures outperform relevant competitors as well as their robustness to model misspecification.

Keywords: High-dimensional multivariate linear regression, equicorrelation

1. Introduction

Multivariate linear regression simultaneously models multiple response variables in terms of one or more predictors. It is well studied, and we direct readers to Reinsel et al. [10] for a detailed review.

We focus on fitting multivariate linear regression models by penalized or constrained Gaussian likelihood. One of the first approaches maximizes the Gaussian likelihood subject to a rank constraint on the regression coefficient matrix [5, 10]. Like other dimension reduction methods, interpreting the fitted model in terms of the original predictors may be difficult.

Rothman et al. [12] proposed to jointly estimate the error precision matrix and the regression coefficient matrix by penalized Gaussian likelihood. They used L_1 -penalties to encourage sparsity in estimates of the regression coefficients and error precision matrix, which can lead to easy-to-interpret fitted models. They showed that using the Gaussian loglikelihood, which accounts for the association between the response components, leads to better parameter estimation than using a multivariate residual sum of squares criterion, which does not account for this association.

Similar approaches that jointly estimate the error precision matrix and the regression coefficient matrix have been proposed. For instance, Lee and Liu [6] assumed that the response variables and the predictors have a joint multivariate normal distribution, and Wang [14] decomposed

*Corresponding author

Email addresses: ham00024@umn.edu (Daeyoung Ham), brad.price@mail.wvu.edu (Bradley S. Price), arothman@umn.edu (Adam J. Rothman)

the multivariate regression problem into a series of penalized conditional log-likelihood of each response conditional on the predictors and other responses. Navon and Rosset [7] extended this to multivariate linear mixed effects models, and Chang and Welsh [3] considered an extension of Rothman et al. [12]’s method to multivariate robust linear regression. Zhu [17] considered a convex reparametrization of Rothman et al. [12]’s joint optimization problem. These methods assumed that the error precision matrix is sparse, which may be unreasonable in some applications with highly correlated response components. In addition, in high-dimensional settings, the graphical lasso subproblem [4] used in the block-wise coordinate decent algorithm of Rothman et al. [12] struggles when the error precision matrix is dense. These dense cases call for values of the penalty tuning parameter near zero, which lead to algorithm failures or very long computing times when solving the graphical lasso subproblem.

This motivated us to develop a new multivariate linear regression method for high-dimensional settings that works when the error precision matrix is dense. Similarly to Rothman et al. [12], we jointly estimate the regression coefficient matrix and the error precision matrix by minimizing the negative Gaussian loglikelihood. However, unlike their approach, we assume the error covariance matrix has compound symmetry (or equicorrelation). Our primary goal is to estimate the regression coefficient matrix when the responses are highly correlated. Although our assumed error correlation structure is simple, our estimation of the regression coefficient matrix is robust to misspecification of the error correlation. We propose an efficient computational algorithm to compute our estimators and we also propose an approximation to the validation likelihood for tuning parameter selection.

2. Problem setup and proposed estimator

Let $x_i = (x_{i1}, \dots, x_{ip})^T$ be the p -dimensional vector of nonrandom predictor values; let $y_i = (y_{i1}, \dots, y_{iq})^T$ be the observed q -dimensional response; and let $\epsilon_i = (\epsilon_{i1}, \dots, \epsilon_{iq})^T$ be the error for the i th subject ($i = 1, \dots, n$). The multivariate linear regression model assumes that y_i is a realization of

$$Y_i = B_*^T x_i + \epsilon_i, \quad i = 1, \dots, n, \quad (1)$$

where $B_* \in \mathbb{R}^{p \times q}$ is the unknown regression coefficient matrix; and $\epsilon_1, \dots, \epsilon_n$ are iid $N_q(0, \Sigma_*)$. To allow for highly correlated response variables, we assume that

$$\Sigma_* = \eta_*^2 \{ (1 - \theta_*) I_q + \theta_* \mathbf{1}_q \mathbf{1}_q^T \}, \quad (2)$$

where $\eta_* \in (0, \infty)$ and $\theta_* \in [0, 1)$ are unknown. This implies that $\text{var}(\epsilon_{i,j}) = \eta_*^2$ for $(i, j) \in \{1, \dots, n\} \times \{1, \dots, q\}$ and that $\text{corr}(\epsilon_{i,j}, \epsilon_{i,k}) = \theta_*$ when $j \neq k$. This implicitly assumes that all of the response components are on the same scale. When they are not, we propose a different method described in Section 4. Our numerical experiments suggest that our estimation of B_* , which is our primary target, is robust to misspecification of Σ_* .

To write the negative loglikelihood, we first express (1) in terms of matrices: let $Y \in \mathbb{R}^{n \times q}$ have i th row Y_i^T ; let $X \in \mathbb{R}^{n \times p}$ have i th row x_i^T ; and let $E \in \mathbb{R}^{n \times q}$ have i th row ϵ_i^T . Then (1) is

$Y = XB_* + E$. The negative log-likelihood function evaluated at (B, Ω) , where Ω is the variable corresponding to the inverse of Σ_* , is

$$\mathcal{L}(B, \Omega) = \text{tr} \left[\frac{1}{n} (Y - XB)^T (Y - XB) \Omega \right] - \log |\Omega|.$$

We propose the following penalized likelihood estimator of $(B_*, \eta_*^2, \theta_*)$:

$$(\hat{B}, \hat{\eta}^2, \hat{\theta}) = \arg \min_{(B, \eta^2, \theta) \in \mathbb{R}^{p \times q} \times (0, \infty) \times [0, 1]} \left\{ \mathcal{L}(B, \Omega(\eta^2, \theta)) + \lambda \sum_{j=1}^p \sum_{k=1}^q |B_{jk}| \right\}, \quad (3)$$

where $\Omega(\eta^2, \theta) = [\eta^2 \{\theta 1_q 1_q' + (1 - \theta) I_q\}]^{-1}$ and $\lambda \in [0, \infty)$ is a tuning parameter. Similarly to Rothman et al. [12], the L_1 penalty on B encourages sparse regression coefficient estimation. We label the solution to this optimization as the Multivariate Regression with Compound Symmetry [MRCS] estimator. When the response components are on different scales, we define an alternative estimator described in Section 4.

Our goal is to estimate B_* and predict future response values: we expect that the assumed error covariance structure in (2) will be an oversimplification in many applications. When $\lambda = 0$, it is known that the regression coefficient estimator that solves (3) would be unchanged if $\Omega(\eta^2, \theta)$ were replaced by any positive definite matrix [12]. So the assumed error correlation structure only influences how the entries in the regression coefficient matrix estimator are shrunk towards zero when $\lambda > 0$. Our numerical experiments suggest that our estimation of B_* is robust to misspecification of the error covariance.

3. Computational algorithms

3.1. Algorithm for exact computation

By the derivation illustrated in Appendix A of our supplementary material, the penalized estimator in (3) is equivalent to the following:

$$\arg \min_{(B, \eta^2, \theta) \in \mathbb{R}^{p \times q} \times (0, \infty) \times [0, 1]} F_\lambda(B, \eta^2, \theta; Y, X), \quad (4)$$

where

$$\begin{aligned} F_\lambda(B, \eta^2, \theta; Y, X) &= \frac{1}{n\eta^2(1 - \theta)} \|Y - XB\|_F^2 - \frac{\theta}{n\eta^2(1 - \theta)(1 - \theta + q\theta)} \|(Y - XB)1_q\|^2 \\ &\quad + (q - 1) \log(1 - \theta) + \log(1 + \{q - 1\}\theta) + q \log(\eta^2) \\ &\quad + \lambda \sum_{j=1}^p \sum_{k=1}^q |B_{jk}|. \end{aligned}$$

We solve (4) by blockwise coordinate descent. We treat (η^2, θ) as the first block, and B as the second block. We let the superscript (k) denote the k th iterate of each component that is being

updated.

For a fixed $\hat{B}^{(k)}$, we reparametrize the problem via $\alpha = \eta^2(1 - \theta)$, $\gamma = \eta^2(1 + (q - 1)\theta)$, which is a one-to-one mapping from (η^2, θ) . Then (4) with $\hat{B}^{(k)}$ fixed becomes

$$(\hat{\alpha}^{(k+1)}, \hat{\gamma}^{(k+1)}) = \arg \min_{0 < \alpha \leq \gamma < \infty} \left\{ \frac{M_1^{(k)}}{\alpha} - \frac{1}{q} \left(\frac{1}{\alpha} - \frac{1}{\gamma} \right) M_2^{(k)} + \log(\gamma) + (q - 1) \log(\alpha) \right\}, \quad (5)$$

where $M_1^{(k)} = \frac{1}{n} \|Y - X \hat{B}^{(k)}\|_F^2$ and $M_2^{(k)} = \frac{1}{n} \|(Y - X \hat{B}^{(k)}) 1_q\|^2$. Since the objective function in (5) is separable, by first order condition, we get

$$\hat{\alpha}^{(k+1)} = \frac{qM_1^{(k)} - M_2^{(k)}}{q(q - 1)}, \quad (6)$$

$$\hat{\gamma}^{(k+1)} = \hat{\gamma}^{(k+1)}(\hat{\alpha}^{(k+1)}) = \max \left\{ \hat{\alpha}^{(k+1)}, \frac{M_2^{(k)}}{q} \right\}, \quad (7)$$

where $M_1^{(k)} \geq M_2^{(k)}/q$ holds by the Cauchy-Schwarz inequality. Finally,

$$((\hat{\eta}^2)^{(k)}, \hat{\theta}^{(k)}) = \left(\hat{\alpha}^{(k)} + \frac{\hat{\gamma}^{(k)} - \hat{\alpha}^{(k)}}{q}, \frac{\hat{\gamma}^{(k)} - \hat{\alpha}^{(k)}}{\hat{\gamma}^{(k)} + (q - 1)\hat{\alpha}^{(k)}} \right). \quad (8)$$

Now, when $\hat{\Omega}^{(k+1)}((\hat{\eta}^2)^{(k+1)}, \hat{\theta}^{(k+1)})$ is fixed, the corresponding optimization problem is given by

$$\hat{B}^{(k+1)}(\hat{\Omega}^{(k+1)}) = \arg \min_B \left\{ \text{tr} \left[\frac{1}{n} (Y - XB)^T (Y - XB) \hat{\Omega}^{(k+1)} \right] \right\} + \lambda \sum_{j=1}^p \sum_{k=1}^q |B_{jk}|. \quad (9)$$

We solve (9) through a function `rblasso` in the R package MRCE [11].

To improve the performance with a better initializer, we suggest the following procedure. We first perform q lasso regressions for each response with the same optimal tuning parameter $\hat{\lambda}_0$ selected with a cross validation. Let $\hat{B}_{\hat{\lambda}_0}$ be the solution. We refer this as combined lasso initializer. We initialize the algorithm from $\hat{B}^{(0)} = \hat{B}_{\hat{\lambda}_0}$. We set the convergence tolerance parameter $\varepsilon = 10^{-7}$. We summarize the algorithmic procedure in Algorithm 1 below. Steps 1 and 2 both guarantee a decrease in the objective function value.

Algorithm 1 Multivariate Regression with Compound Symmetry [MRCS]

For each fixed value of λ , initialize $\hat{B}^{(0)} = \hat{B}_{\hat{\lambda}_0}$. Set $k = 0$ and $((\hat{\eta}^2)^{(0)}, \hat{\theta}^{(0)}) = (1, 0)$.

Step 1: Compute $((\hat{\eta}^2)^{(k+1)}, \hat{\theta}^{(k+1)})(\hat{B}^{(k)})$ by (8).

Step 2: Compute $\hat{B}^{(k+1)}((\hat{\eta}^2)^{(k+1)}, \hat{\theta}^{(k+1)})$ by (9).

Step 3: If $|F_\lambda(\hat{B}^{(k+1)}, (\hat{\eta}^2)^{(k+1)}, \hat{\theta}^{(k+1)}) - F_\lambda(\hat{B}^{(k)}, (\hat{\eta}^2)^{(k)}, \hat{\theta}^{(k)})| < \varepsilon \text{tr}(Y'Y)/n$ then stop. Otherwise go to Step 1 and $k \leftarrow k + 1$.

3.2. Algorithm for approximate computation

When $p \geq n$, the residual sample covariance matrix, $(Y - XB)^T(Y - X)/n$, is singular. When there exists \bar{B} such that any one of the columns of $Y - X\bar{B}$ is zero, then the objective function value for updating Ω can be made arbitrarily negative by increasing the corresponding diagonal element of Ω sufficiently, which implies that a global minimizer does not exist. In addition, the computational time of the blockwise coordinate descent for fitting both regression coefficients and the error precision matrix tends to be significantly higher in increased dimensions of p , q [12]. To improve computational efficiency and ensure the well-posed optimization problem in high dimensions, we provide an approximate solution to our procedure by following the idea of approximate MRCE proposed in Rothman et al. [12]. As in Algorithm 1, we compute the initial $\hat{B}^{(0)} = \hat{B}_{\hat{\lambda}_0}$. Then, for each λ , we compute $(\hat{\eta}^2(\hat{B}_{\hat{\lambda}_0}), \hat{\theta}(\hat{B}_{\hat{\lambda}_0}))$ by (8). After this step for (inverse) covariance update, we compute the proposed approximate solution \hat{B} with known $(\hat{\eta}^2(\hat{B}_{\hat{\lambda}_0}), \hat{\theta}(\hat{B}_{\hat{\lambda}_0}))$ by (9). We suppress the dependence of \hat{B} and $(\hat{\eta}^2(\hat{B}_{\hat{\lambda}_0}), \hat{\theta}(\hat{B}_{\hat{\lambda}_0}))$ on λ for notational simplicity. We refer the approximate solution to (4) as ap.MRCS. We summarize the procedure in Algorithm 2 below.

Algorithm 2 Approximated version of Multivariate Regression with Compound Symmetry [ap.MRCS]

For each fixed value of λ , initialize $\hat{B}^{(0)} = \hat{B}_{\hat{\lambda}_0}$.
Step 1: Compute $(\hat{\eta}^2, \hat{\theta})(\hat{B}^{(0)})$ by (8).
Step 2: Compute $\hat{B}(\hat{\eta}^2, \hat{\theta})$ by (9).

4. Extension to general equicorrelation covariance matrix

When the response components are on different scales, then it may be unreasonable to assume that the components of the errors have the same variance η_*^2 . We extend our model by allowing different η_{*j} 's for each response component. The model follows (1) except that we use the following error covariance matrix:

$$\Sigma_* = \text{diag}(\{\eta_{*j}\}_{j=1}^q) \left[(1 - \theta)I_q + \theta 1_q 1_q^T \right] \text{diag}(\{\eta_{*j}\}_{j=1}^q),$$

where $(\eta_{*1}, \dots, \eta_{*q}) \in (0, \infty)^q$ are the unknown standard deviations of the q marginal distributions of the error, i.e. $\text{var}(\epsilon_{i,j}) = \eta_{*j}^2$ for $(i, j) \in \{1, \dots, n\} \times \{1, \dots, q\}$. The inverse error covariance matrix is

$$\Omega_* = \frac{1}{1 - \theta_*} \text{diag}(\{\eta_{*i}^{-1}\}_{i=1}^q) \left[I_q - \frac{\theta_*}{1 + (q - 1)\theta_*} 1_q 1_q^T \right] \text{diag}(\{\eta_{*i}^{-1}\}_{i=1}^q). \quad (10)$$

Then the corresponding penalized negative log-likelihood optimization is

$$\arg \min_{(B, \{\eta_i\}_{i=1}^q, \theta) \in \mathbb{R}^{p \times q} \times \mathbb{R}_+^q \times [0, 1]} F_\lambda^{\text{gen}}(B, \{\eta_i\}_{i=1}^q, \theta; Y, X), \quad (11)$$

where

$$\begin{aligned}
F_\lambda^{gen}(B, \{\eta_i\}_{i=1}^q, \theta; Y, X) &= \frac{1}{n(1-\theta)} \|(Y - XB)\text{diag}(\{\eta_i^{-1}\})\|_F^2 \\
&\quad - \frac{\theta}{n(1-\theta)(1-\theta+q\theta)} \|[(Y - XB)\text{diag}(\{\eta_i^{-1}\})]1_q\|^2 \\
&\quad + (q-1)\log(1-\theta) + \log(1 + \{q-1\}\theta) + 2\sum_{i=1}^q \log(\eta_i) \\
&\quad + \lambda \sum_{j=1}^p \sum_{k=1}^q |B_{jk}|,
\end{aligned}$$

and $\lambda \in [0, \infty)$ is a tuning parameter. Note that the problem (11) is bi-convex in B and $(\{\eta_i\}_{i=1}^q, \theta)$. As in Algorithm 3.2, we treat $(\{\eta_i\}_{i=1}^q, \theta)$ as the first block and B as the second block in blockwise coordinate descent.

For a fixed $\hat{B}^{(k)}$, we solve for $(\{\eta_i\}_{i=1}^q, \theta)$ cyclically. By simple algebra (see Appendix A in our supplementary material), we compute the update for η_j by

$$\hat{\eta}_j^{(k+1)} = \frac{-K_1^{(k)} + \sqrt{(K_1^{(k)})^2 + 4K_2^{(k)}}}{2}, \quad (12)$$

where

$$\begin{aligned}
K_1^{(k)} &= \frac{\hat{\theta}^{(k)}}{n(1-\hat{\theta}^{(k)})(1+(q-1)\hat{\theta}^{(k)})} \sum_{i=1}^n e_{ij}^{(k)} \left(\sum_{k \neq j} e_{ik}^{(k)} \frac{1}{\hat{\eta}_k^{(k)}} \right), \\
K_2^{(k)} &= \frac{1+(q-2)\hat{\theta}^{(k)}}{n(1+(q-1)\hat{\theta}^{(k)})(1-\hat{\theta}^{(k)})} \left(\sum_{i=1}^n (e_{ij}^{(k)})^2 \right),
\end{aligned}$$

and $e_{ij}^{(k)}$ is the (i, j) -th element of $Y - X\hat{B}^{(k)}$. After sequentially solving for $\{\eta_i\}_{i=1}^q$, we solve the following by line search:

$$\begin{aligned}
\hat{\theta}^{(k+1)} &= \arg \min_{\theta \in [0,1]} \frac{1}{n(1-\theta)} \|(Y - X\hat{B}^{(k)})\text{diag}(\{\hat{\eta}_i^{(k+1)-1}\})\|_F^2 \\
&\quad - \frac{\theta}{n(1-\theta)(1-\theta+q\theta)} \|[(Y - X\hat{B}^{(k)})\text{diag}(\{\hat{\eta}_i^{(k+1)-1}\})]1_q\|^2 \\
&\quad + (q-1)\log(1-\theta) + \log(1 + \{q-1\}\theta). \quad (13)
\end{aligned}$$

For efficiency, we do not require full convergence in each inner loop over $(\{\eta_i\}_{i=1}^q, \theta)$. Instead, we conduct single-iteration updates for each $\{\eta_i\}_{i=1}^q$ and θ by (12) and (13).

We compute $\hat{B}^{(k+1)}$ using (9) with $\hat{\Omega}^{(k+1)}$ set to the right side of (10) with $\{\eta_i\}_{i=1}^q$ and θ replaced by $\{\hat{\eta}_i^{(k+1)}\}_{i=1}^q$ and $\hat{\theta}^{(k+1)}$, respectively. We call the solution to (11) MRGCS.

We again start the algorithm with combined lasso initializer as in Algorithm 1. We compared the combined lasso initializer with a separate lasso initializer that fits q separate lasso regressions for each response with the different tuning parameters selected by cross validation for each response. However, we found that the combined lasso initializer generally performed better than the separate lasso except for a few cases. We again set the convergence tolerance parameter $\varepsilon = 10^{-7}$ for the following Algorithm 3 which summarizes the entire procedure.

Algorithm 3 Multivariate Regression with Generalized Compound Symmetry [MRGCS]

For each fixed value of λ , initialize $\hat{B}^{(0)} = \hat{B}_{\lambda_0}$. Set $k = 0$ and $(\{\hat{\eta}_i^{(0)}\}_{i=1}^q, \hat{\theta}^{(0)}) = (1_q, 0)$.

Step 1: Compute one-step update of $(\{\hat{\eta}_i^{(k+1)}\}_{i=1}^q, \hat{\theta}^{(k+1)})$ by solving (12)–(13) cyclically.

Step 2: Compute $\hat{B}^{(k+1)}$ by solving (9).

Step 3: If $|F_\lambda^{gen}(\hat{B}^{(k+1)}, \{\hat{\eta}_i^{(k+1)}\}_{i=1}^q, \hat{\theta}^{(k+1)}) - F_\lambda^{gen}(\hat{B}^{(k)}, \{\hat{\eta}_i^{(k)}\}_{i=1}^q, \hat{\theta}^{(k)})| < \varepsilon \text{tr}(Y'Y)/n$ then stop. Otherwise go to Step 1 with $k \leftarrow k + 1$.

4.1. Approximate solutions II

As in Section 3.2, we propose an approximate solution to (11). Again, we start the algorithm with $\hat{B}^{(0)} = \hat{B}_{\lambda_0}$, the combined lasso initializer. Then, for each λ , we compute $(\{\hat{\eta}_i\}_{i=1}^q, \hat{\theta})$ from (11). However, the difference between this approximation and the canonical MRGCS is that we conduct the updating step for $(\{\hat{\eta}_i\}_{i=1}^q, \hat{\theta})$ until convergence instead of a single-iteration update. This subproblem is obviously convex in $(\{\eta_i\}_{i=1}^q, \theta)$. Next, we compute the final \hat{B} by solving (9) once. We call this approximation ap.MRGCS. We summarize it in Algorithm 4 below.

Algorithm 4 Approximated version of Multivariate Regression with generalized Compound Symmetry [ap.MRGCS]

For each fixed value of λ , initialize $\hat{B}^{(0)} = \hat{B}_{\lambda_0}$.

Step 1: Compute $(\{\hat{\eta}_i\}_{i=1}^q, \hat{\theta})$ cyclically by solving (12) and (13) until convergence.

Step 2: Compute $\hat{B}(\{\hat{\eta}_i\}_{i=1}^q, \hat{\theta})$ by solving (9).

5. Asymptotic statistical properties

We study large sample asymptotic behavior of our estimator MRCS defined by (4) using the same asymptotic framework as Lee and Liu [6]. We study high-dimensional statistical properties of ap.MRCS (see Algorithm 3.2) in Appendix C of the supplementary material. We keep p and q fixed with $n > p + q$ throughout this section. As stated in Proposition 1 of Zou [18], the equally-weighted lasso-penalized estimator does not possess the oracle property. Thus, to ensure the oracle property, it is encouraged to assign weights, w_{jk} , to each $|B_{jk}|$ in the penalty term. We let $w_{jk} = 1/|B_{jk}^{(ols)}|^r$ ($r > 1$) be the weight for $|B_{jk}|$, where $B_{jk}^{(ols)}$ is (j, k) -th element of the regression coefficient matrix obtained from ordinary least squares. Using these weights, the slightly modified

optimization (than (4)) we consider in this section is as follows:

$$\begin{aligned} \arg \min_{(B, \eta^2, \theta) \in \mathbb{R}^{p \times q} \times (0, \infty) \times [0, 1]} & \frac{1}{\eta^2(1 - \theta)} \operatorname{tr} \left\{ n^{-1} (Y - XB)^T (Y - XB) \left[I_q - \frac{\theta}{1 - \theta + q\theta} \mathbf{1}_q \mathbf{1}_q^T \right] \right\} \\ & + (q - 1) \log(1 - \theta) + \log(1 + \{q - 1\}\theta) + q \log(\eta^2) \\ & + \lambda \sum_{j=1}^p \sum_{k=1}^q w_{jk} |B_{jk}|. \end{aligned} \quad (14)$$

We make the following assumptions to state large sample asymptotics of MRCS.

Assumption A.

- (A1) : $X^T X/n \rightarrow Z$, where Z is a positive definite matrix.
- (A2) : There exists \tilde{B}_{jk} a \sqrt{n} -consistent estimator of B_{jk*} , where B_{jk*} is the (j, k) -th element of B_* for $(j, k) \in \{1, \dots, p\} \times \{1, \dots, q\}$.
- (A3) : There exists $(\tilde{\eta}^2, \tilde{\theta})$ \sqrt{n} -consistent estimator of (η_*^2, θ_*) .
- (A4) : The distribution of E has finite joint fourth moments.

Condition (A1) is a standard condition in linear regression large sample asymptotics literature, and was also assumed in Zou [18], Lee and Liu [6], and Chang and Welsh [3]. It implies that the design matrix has good asymptotic behavior. We note that (A2) and (A3) are generally satisfied by maximum likelihood estimators [MLEs] or L_2 -penalized MLEs. (A4) is satisfied by broad class of error distributions such as multivariate sub-exponential distributions.

For a matrix $R \in \mathbb{R}^{p \times q}$, we let $\operatorname{vec}(R) \in \mathbb{R}^{pq}$ be the vector formed by stacking the columns of R . Define $S := \{i : \operatorname{vec}(B_*)_i \neq 0\}$. Let v_A be the subvector of the of the entries in v with indices in A . For a square matrix $M \in \mathbb{R}^{q \times q}$, we further define M_A as the $|A| \times |A|$ matrix obtained by removing the i -th row and column of M for $i \in A^c$, where $A \subseteq \{1, \dots, q\}$. We let \otimes denote the Kronecker product of two matrices. Recall that the inverse of compound symmetry error covariance is computed as

$$\Omega_* = \frac{1}{\eta_*^2(1 - \theta_*)} \left[I_q - \frac{\theta_*}{1 + (q - 1)\theta_*} \mathbf{1}_q \mathbf{1}_q^T \right].$$

In the following theorem, we provide the oracle guarantee, the limit distribution of \hat{B} , and the joint limit distribution of $(\hat{\eta}^2, \hat{\theta})$. This result is analogous to Theorem 3 of Lee and Liu [6].

Theorem 1. *Under the conditions (A1)–(A4), assuming that $\lambda\sqrt{n} \rightarrow 0$ and $\lambda n^{(r+1)/2} \rightarrow \infty$, then, there exists a local minimizer $(\hat{B}, \hat{\eta}^2, \hat{\theta})$ to the optimization problem (14) that satisfies*

$$\begin{aligned} \lim_{n \rightarrow \infty} P(\hat{B}_{jk} = 0) &= 1 && \text{if } B_{jk*} = 0, \\ \sqrt{n}(\operatorname{vec}(\hat{B})_S - \operatorname{vec}(B_*)_S) &\rightarrow_d N(0, D^{-1}), \\ \left\| (\hat{\eta}^2, \hat{\theta}) - (\eta_*^2, \theta_*) \right\| &= O_p(1/\sqrt{n}), \end{aligned}$$

where $D = (\Omega_* \otimes Z)_S$. Furthermore, if $\theta_* \in (0, 1)$, then

$$\sqrt{n}((\hat{\eta}^2, \hat{\theta}) - (\eta_*^2, \theta_*)) \rightarrow_d W^T N_2(0, V),$$

where $W = (1, -1/\eta_*^2)^T$, and V is defined in [Appendix B](#) of the supplementary material (see [\(B.1\)](#)).

6. Tuning parameter selection

We suggest the following tuning parameter selection procedure for MRCS, ap.MRCS, MRGCS, and ap.MRGCS:

$$\hat{\lambda} = \arg \min_{\lambda \in \Lambda} \sum_{k=1}^K \text{tr} \left\{ n^{-1} (Y_k - X_k \hat{B}_{-k})^T (Y_k - X_k \hat{B}_{-k}) \hat{\Omega}_{-k} \right\}, \quad (15)$$

where

$$\hat{\Omega}_{-k} = \left[\hat{\eta}_{-k} \left\{ \hat{\theta}_{-k} 1_q 1_q^T + (1 - \hat{\theta}_{-k}) I_q \right\} \right]^{-1}.$$

In [\(15\)](#), Λ is a candidate set of tuning parameter values, K is the number of folds used for the cross validation, \hat{B}_{-k} is the estimated regression coefficient matrix from each method based on the observations that excludes the k th fold, Y_k , X_k are the responses and predictors corresponding to k th fold, and $\hat{\eta}_{-k}$, $\hat{\theta}_{-k}$ are the estimated parameters based on the observations that excludes the k th fold. The loss function in [\(15\)](#) is the negative Gaussian validation loglikelihood without the log determinant term. Including this term was slightly less stable than excluding it in our numerical experiments. Similar Gaussian validation likelihood minimization is presented in Lee and Liu [\[6\]](#), which used this loss criterion for finding an optimal tuning parameter associated graphical lasso applied to the error precision.

We note that we do not use $\hat{\eta}_{-k}$, $\hat{\theta}_{-k}$ from the output of MRCS. Rather we use the one-step estimators used for ap.MRCS that are computed in the Step 1 of [Algorithm 3.2](#). We use the same $\hat{\eta}_{-k}$, $\hat{\theta}_{-k}$ for both MRCS and ap.MRCS. This is because the stability of ap.MRCS output turned out to be significantly better than that of the canonical MRCS. Furthermore, we use $\hat{\eta}_{-k}$, $\hat{\theta}_{-k}$ which assumes compound symmetry error covariance even when we fit MRGCS or ap.MRGCS which assume varying marginal error variances. This is because the output of ap.MRCS was significantly more stable in the tuning parameter selection compared with that of ap.MRGCS as well as the MRGCS output. We provide further support regarding this tuning parameter selection procedure through extensive simulations in [Appendix G.1](#) and [Appendix G.2](#) of the supplementary material.

7. Simulations

The data for our simulations are generated from the following model:

$$Y_i = \mu + X_i B_* + \epsilon_i, \quad X_i \sim N(0, \Sigma_X) \in \mathbb{R}^p, \quad \epsilon_i \sim N(0, \Sigma_*) \in \mathbb{R}^q, \quad i = 1, \dots, n \quad (16)$$

where $\mu = (1, 1 + 4/(q - 1), \dots, 5)$, $(\Sigma_X)_{i,j} = (0.7)^{|i-j|}$ for $1 \leq i, j \leq p$, and

$$\Sigma_* = \text{diag}(\{\eta_k\}_{k=1}^q) [(1 - \theta)I_q + \theta 1_q 1_q^T] \text{diag}(\{\eta_k\}_{k=1}^q). \quad (17)$$

We use $n = 50$ training observations throughout. To generate B_* , we follow the same regression coefficient matrix generating procedure used in Section 3 of Rothman et al. [12]. We define the operation $*$ as the element-wise matrix product. The coefficients matrix B_* is generated by

$$B_* = W * K * Q, \quad (18)$$

where W has iid entries from $N(0, 1)$; K has entries from iid $Ber(s_1)$ (a Bernoulli distribution which returns 1 with probability s_1); $Q = 1_p 1_q^T Q_1$ where a $q \times q$ diagonal matrix Q_1 has diagonal elements from iid $Ber(s_2)$. This results in, Q has rows that are either all one or all zero, where the population proportion of having all-one row ($1'_q$) equals to s_2 . Under this setting each model is expected to have $(1 - s_2)p$ predictors that are irrelevant for all q responses, and each relevant predictor is expected to have contribution to $s_1 q$ of the response variables.

We compare a separate lasso regression with a uniquely selected tuning parameter for each response [LASP], combined lasso [LAS] which employs the same tuning parameter for all responses, MRCE, approximate MRCE [ap.MRCE] [12], MRCS (the solution to (4)), MRGCS (the solution to (11)). In addition to the canonical estimators, MRCS and MRGCS, we also consider their approximate versions: ap.MRCS (see Section 3.2), as well as ap.MRGCS (see Section 4.1). Moreover, we compare these methods to an oracle procedure that assumes the true error precision $\Omega_* = \Sigma_*^{-1}$ is known, and only estimates B by L_1 -penalty.

$$\hat{B}_{\text{Or}} := \arg \min_{B \in \mathbb{R}^{p \times q}} \text{tr} \{n^{-1}(Y - XB)^T(Y - XB)\Omega_*\} + \lambda \sum_{j=1}^p \sum_{k=1}^q |B_{jk}|. \quad (19)$$

We refer this estimator as MRCS-Or. In MRCE, we penalized the diagonals of the inverse covariance matrix only when $p \geq n$.

Tuning parameters are selected using 5 fold cross validation from $\lambda \in \Lambda$, where $\Lambda = \{10^{-4+0.5k} : k = 0, 1, \dots, 14\}$. The optimal tuning parameter selection procedures for our methods are discussed in Section 6 (see (15)). The optimal tuning parameter for MRCS-Or is also selected by (15) except that we use Ω_* in place of $\hat{\Omega}_{-k}$ in (15). For the other competitors, we select each tuning parameter that minimizes validation prediction error with 5 fold cross validation. For the estimators which require a single tuning parameter, we again use the candidate set as $\lambda \in \{10^{-4+0.5k} : k = 0, 1, \dots, 14\}$. And for MRCE, we use $(\lambda_1, \lambda_2) \in \Lambda_1 \times \Lambda_2$, where $\Lambda_1 = \Lambda_2 = \{10^{-4+0.5k} : k = 0, 1, \dots, 14\}$.

For the primary criterion for the model comparison, we measure the model error, $\text{tr}[(\hat{B} - B_*)^T \Sigma_X (\hat{B} - B_*)]$ [1, 16] with \hat{B} provided by each method. We also measure the prediction error, $\|\hat{Y} - Y\|_F^2$, on the test set which has 200 observations which are generated from the same data generating process as in the training set. We further measure the true negative rate [TNR] and true

positive rate [TPR] for the regression coefficient matrix estimation as follows [12]:

$$\text{TNR}(\hat{B}) = \frac{\#\{(i, j) \in [p] \times [q] : \hat{B}_{ij} = 0, B_{ij^*} = 0\}}{\#\{(i, j) \in [p] \times [q] : B_{ij^*} = 0\}}, \quad (20)$$

$$\text{TPR}(\hat{B}) = \frac{\#\{(i, j) \in [p] \times [q] : \hat{B}_{ij} \neq 0, B_{ij^*} \neq 0\}}{\#\{(i, j) \in [p] \times [q] : B_{ij^*} \neq 0\}}, \quad (21)$$

where $[k] = \{1, \dots, k\}$ for $k \in \mathbb{N}$; $\#A$ stands for the number of elements in the set A .

7.1. Setting I: Constant η

In this section, we consider $(p, q) \in \{(20, 50), (50, 20), (80, 80)\}$, We refer the readers to [Appendix H.1](#) in the supplementary material for the results of low dimensional simulations ($p = q = 20$). We vary $s_1 \in \{0.1, 0.5\}$, $s_2 \in \{0.1, 0.5, 1\}$, $\theta \in \{0, 0.5, 0.75, 0.9, 0.95\}$, and fix $\eta_i = 1$ for all $i = 1, \dots, q$. We drop MRCE due to its substantially high computation time. When $p \geq n$ we exclude MRCS, MRGCS from the set of competitors, where we still consider ap.MRCS, and ap.MRGCS, since they can avoid the residual covariance instability (see Section 3.2). The results for each setting are based on 50 independent replications. Throughout the results, the trend across the estimators in the prediction error is nearly equivalent to that in the model error. Hence, we mainly discuss the model error as our primary criterion.

7.1.1. Results when $(p, q) = (20, 50)$

The complete simulation results are in Figure [I.19–I.22](#). As θ increases, all our equicorrelation based estimators consistently outperforms ap.MRCE as well as two lasso methods. The best non-oracle estimators were MRCS and ap.MRCS. MRGCS and ap.MRGCS also showed competitive performance. In TNR, sep.lasso showed the best rate in general, MRCS and ap.MRCS outperformed MRGCS and ap.MRGCS, and ap.MRCE was the worst. On the other hand, in TPR, two lasso solutions were generally the worst, and all joint optimization methods showed increasing TPR with θ . This indicates the joint optimization methods tend to provide more dense solution than lasso as θ gets increased.

7.1.2. Results when $(p, q) = (50, 20)$

The complete simulation results are in Figure [I.23–I.26](#). The best non-oracle estimators was ap.MRCS. In addition, ap.MRGCS showed comparable performance to ap.MRCS except for $(s_1, s_2) = (0.5, 0.1)$, where ap.MRCE outperformed it at $\theta = 0, 0.95$. Generally, our non-oracle estimators outperformed ap.MRCE (and the two lasso methods as well). The general trends in TNR/TPR are the same as in $(p, q) = (20, 50)$, but ap.MRCE improved in TNR.

7.1.3. Results when $(p, q) = (80, 80)$

The computing time for ap.MRCE is substantially higher than other procedures, specifically when the tuning parameter associated with the graphical lasso subproblem is close to 10^{-4} . Given this issue we restricted the tuning parameter set for the L_1 penalty on the error precision into

$\{10^{-2+0.5k} : k = 0, 1, \dots, 8\}$. We note that this computational setup for ap.MRCE is used for the other simulations where $(p, q) = (80, 80)$ in Section 7.2 and Appendix H.2 (of the supplementary material).

The complete simulation results are in Figure I.27–I.30. The best non-oracle estimator was ap.MRCS. Again ap.MRGCS suffered only when $(s_1, s_2) = (0.5, 0.1)$, and it showed competitive performance in the other settings. The general performance of ap.MRCE was significantly worse than the previous (p, q) pairs.

7.2. Setting II: Equicorrelation of Σ_* with heterogeneous and asymmetrically distributed η_i 's

In this section, we study the performance of our equicorrelation based estimators under generalized Σ_* in which η_i 's are now heterogeneous. In Appendix H.2 of the supplementary material, we compared our methods to the others in the settings where η_i 's are still heterogeneous but symmetrically distributed. We discovered that MRCS and ap.MRCS showed comparable performance to MRGCS and ap.MRGCS, the two best non-oracle methods in that setting. This may be due to the symmetrically distributed η_i 's ($i \in \{1, \dots, q\}$) which can smooth out heterogeneous marginal error variances. Now we consider asymmetric cases in this section. We used the same data generating process (16)–(18) except that we considered

$$\begin{aligned} \eta_1, \dots, \eta_{10} &= 1/2, \eta_{11}, \dots, \eta_{20} = 1/\sqrt{2}, \eta_{21}, \dots, \eta_{30} = 1, \\ \eta_{31}, \dots, \eta_{40} &= \sqrt{3}, \eta_{41}, \dots, \eta_{50} = 3, \end{aligned} \quad (22)$$

when $(p, q) = (20, 50)$, and

$$\begin{aligned} \eta_1, \dots, \eta_4 &= 1/2, \eta_5, \dots, \eta_8 = 1/\sqrt{2}, \eta_9, \dots, \eta_{12} = 1, \\ \eta_{13}, \dots, \eta_{16} &= \sqrt{3}, \eta_{17}, \dots, \eta_{20} = 3, \end{aligned} \quad (23)$$

when $(p, q) = (50, 20)$. Lastly, when $(p, q) = (80, 80)$, we used

$$\begin{aligned} \eta_1, \dots, \eta_{10} &= 1/2, \eta_{11}, \dots, \eta_{20} = 1/\sqrt{2}, \eta_{21}, \dots, \eta_{30} = 1/\sqrt[4]{2}, \eta_{31}, \dots, \eta_{40} = 1 \\ \eta_{41}, \dots, \eta_{50} &= \sqrt{3}, \eta_{51}, \dots, \eta_{65} = 2, \eta_{66}, \dots, \eta_{80} = 3. \end{aligned} \quad (24)$$

To see the effect of varying η_i on the regression coefficient shrinkage, we also compared the original L_1 -penalty on B , $\lambda \sum_{j,k} |B_{jk}|$, with an adaptive L_1 -penalty, $\lambda \sum_{j,k} |\eta_k^{-1} B_{jk}|$, for MRCS-Or. However, we did not find any supporting evidence on the use of the adaptive penalty instead of the original penalty. Thus, we still suggest the use of the original L_1 -penalty function even in the case of varying η_i .

7.2.1. Results when $(p, q) = (20, 50)$

The complete results can be found in Figure I.31–I.34. MRGCS and ap.MRGCS were the two best non-oracle methods, and consistently outperformed the other methods. Note that MRGCS was slightly better than its approximate counterpart. As opposed to the results shown in Appendix H.2.1 of the supplementary material where η_i 's are symmetrically distributed, MRCS and ap.MRCS struggled under the asymmetric setting discussed in this section. With relatively higher

$s_1 s_2$ values, ap.MRCE even outperformed these two methods for higher values of θ . TNR/TPR results and trends are similar to those shown in Section 7.1.1.

7.2.2. Results when $(p, q) = (50, 20)$

The complete results are in Figure I.35–I.38. ap.MRGCS was the best non-oracle method, although it suffered again when $(s_1, s_2) = (0.5, 0.1)$. As opposed to the results in $(p, q) = (20, 50)$, ap.MRCS was the second-best non-oracle competitor, and it outperformed ap.MRGCS when $s_2 = 0.1$. ap.MRCE showed poor performance generally. Note, the prediction performance of MRCS-Or, ap.MRGCS, and ap.MRCS was substantially better than the others. In TNR, surprisingly, ap.MRGCS was the worst, and ap.MRCS was significantly better than ap.MRGCS. In TPR, ap.MRCE and two lasso methods showed poor performance.

7.2.3. Results when $(p, q) = (80, 80)$

The complete simulation results are in Figure I.39–I.42. The results show the best non-oracle estimator in this setting is ap.MRGCS. Again, ap.MRGCS suffered only when $(s_1, s_2) = (0.5, 0.1)$ where it was outperformed by ap.MRCE as well as sep.lasso (see similar results in Appendix H.2.3 of the supplementary material where η_i 's are symmetrically distributed). ap.MRCS was outperformed by ap.MRCE for some values of θ 's, when $(s_1, s_2) = (0.1, 0.5), (0.1, 1)$. Note that this can be compared with the results in Appendix H.2.3 of the supplementary material where ap.MRCS and ap.MRGCS substantially outperformed ap.MRCE. The relative performance of ap.MRCE was improved. ap.MRCE showed substantially lower TNR compared with the other procedures as θ gets increased. But, it was the best non-oracle method in TPR.

8. Simulation under the model misspecification

8.1. Misspecification of B_* : When the true B_* is non-sparse

In this section, we study how non-sparse true regression coefficient matrix affects the proposed methods. As in previous simulations we measure the prediction and model error for evaluation. We follow the same data generating process (16)–(17). We consider η_i 's in (17) over three different settings: constant η_i 's (Setting A; Section 7.1), heterogeneous and symmetrically distributed η_i 's (Setting B; Appendix H.2), heterogeneous and asymmetrically distributed η_i 's (Setting C; Section 7.2). We do not consider different sparsity levels for B_* . Rather than using (18) for generating regression coefficients matrix B_* , for each element of B_* , we generate iid draws from a uniform distribution on $(-1/4, 1/4)$ when $(p, q) = (20, 50), (50, 20)$, and on $(-1/10, 1/10)$ when $(p, q) = (80, 80)$. This regression coefficient matrix is non-sparse, and includes many non-zero, small signals. One can expect that sep.lasso and comb.lasso are likely to suffer from this design. We again set $\theta \in \{0, 0.5, 0.75, 0.9, 0.95\}$. In addition to the same set of competitors in Section 7, we also considered combined ridge [c.ridge], and separate ridge [s.ridge]. c.ridge and s.ridge are analogously defined as combined lasso and separate lasso.

The complete results are in Figure I.43–I.44. Under the setting A, we denote the sub-settings $(p, q) = (20, 50), (50, 20), (80, 80)$ by A1, A2, and A3, respectively. And, we similarly denote the sub-settings for B and C. MRGCS and ap.MRGCS were the best non-oracle method in all settings, and outperformed ap.MRCE as well as lasso and ridge estimators as θ increases. We note that

ap.MRCE was the third-best non-oracle method. In Setting A, the setting with constant η_i 's, MRCS and ap.MRCS were also regarded as the best non-oracles. Although they showed competitive performance with symmetric and heterogeneous η_i 's when B_* has sparsity (see [Appendix H.2](#) of the supplementary material), both methods struggled in non-sparse cases (settings B and C). The results from this section indicate that if non-sparse B_* has sufficiently small (in absolute value) elements, then there is more gain by joint optimization than lose by misspecified L_1 penalty.

8.2. Misspecification of Σ_* : Corrupted compound symmetry to general non-sparse covariance

In this section, we conduct simulation studies to study the effect of misspecification of Σ_* to our procedure. We are interested in how our equicorrelation based procedures react to a different class of error covariance Σ_* , which is assumed to have a corrupted compound symmetry structure that is defined in (25) below. To generate the data, we used the same procedure that is used throughout Section 7 except that we considered different sparsity level of B_* (which will be explained below) and used a corrupted compound symmetry Σ_* which is computed as follows:

$$\Sigma_* = (1 - \omega) [0.5 ((1 - 0.9)I_q + 0.9\mathbf{1}_q\mathbf{1}_q^T)] + \omega V D V^T, \quad (25)$$

where the columns of $V \in \mathbb{R}^{q \times q}$, v_1, \dots, v_q are generated by the Gram-Schmidt orthogonalization of a $q \times q$ random matrix whose entries are iid standard normal draws; $D \in \mathbb{R}^{q \times q}$ is a diagonal matrix. For the diagonal entries of D , we generated iid draws from a two point distribution that is explained below. Through this we vary the condition number of Σ_* . (25) can be interpreted as a convex combination of a general poorly conditioned matrix and a compound symmetry with variance 0.5 and correlation 0.9, which is also poorly conditioned. We considered the corruption level $\omega \in \{0.05, 0.5, 1\}$. $\omega = 1$ leads to a general non-sparse Σ_* that is completely different than compound symmetry. As ω decreases, the similarity extent of Σ_* to the compound symmetry class increases. Denoting $\text{Ber}(p, a, b)$ by the generic two point distribution that returns a numeric value a (resp. b) with the probability p (resp. $1 - p$), the following is the condition numbers according to each setting:

- When $(p, q) = (20, 50)$,
 - D constructed upon iid $\text{Ber}(0.5, 0.1, 10)$ draws: 100 / 189.9075 / 412.7517 (setting A / B / C according to $w = 1/0.5/0.05$)
 - D constructed upon iid $\text{Ber}(0.4, 0.01, 10)$ draws: 1000 / 507.617 / 453.8222 (setting D / E / F according to $w = 1/0.5/0.05$)
- When $(p, q) = (50, 20)$,
 - D constructed upon iid $\text{Ber}(0.2, 0.2, 10)$ draws: 50 / 64.29671 / 153.7895 (setting G / H / I according to $w = 1/0.5/0.05$)
 - D constructed upon iid $\text{Ber}(0.6, 0.02, 10)$ draws: 500 / 265.719 / 186.6711 (setting J / K / L according to $w = 1/0.5/0.05$)

Note that a $q \times q$ compound symmetry matrix with $q = 50$ (resp. $q = 20$) and $\theta = 0.9$ has condition number 451 (resp. 181). We considered this setting for the elements of D to avoid the diagonally dominant Σ_* , which can be similar to a diagonal matrix. We present numerical experiments that use the diagonally dominant Σ_* (where the diagonals of D are generated by a chi-square distribution) in [Appendix H.3](#) of the supplementary material. For the sparsity levels of B_* , we considered $(s_1, s_2) \in \{(0.5, 0.5), (0.5, 1), (1, 1)\}$ where the last pair accounts for dense B_* . For setting A, we denote the sub-setting of sparsity $(0.5, 0.5), (0.5, 1), (1, 1)$ by A-1, A-2, and A-3, respectively. We use similar notation to denote the sub-settings from B to L. We consider the same set of competitors methods to those described in [Section 8.1](#).

The complete results are in [Table I.7–I.10](#) in [Appendix I.1](#) of the supplementary material. In general, the oracle estimator the best, except for cases: A-3, D-3, G-3, H-3, I-3, J-3, K-3, L-3, where sparsity is violated and ridge estimators performed the best. We note these setting settings utilize a dense B_* that allows large signal. When there exists sparsity in B_* and $\omega = 1, 0.5$, our estimators not only showed comparable performance to lasso methods but also outperformed the others in several cases. When the corruption level is sufficiently low ($\omega = 0.05$), our equicorrelation based estimators outperformed the others substantially. Even though the true error covariance has varying marginal variances, MRCS and ap.MRCS performed nearly equal to MRGCS and ap.MRGCS, and they often outperformed the latter two. The results from this section (as well as from [Appendix H.3](#) of the supplementary material) indicate that our methods are robust to the model misspecification unless B_* is almost completely non-sparse with non-small signals and the true error covariance is extremely different than an equicorrelation.

9. Data analysis

We examined a data set from Korea water resources management information system (WAMIS) on the river flow chart of the Han river and its branches. The entire raw data set is public and can be downloaded from the portal (http://www.wamis.go.kr/wkw/flw_dubobsif.do). We used the daily stream flow measured in m^3/s throughout the calendar year 2023 from February 1st to December 25th. The 6 selected measurement points (bridges) for the analysis are: Haengju (HJ), Hankang (HK), Gwangjin (GJ), Paldang (PD), Yeojoo (YJ), Nahmhankang (NHK). The first four points are in the main stream of the Han river, and the next two points are in the relatively northern region. Within these 6 points, when considering the average flux in February to April as a reference, flows in YJ, NHK are generally on the same scale ($70\text{--}100 m^3/s$), but the other 4 points are generally on much higher scale ($120\text{--}300 m^3/s$). We set the predictors as the stream flux observations from 1 to 7 days before and the responses as the daily flux at each measurement point. Hence, there are 42 predictors and the leading intercept term, as well as 6 response variables in the model. We used a training set that has 52 observations from February 8th to March 31th. This indicates $(n, p, q) = (52, 43, 6)$. The test set has 139 observations from August 8th to December 25th. The competitors are MRCE, ap.MRCE, comb.lasso, sep.lasso, MRCS, MRGCS, ap.MRCS, ap.MRGCS. The labels are defined in [Section 7](#). The prediction performance results are summarized in [Table 1–2](#). For the grand average prediction taken by all the responses (see [Table 1](#)), ap.MRCS was the best model, and MRCS was the second-best. MRCE, ap.MRCE, combined lasso followed the next. ap.MRGCS, MRGCS were slightly outperformed by combined

lasso but outperformed separate lasso as well as OLS. ap.MRCS also performed the best in three responses (see Table 2), and MRCS was the best in two responses.

| Performance comparison table | | | | | | | | | |
|------------------------------|----------|------------|-----------|-----------------|----------|-----------------|----------|----------|----------|
| Competitors | OLS | comb.Lasso | sep.Lasso | MRCS | MRGCS | ap.MRCS | ap.MRGCS | MRCE | ap.MRCE |
| River flow | 434634.6 | 265887.3 | 283362.8 | 246039.1 | 268250.1 | 241223.4 | 268187.2 | 261599.1 | 263000.8 |

Table 1: The prediction performance comparison table for the combined response. We measured grand averaged squared error from 139 observations in the test set; $\|\hat{Y} - Y\|_F^2/139$. Boldface indicates the best model [ap.MRCS] and its canonical version [MRCS] which is the second-best.

| Performance comparison table by each response | | | | | | |
|---|-----------------|-----------------|-----------------|-----------------|-----------------|-----------------|
| Competitors \ Responses | HJ | HK | GJ | NHK | YJ | PD |
| OLS | 1438608 | 179435.4 | 217457.6 | 76625.49 | 158738.3 | 536943.0 |
| sep.Lasso | 601845.6 | 246680.3 | 200497.8 | 89415.67 | 147132.8 | 309751.8 |
| comb.Lasso | 601845.6 | 246680.3 | 231999.8 | 95087.78 | 159095.3 | 365468.2 |
| MRCS | 537848.0 | 239304.6 | 200497.8 | 79507.57 | 134387.3 | 284689.6 |
| MRGCS | 533929.2 | 229286.2 | 210172.7 | 81730.28 | 164394.0 | 389988.1 |
| ap.MRCS | 515088.8 | 233800.8 | 200497.8 | 79817.72 | 134401.6 | 283733.4 |
| ap.MRGCS | 537831.2 | 224128.6 | 214104.0 | 101772.8 | 164287.5 | 366998.9 |
| MRCE | 525804.0 | 227598.0 | 210888.4 | 80369.34 | 164309.4 | 360625.6 |
| ap.MRCE | 531651.2 | 223977.3 | 215168.6 | 101128.7 | 163408.5 | 342670.8 |

Table 2: The river flow prediction performance comparison table for each response. We measured average squared error for each response variable from 139 observations in the test set; $(\|\hat{Y}^i - Y^i\|^2)/139$, for $1 \leq i \leq 6$. Boldface indicates the best model for each response.

10. Acknowledgement

The authors would like to express gratitude to Professor Aaron Molstad for helpful comments on the proof details. Computational resources were provided by the WVU Research Computing Thorny Flat HPC cluster, which is funded in part by NSF OAC-1726534. Price was partially supported by the National Institute of General Medical Sciences, 5U54GM104942-04. The content is solely the responsibility of the authors and does not necessarily represent the official views of the NIH.

Appendix A. Derivation of the optimization problems (4)

We first check the derivation of the optimization problem (4). Recall that

$$\Sigma_* = \eta_*^2 \{ (1 - \theta_*) I_q + \theta_* \mathbf{1}_q \mathbf{1}_q^T \}$$

Since $\det(I + uv^T) = 1 + u^T v$ for $u, v \in \mathbb{R}^q$ and $\det(cA) = c^q A$ for $A \in \mathbb{R}^{q \times q}$, we have

$$\begin{aligned} \det(\Sigma_*) &= \det \left(\eta_*^2 (1 - \theta_*) \left[I_q + \frac{\theta_*}{1 - \theta_*} \mathbf{1}_q \mathbf{1}_q^T \right] \right) \\ &= \eta_*^{2q} (1 - \theta_*)^q \left(1 + q \frac{\theta_*}{1 - \theta_*} \right). \end{aligned}$$

This yields

$$\begin{aligned} \log \det(\Sigma_*) &= q \log(\eta_*^2) + q \log(1 - \theta_*) + \log \left(1 + q \frac{\theta_*}{1 - \theta_*} \right) \\ &= q \log(\eta_*^2) + q \log(1 - \theta_*) + \log \left(\frac{1 - \theta_* + q\theta_*}{1 - \theta_*} \right) \\ &= q \log(\eta_*^2) + (q - 1) \log(1 - \theta_*) + \log(1 + (q - 1)\theta_*). \end{aligned}$$

To compute Σ_*^{-1} , we use the following so-called Woodbury identity:

$$(A + CDC')^{-1} = A^{-1} - A^{-1}C(D^{-1} + C'A^{-1}C)^{-1}C'A^{-1},$$

with $A = (1 - \theta_*) I_q$, $D = \theta_*$, and $C = \mathbf{1}_q$. Then $A^{-1} = (1 - \theta_*)^{-1} I_q$, $D^{-1} = \theta_*^{-1}$, and

$$\begin{aligned} \Sigma_*^{-1} &= (\eta_*^2)^{-1} \left((1 - \theta_*) I_q + \theta_* \mathbf{1}_q \mathbf{1}_q^T \right)^{-1} \\ &= (\eta_*^2)^{-1} (A + CDC^T)^{-1} \\ &= (\eta_*^2)^{-1} \left[A^{-1} - A^{-1}C(D^{-1} + C'A^{-1}C)^{-1}C^T A^{-1} \right] \\ &= (\eta_*^2)^{-1} \left[(1 - \theta_*)^{-1} I_q - (1 - \theta_*)^{-1} I_q \mathbf{1}_q (\theta_*^{-1} + (1 - \theta_*)^{-1} \mathbf{1}_q^T I_q \mathbf{1}_q)^{-1} \mathbf{1}_q^T (1 - \theta_*)^{-1} I_q \right] \\ &= (\eta_*^2)^{-1} \left[(1 - \theta_*)^{-1} I_q - (1 - \theta_*)^{-1} I_q \mathbf{1}_q (\theta_*^{-1} + (1 - \theta_*)^{-1} q)^{-1} \mathbf{1}_q^T (1 - \theta_*)^{-1} I_q \right] \\ &= (\eta_*^2)^{-1} \left[(1 - \theta_*)^{-1} I_q - (1 - \theta_*)^{-2} (\theta_*^{-1} + (1 - \theta_*)^{-1} q)^{-1} \mathbf{1}_q \mathbf{1}_q^T \right] \\ &= (\eta_*^2)^{-1} (1 - \theta_*)^{-1} \left(I_q - \frac{\theta_*}{1 - \theta_* + q\theta_*} \mathbf{1}_q \mathbf{1}_q^T \right). \end{aligned}$$

This identifies

$$\begin{aligned}
F_\lambda(B, \eta^2, \theta; Y, X) &= \frac{1}{\eta^2(1-\theta)} \operatorname{tr} \left\{ n^{-1}(Y - XB)^T(Y - XB) \left[I_q - \frac{\theta}{1-\theta+q\theta} \mathbf{1}_q \mathbf{1}_q^T \right] \right\} \\
&\quad + (q-1) \log(1-\theta) + \log(1 + \{q-1\}\theta) + q \log(\eta^2) \\
&\quad + \lambda \sum_{j=1}^p \sum_{k=1}^q |B_{jk}|.
\end{aligned} \tag{A.1}$$

Its equivalence to the optimization problem (4) is based on the following:

$$\begin{aligned}
&\frac{1}{\eta^2(1-\theta)} \operatorname{tr} \left\{ n^{-1}(Y - XB)^T(Y - XB) \left[I_q - \frac{\theta}{1-\theta+q\theta} \mathbf{1}_q \mathbf{1}_q^T \right] \right\} \\
&= \frac{1}{n\eta^2(1-\theta)} \|Y - XB\|_F^2 - \frac{\theta}{n\eta^2(1-\theta)(1-\theta+q\theta)} \operatorname{tr} \{ (Y - XB)^T(Y - XB) \mathbf{1}_q \mathbf{1}_q^T \} \\
&= \frac{1}{n\eta^2(1-\theta)} \|Y - XB\|_F^2 - \frac{\theta}{n\eta^2(1-\theta)(1-\theta+q\theta)} \|(Y - XB) \mathbf{1}_q\|^2.
\end{aligned}$$

We now check the derivation of the optimization problem (11). We cyclically update η_j while fixing B , θ , and η_{-j} , where $\eta_{-j} = (\eta_1, \dots, \eta_{j-1}, \eta_{j+1}, \dots, \eta_q)$ for each $j \in \{1, \dots, q\}$. By simple algebra, one can derive that the objective function with respect to η_j is computed as the following:

$$g_j(\eta_j) = \frac{1}{n(1-\theta)} \sum_{i=1}^n e_{ij}^2 \frac{1}{\eta_j^2} - \frac{\theta}{n(1-\theta)(1+(q-1)\theta)} \sum_{i=1}^n \left(\sum_{j=1}^q e_{ij} \frac{1}{\eta_j} \right)^2 + 2 \log(\eta_j),$$

We suppress the dependence of g_j on η_{-j} , B , and θ for notational simplicity. From the above computation, we have

$$\begin{aligned}
\frac{1}{2} g'_j(\eta_j) &= \frac{1}{\eta_j} + \frac{\theta}{n(1-\theta)(1+(q-1)\theta)} \sum_{i=1}^n \left(\sum_{k \neq j} e_{ik} \frac{1}{\eta_j^2 \eta_k} \right) \\
&\quad - \frac{1+(q-2)\theta}{n(1+(q-1)\theta)(1-\theta)} \left(\sum_{i=1}^n e_{ij}^2 \right) \frac{1}{\eta_j^3}.
\end{aligned}$$

Then $g'_j = 0$ yields (12), since $\eta_j > 0$.

Appendix B. Proof of Theorem 1

We first provide two lemmas which are used for the proof of Theorem 1. Recall $S = \{i : \text{vec}(B_*)_i \neq 0\}$, and

$$\Omega_* = \frac{1}{\eta_*^2(1-\theta_*)} \left[I_q - \frac{\theta_*}{1+(q-1)\theta_*} \mathbf{1}_q \mathbf{1}_q^T \right].$$

Lemma 1. *Under the conditions (A1) and (A3), assuming that $(\hat{\eta}^2, \hat{\theta})$ are \sqrt{n} -consistent estimators of (η_*^2, θ_*) , then, if $\lambda\sqrt{n} \rightarrow 0$ and $\lambda n^{(r+1)/2} \rightarrow \infty$, the following holds.*

$$\begin{aligned} \lim_{n \rightarrow \infty} P(\hat{B}_{jk} = 0) &= 1 && \text{if } B_{jk*} = 0, \\ \sqrt{n}(\text{vec}(\hat{B})_S - \text{vec}(B_*)_S) &\rightarrow_d N(0, D^{-1}), \end{aligned}$$

where \hat{B} is a solution to the optimization problem (14) for fixed $(\hat{\eta}^2, \hat{\theta})$, and $D = (\Omega_* \otimes Z)_S$.

Proof. The diagonals of Ω_* are $\frac{1+(q-2)\theta_*}{\eta_*^2(1-\theta_*)(1+(q-1)\theta_*)} = \frac{1}{\eta_*^2(1-\theta_*)} \left(1 - \frac{\theta_*}{1+(q-1)\theta_*}\right)$ and the off-diagonals are $-\frac{\theta_*}{\eta_*^2(1-\theta_*)(1+(q-1)\theta_*)}$. Let $v_* = \frac{1}{\eta_*^2(1-\theta_*)}$ and $w_* = \frac{\theta_*}{\eta_*^2(1-\theta_*)(1+(q-1)\theta_*)}$. We further denote $\hat{v} = \frac{1}{\hat{\eta}^2(1-\hat{\theta})}$ and $\hat{w} = \frac{\hat{\theta}}{\hat{\eta}^2(1-\hat{\theta})(1+(q-1)\hat{\theta})}$. Then,

$$\begin{aligned} |\hat{v} - v_*| &= \left| \frac{\hat{\eta}^2(1-\hat{\theta}) - \eta_*^2(1-\theta_*)}{\eta_*^2(1-\theta_*)\hat{\eta}^2(1-\hat{\theta})} \right| \\ &\leq \frac{|\hat{\eta}^2 - \eta_*^2| + \hat{\eta}^2|\hat{\theta} - \theta_*| + \theta_*|\hat{\eta}^2 - \eta_*^2|}{\eta_*^2(1-\theta_*)\hat{\eta}^2(1-\hat{\theta})} = O_p(1/\sqrt{n}), \end{aligned}$$

since $\hat{\eta}^2, 1/\hat{\eta}^2, 1/(1-\hat{\theta}) = O_p(1)$ and $|\hat{\eta}^2 - \eta_*^2|, |\hat{\theta} - \theta_*| = O_p(1/\sqrt{n})$. Similarly, one can check that $|\hat{w} - w_*| = O_p(1/\sqrt{n})$. This implies that the \sqrt{n} -consistent estimator of (η_*^2, θ_*) guarantees the existence of \sqrt{n} -consistent estimator of Ω . The rest of the proof follows the same derivation steps provided in the proofs of Lemma 1 and Theorem 1 of Lee and Liu [6]. Hence, we omit the proof. \square

We define a matrix, $V \in \mathbb{R}^{2 \times 2}$, which characterizes the limiting covariance of $(\hat{\eta}, \hat{\theta})$. This symmetric matrix has the following four elements:

$$\begin{aligned} V_{11} &= \frac{1}{q^2} \left(\sum_{j=1}^q \text{var}(E_{ij}^2) + 2 \sum_{j < k} \text{cov}(E_{ij}^2, E_{ik}^2) \right), \\ V_{22} &= \frac{1}{q^2(q-1)^2} \sum_{j,k,l,m} Q_{jk} Q_{lm} \text{cov}(E_{ij} E_{ik}, E_{il} E_{im}), \\ V_{12} = V_{21} &= \frac{1}{q^2} \text{var} \left(\sum_{j=1}^q E_{ij}^2 \right) - \frac{2}{q^2(q-1)} \text{cov} \left(\sum_{j < k} E_{ij} E_{ik}, \sum_{j=1}^q E_{ij}^2 \right), \end{aligned} \tag{B.1}$$

where $Q = (qI_q - 1_q 1_q^T)$.

Lemma 2. *Under the conditions (A1), (A2) and (A4), assuming that \hat{B} is \sqrt{n} -consistent to B_* , then, for $W = (1, -1/\eta_*^2)^T$, the following holds.*

$$\left\| (\hat{\eta}^2, \hat{\theta}) - (\eta_*^2, \theta_*) \right\| = O_p(1/\sqrt{n}),$$

where $(\hat{\eta}^2, \hat{\theta})$ is a solution to the optimization problem (14) for fixed \hat{B} . Furthermore, if $\theta_* \in (0, 1)$, then

$$\sqrt{n}(\hat{\eta}^2, \hat{\theta}) - (\eta_*^2, \theta_*) \rightarrow_d W^T N_2(0, V),$$

where $W = (1, -1/\eta_*^2)^T$, and V is defined in B.1.

Proof. It suffices to assume that true B_* is known, since the natural following step which is the replacement of B_* with \hat{B} can be directly obtained by application of the derivation used in the proof of Theorem 2 in Lee and Liu [6]. Recall the reparametrization of (η^2, θ) to (α, γ) via $\alpha = \eta^2(1-\theta)$, $\gamma = \eta^2(1 + (q-1)\theta)$ by which we derived the closed form solutions to $\hat{\alpha}$ and $\hat{\gamma}$. The solutions were $\hat{\alpha} = \frac{qM_1^* - M_2^*}{q(q-1)}$, $\hat{\gamma} = \max\{\hat{\alpha}, M_2^*/q\}$, where $M_1^* = \frac{1}{n}\|E\|_F^2$ and $M_2^* = \frac{1}{n}\|E1_q\|^2$ (see (6), (7)). We define $\hat{\delta} = \frac{M_1^*}{q}$. We first find the joint limiting distribution of $(\hat{\delta}, \hat{\alpha})$. We have

$$\begin{aligned} \frac{qM_1^* - M_2^*}{q(q-1)} &= \frac{1}{nq(q-1)} \left\{ \sum_{i=1}^n \left[\sum_{j=1}^q (q-1)E_{ij}^2 - 2 \sum_{1 \leq j < k \leq q} E_{ij}E_{ik} \right] \right\} \\ &= \frac{1}{nq(q-1)} \sum_{i=1}^n E_i^T Q E_i, \end{aligned}$$

where $E_i = (E_{i1}, \dots, E_{iq})^T \in \mathbb{R}^q$ and $Q = (qI_q - 1_q 1_q^T)$. We further have

$$\begin{aligned} \mathbb{E}(E_i^T Q E_i / (q(q-1))) &= \eta_*^2(1 - \theta_*), \\ \text{var}(E_i^T Q E_i / (q(q-1))) &= \frac{1}{q^2(q-1)^2} \sum_{j,k,l,m} Q_{jk} Q_{lm} \text{cov}(E_{ij}E_{ik}, E_{il}E_{im}). \end{aligned}$$

In addition, $\hat{\delta}$ can be expressed as $\frac{1}{nq} \sum_{i=1}^n \sum_{j=1}^q E_{ij}^2 = \frac{1}{nq} \sum_{i=1}^n E_i^T I_q E_i$, which satisfies

$$\begin{aligned} \mathbb{E}(E_i^T I_q E_i / q) &= \eta_*^2, \\ \text{var}(E_i^T I_q E_i / q) &= \frac{1}{q^2} \left(\sum_{j=1}^q \text{var}(E_{ij}^2) + 2 \sum_{j < k} \text{cov}(E_{ij}^2, E_{ik}^2) \right). \end{aligned}$$

Likewise, we obtain

$$\text{cov} \left(E_i^T I_q E_i / q, E_i^T Q E_i / (q(q-1)) \right) = \frac{1}{q^2} \text{var} \left(\sum_{j=1}^q E_{ij}^2 \right) - \frac{2}{q^2(q-1)^2} \text{cov} \left(\sum_{j < k} E_{ij} E_{ik}, \sum_{j=1}^q E_{ij}^2 \right).$$

Thus, we have

$$\sqrt{n}((\hat{\delta}, \hat{\alpha}) - (\eta_*^2, \eta_*^2(1 - \theta_*))) \rightarrow_d N_2(0, V). \quad (\text{B.2})$$

And, since $\hat{\eta}^2 = (1 - 1/q)\hat{\alpha} + \hat{\gamma}/q$, we have

$$\hat{\eta}^2 - \hat{\delta} = \frac{\hat{\gamma}}{q} - \frac{M_2^*}{q^2} = \max \left\{ \frac{\hat{\alpha}}{q}, \frac{M_2^*}{q^2} \right\} - \frac{M_2^*}{q^2}.$$

When $\theta_* \in (0, 1)$, $\hat{\alpha} \rightarrow_p \eta_*^2(1 - \theta)$, and $\max\{\hat{\alpha}, M_2^*/q\} = M_2^*/q$ with probability tending to 1, since $M_2^*/q \rightarrow_p \eta_*^2$. This yields, $\hat{\eta}^2 = \hat{\delta}$ with probability tending to 1 and it further implies

$$\sqrt{n}((\hat{\eta}^2, \hat{\alpha}) - (\eta_*^2, \eta_*^2(1 - \theta_*))) \rightarrow_d N_2(0, V).$$

Then, by the same Delta method via $g(x, y) = (x, (x - y)/x)$, we have

$$\sqrt{n} \left(\left(\hat{\eta}^2, \frac{\hat{\eta}^2 - \hat{\alpha}}{\hat{\eta}^2} \right) - (\eta_*^2, \theta_*) \right) \rightarrow_d W^T N_2(0, V),$$

where $W = (1, -1/\eta_*^2)^T$, since $\hat{\delta} > 0$ almost surely. It is obvious that $\frac{\hat{\eta}^2 - \hat{\alpha}}{\hat{\eta}^2} = \frac{\hat{\gamma} - \hat{\alpha}}{\hat{\gamma} + (q-1)\hat{\alpha}} = \hat{\theta}$. On the other hand, when $\theta_* = 0$, (B.2) with the Delta method yields,

$$\sqrt{n} \left(\left(\hat{\delta}, \frac{\hat{\delta} - \hat{\alpha}}{\hat{\delta}} \right) - (\eta_*^2, \theta_*) \right) \rightarrow_d W^T N_2(0, V).$$

Then it suffices to show $|\hat{\delta} - \hat{\eta}^2| = O_p(1/\sqrt{n})$ and $|\hat{\alpha}(1/\hat{\eta}^2 - 1/\hat{\delta})| = O_p(1/\sqrt{n})$. Indeed, we have

$$q|\hat{\delta} - \hat{\eta}^2| \leq \left| \frac{M_2^*}{q} - \hat{\alpha} \right| = \left| \frac{M_2^*}{q} - \frac{qM_1^* - M_2^*}{q(q-1)} \right| = \left| \frac{M_2^* - M_1^*}{q-1} \right|,$$

and $M_2^* - M_1^* = \frac{1}{n} \sum_{i=1}^n E_i^T Q_0 E_i$, where Q_0 has 0 for all diagonal elements and 1 for all off-diagonal elements. Thus, by similar asymptotic derivation steps above, one can easily check $|\hat{\delta} - \hat{\eta}^2| = O_p(1/\sqrt{n})$. Since $\hat{\eta}^2, \hat{\delta}, \hat{\alpha} \rightarrow_p \eta_*^2 > 0$, $|1/\hat{\eta}^2|, |1/\hat{\delta}|, |\hat{\alpha}| = O_p(1)$. This implies

$$|\hat{\alpha}(1/\hat{\eta}^2 - 1/\hat{\delta})| = |\hat{\alpha}| |1/\hat{\delta}| |1/\hat{\eta}^2| |\hat{\eta}^2 - \hat{\delta}| = O_p(1/\sqrt{n}).$$

Finally, we have

$$\left\| \left(\hat{\delta}, \frac{\hat{\delta} - \hat{\alpha}}{\hat{\delta}} \right) - \left(\hat{\eta}^2, \frac{\hat{\eta}^2 - \hat{\alpha}}{\hat{\eta}^2} \right) \right\| \leq |\hat{\eta}^2 - \hat{\delta}| + |\hat{\alpha}(1/\hat{\eta}^2 - 1/\hat{\delta})| = O_p(1/\sqrt{n}),$$

and it completes the proof. \square

Now we give the proof of Theorem 1.

Proof. We already verified that a \sqrt{n} -consistent estimator of (η_*^2, θ_*) guarantees the existence of the \sqrt{n} -consistent estimator of Ω_* by Lemma 1. Combining the result in Lemma 2, the rest of the proof follows the same derivation used in the proofs of Lemma 3 and Theorem 3 of Lee and Liu [6]. Hence, we omit the proof. \square

Appendix C. High-dimensional statistical guarantees

In this section, we study the statistical properties of an oracle estimator, MRCS-Or that assumes the true covariance is known (see (19)), and a surrogate version of ap.MRCS (see Section 3.2) that leverages pilot estimators η_n^2 and θ_n for η_*^2 and θ_* . Our theoretical results accommodate scenarios where the sample size n and the dimensional parameters p and q are allowed to grow simultaneously.

For a matrix $M \in \mathbb{R}^{p \times q}$, we let $\text{vec}(M) \in \mathbb{R}^{pq}$ denote the vector formed by stacking the columns of M . We denote i -th row of M by $M_{i\cdot}$, and j -th column of it by $M_{\cdot j}$. Recall $S = \{i : \text{vec}(B_*)_{i\cdot} \neq 0\}$, which is the support of the true regression coefficients matrix B_* . We define the subspace that corresponds to S as follows:

$$\mathcal{M}(S) \equiv \{v \in \mathbb{R}^{pq} : v_i = 0 \text{ if } i \notin S\}.$$

We further define a projection of a generic vector u onto the subspace $\mathcal{M}(S)$ by

$$u_{\mathcal{M}(S)} \equiv \arg \min_{v \in \mathcal{M}(S)} \|u - v\|_2.$$

We let $\mathcal{M}^\perp(S)$ denote the orthogonal complement of $\mathcal{M}(S)$, which is given by

$$\mathcal{M}^\perp(S) \equiv \{v^{pq} : \langle u, v \rangle = 0, \forall u \in \mathcal{M}(S)\}.$$

To prove consistency of the oracle procedure, we make the following assumptions:

(C1) : Each column of X is scaled so that $\|X_{\cdot j}\|_2 = \sqrt{n}$ for all $j = 1, \dots, p$.

(C2) : The errors $E_i = (E_{i1}, \dots, E_{iq})$ are iid $N_q(0, \Sigma_*)$, for $i = 1, \dots, n$, where

$$\Sigma_* = \eta_*^2 [(1 - \theta_*)I_q + \theta_* \mathbf{1}_q \mathbf{1}_q^T],$$

for $\eta_* \in (0, \infty)$ and $\theta_* \in [0, 1)$.

(C3) : Let $\bar{X} = I_q \otimes X$, where \otimes stands for the standard Kronecker product. There exists a positive constant κ which satisfies

$$\kappa \|v\|_2^2 \leq \min_{v \in \mathcal{C}} \|\bar{X}v\|_2^2/n,$$

where

$$\mathcal{C} := \{v \in \mathbb{R}^{pq} \mid \|v_{\mathcal{M}^+(S)}\|_1 \leq 3\|v_{\mathcal{M}}\|_1\}. \quad (\text{C.1})$$

Assumption (C1) is a standard assumption in the penalized regression literature [8, 9, 15]. This condition can be easily satisfied with appropriate standardization. Assumption (C2) implies that the error follows multivariate normal distribution, which has zero mean and exhibits compound symmetry variance. Assumption (C3) is so-called the restricted eigenvalue condition. We refer the readers to Negahban et al. [8] for more details of this condition. Now we state the consistency result of \hat{B}_{Or} .

Theorem 2. *If Assumptions (C1)–(C3) hold and $\lambda_n = 8\sqrt{\frac{\log(pq)}{n\eta_*^2(1-\theta_*)}}$, then there exist positive constants c_1, c_2, c_3 such that*

$$\|\text{vec}(\hat{B}_{Or} - B^*)\|_2 \leq c_3 \frac{\eta_*}{\sqrt{1-\theta_*}} \frac{1 + (q-1)\theta_*}{\kappa} \sqrt{\frac{s \log(pq)}{n}},$$

with probability at least $1 - c_1 \exp(-c_2 \log(pq))$.

Proof of Theorem 2 is postponed to [Appendix D](#) of the supplementary material. Except for the scalar factor $(1+(q-1)\theta_*)/\sqrt{1-\theta_*}$, which is related to the eigenspectrum of the correlation matrix of Σ_* , the rate $O_p(\sqrt{s \log(pq)/n})$ is standard rate of convergence in lasso-penalized multivariate linear regression [9, 13, 17]. However, since the largest eigenvalue of Σ_* is proportional to q , it is required that $q\sqrt{s \log(pq)/n} \rightarrow 0$ when $\theta_* > 0$ to obtain $\|\text{vec}(\hat{B}_{Or} - B^*)\|_2 = o_p(1)$.

Assume that we have consistent pilot estimators η_n^2, θ_n of η_*^2, θ_* . We consider the following updated optimization problem of (19) with replacement of η_*^2, θ_* with plug-in pilot estimators η_n^2, θ_n .

$$\begin{aligned} \hat{B}_{Pl} := \arg \min_{B \in \mathbb{R}^{p \times q}} \text{tr} \left\{ n^{-1} (Y - XB)^T (Y - XB) \left[\eta_n^2 \{ \theta_n \mathbf{1}_q \mathbf{1}_q^T + (1 - \theta_n) I_q \} \right]^{-1} \right\} \\ + \lambda \sum_{j=1}^p \sum_{k=1}^q |B_{jk}| \end{aligned} \quad (\text{C.2})$$

We define

$$v(\eta^2, \theta) := \frac{1}{\eta^2(1 + (q-1)\theta)}, \quad (\text{C.3})$$

for $\eta^2 \in (0, \infty)$ and $\theta \in [0, 1)$. To prove consistency of the plug-in optimizer, we make the

following assumption on η_n^2, θ_n .

(C4) : There exists pilot estimators η_n^2, θ_n for η_*^2, θ_* that are independent of E_1, \dots, E_n . The pilot estimators satisfy $\eta_n \in (0, \infty), \theta_n \in [0, 1)$, and the following holds with probability at least $1 - k_1 \exp(-k_2 \log(pq))$ where $k_1 > 0, k_2 \geq 1$:

$$\left| \frac{v(\eta_n^2, \theta_n)}{v(\eta_*^2, \theta_*)} - 1 \right| \leq \frac{1}{2}, \quad (\text{C.4})$$

and

$$s_n := [(1 - \theta_*) + |\theta_n - \theta_*|] \frac{(\eta_*^2)^3 (1 - \theta_*)^2}{(\eta_n^2)^2 (1 - \theta_n)^2} \leq 2\eta_*^2(1 - \theta_*). \quad (\text{C.5})$$

Assumption (C4) holds if η_n^2, θ_n are sufficiently close to η_*^2, θ_* , respectively, with high probability. The independence between (η_n^2, θ_n) and E_1, \dots, E_n can be achieved when (η_n^2, θ_n) are estimated from independent observations generated by the same model. More details can be found in [Appendix E](#) of the supplementary material.

While the following theorem is not directly applicable to ap.MRCS (see [Section 3.2](#)), the theoretical properties of \hat{B}_{Pl} provide better understanding of ap.MRCS. Now we state the consistency result of \hat{B}_{Pl} .

Theorem 3. *If Assumptions (C1)–(C4) hold and $\lambda_n = 8\sqrt{\frac{\log(pq)}{n\eta_*^2(1-\theta_*)}}$, then there exist constants c_4, c_5, c_6 such that*

$$\|\text{vec}(\hat{B}_{Pl} - B_*)\|_2 \leq c_6 \frac{\eta_*}{\sqrt{1 - \theta_*}} \frac{1 + (q - 1)\theta_*}{\kappa} \sqrt{\frac{s \log(pq)}{n}},$$

with probability at least $1 - c_4 \exp(-c_5 \log(pq))$.

Proof of [Theorem 3](#) is provided in [Appendix F](#) of the supplementary material. The convergence rate of $\|\text{vec}(\hat{B}_{Pl} - B_*)\|_2$ is identical to the rate of $\|\text{vec}(\hat{B}_{Or} - B_*)\|_2$. On the other hand, compared with the upper bound of $\|\text{vec}(\hat{B}_{Or} - B_*)\|_2$ in [Theorem 2](#), the upper bound of $\|\text{vec}(\hat{B}_{Pl} - B_*)\|_2$ in [Theorem 3](#) is inflated by $\sqrt{2}$ (see the proof given in [Appendix F](#)), which arises from (C.5) that accounts for additional error introduced by plug-in pilot estimators.

Appendix D. Proof of [Theorem 2](#)

In this section, we give the proof of [Theorem 2](#).

Proof. Let $\bar{Y} = \text{vec}(Y)$, $\bar{B} = \text{vec}(B)$, and $\bar{E} = \text{vec}(E)$. Letting $\Omega_* = \Sigma_*^{-1}$, we can write (19) as

$$\hat{B}_{Or} := \arg \min \mathcal{L}(B) + \lambda_n \|\bar{B}\|_1, \quad (\text{D.1})$$

where

$$\mathcal{L}(B) = \frac{1}{n}(\bar{Y} - \bar{X}\bar{B})^T(\Omega_* \otimes I_n)(\bar{Y} - \bar{X}\bar{B}).$$

We define $\delta\mathcal{L}(\Delta, \bar{B}) = \mathcal{L}(\bar{B} + \Delta) - \mathcal{L}(\bar{B}) - \langle \nabla\mathcal{L}(\bar{B}), \Delta \rangle$. Since $\Omega_* \otimes I_n$ is positive definite symmetric matrix with minimal eigenvalue of $1/(\eta_*^2(1 + (q-1)\theta_*))$, one can easily show

$$\delta\mathcal{L}(\Delta, \bar{B}) = \frac{1}{n}(\bar{X}\Delta)^T(\Omega_* \otimes I_n)(\bar{X}\Delta) \geq \frac{1}{(1 + (q-1)\theta_*)\eta_*^2} \frac{\|\bar{X}\Delta\|_2^2}{n} \quad (\text{D.2})$$

$$\geq \frac{\kappa\|\Delta\|_2^2}{(1 + (q-1)\theta_*)\eta_*^2}, \quad (\text{D.3})$$

for all $\Delta \in \mathcal{C}$, by Assumption (C3). For a general subspace \mathcal{X} , we define a compatibility constant $\psi(\mathcal{M}) = \sup_{u \in \mathcal{M} \setminus \{0\}} \frac{\|u\|_1}{\|u\|_2}$, where $\psi(\mathcal{M}(S)) = \sqrt{s}$. If $\lambda_n \geq 2\|\nabla\mathcal{L}(\bar{B})\|_\infty$, by Theorem 1 of Negahban et al. [8], we have

$$\|\text{vec}(\hat{B}_{\text{Or}} - B_*)\|_2^2 \leq 9\frac{\lambda_n^2}{c^2}s, \quad (\text{D.4})$$

where $c = \kappa/((1 + (q-1)\theta_*)\eta_*^2)$. Indeed,

$$\begin{aligned} \|\nabla\mathcal{L}(\bar{B})\|_\infty &= \frac{2}{n}\|\bar{X}^T(\Omega_* \otimes I_n)(\bar{Y} - \bar{X}\bar{B})\|_\infty \\ &= \frac{2}{n}\|\bar{X}^T(\Omega_* \otimes I_n)\bar{E}\|_\infty = \frac{2}{n}\|\bar{X}^T\bar{W}\|_\infty, \end{aligned}$$

where $(\Omega_* \otimes I_n)\bar{E} = \bar{W}$; $\bar{W} := \text{vec}(W)$, $W \in \mathbb{R}^{n \times q}$, and W_i 's are iid from $N(0, \Omega_*)$, for $i = 1, \dots, n$. We define

$$u(\eta^2, \theta) := \frac{1}{\eta^2(1-\theta)} \frac{1 + (q-2)\theta}{1 + (q-1)\theta}, \quad (\text{D.5})$$

for $\eta \in (0, \infty)$ and $\theta \in [0, 1)$. We define the events

$$\begin{aligned} \mathcal{A}_j &= \left\{ \frac{1}{n}\|X^T W_{\cdot j}\|_\infty \leq \sqrt{u(\eta_*^2, \theta_*) \frac{t + 2 \log p}{n}} \right\}, \\ \mathcal{A} &= \cap_{j=1}^q \mathcal{A}_j. \end{aligned}$$

Since $\mathbb{P}(\mathcal{A}_j^c) \leq 2 \exp(-t/2)$ by Lemma 6.2 of Bühlmann and Van De Geer [2] and Assumption (C1)–(C2), we have

$$\mathbb{P}(\mathcal{A}) = \mathbb{P}(\cap_{j=1}^q \mathcal{A}_j) \geq 1 - \sum_{j=1}^q \mathbb{P}(\mathcal{A}_j^c) \geq 1 - 2q \exp(-t/2).$$

Recall that $\lambda_n = 8\sqrt{\frac{\log(pq)}{n\eta_*^2(1-\theta_*)}}$. Thus, letting $t = 4\log pq + 2\log p$, we have

$$\begin{aligned}\mathbb{P}(\lambda_n \geq 2\|\nabla\mathcal{L}(\bar{B})\|_\infty) &= \mathbb{P}\left(\lambda_n \geq \frac{4}{n}\|\bar{X}^T\bar{W}\|_\infty\right) \\ &\geq 1 - 2\exp(-\log(pq)),\end{aligned}\tag{D.6}$$

since $\frac{1+(q-2)\theta_*}{1+(q-1)\theta_*} \leq 1$. Combining (D.4) and (D.6) completes the proof with $c_1 = 2$, $c_2 = 1$, $c_3 = 24$. \square

Appendix E. Supplementary description of Assumption (C4)

First, we note that

$$\begin{aligned}&\left|\frac{v(\eta_*^2, \theta_*)}{v(\eta_n^2, \theta_n)} - 1\right| \\ &= \left|\frac{(1 + (q-1)\theta_*)(\eta_n^2 - \eta_*^2) + (q-1)\eta_n^2(\theta_n - \theta_*)}{\eta_*^2(1 + (q-1)\theta_*)}\right| \\ &= \left|\frac{\eta_n^2}{\eta_*^2} - 1\right| + q\frac{\eta_n^2}{\eta_*^2}\frac{|\theta_n - \theta_*|}{1 + (q-1)\theta_*} \\ &\leq \left|\frac{\eta_n^2}{\eta_*^2} - 1\right| + \left(\left|\frac{\eta_n^2}{\eta_*^2} - 1\right| + 1\right)\frac{q|\theta_n - \theta_*|}{1 + (q-1)\theta_*}.\end{aligned}$$

Thus, if

$$|\eta_n^2 - \eta_*^2| \leq \frac{\eta_*^2}{6}, \quad \text{and} \quad |\theta_n - \theta_*| \leq \frac{1 + (q-1)\theta_*}{7q}\tag{E.1}$$

on an event \mathcal{A}_0 where $P(\mathcal{A}_0) \geq 1 - k_1 \exp(-k_2 \log(pq))$ for $k_1 > 0$ and $k_2 \geq 1$, then $\left|\frac{v(\eta_n^2, \theta_n)}{v(\eta_*^2, \theta_*)} - 1\right| \leq 1/3$ on \mathcal{A}_0 . This further yields $\left|\frac{v(\eta_n^2, \theta_n)}{v(\eta_*^2, \theta_n)} - 1\right| \leq 1/2$ on \mathcal{A}_0 , which is (C.4).

Next, when

$$\frac{\eta_*^2}{\eta_n^2} \leq \left(\frac{3}{2}\right)^{1/4}, \quad \frac{1 - \theta_*}{1 - \theta_n} \leq \left(\frac{3}{2}\right)^{1/4}, \quad \text{and} \quad |\theta_n - \theta_*| \leq \frac{1 - \theta_*}{3}\tag{E.2}$$

hold on \mathcal{A}_0 , one can easily check that (C.5) holds on \mathcal{A}_0 . Thus, when $\mathbb{E}|\eta_n^2 - \eta_*^2| = O(1/(pq)^{k_2})$ and $\mathbb{E}|\theta_n - \theta_*| = O(q/(pq)^{k_2})$, then the conditions in (E.1)–(E.2) hold.

Appendix F. Proof of Theorem 3

In this section, we give the proof of Theorem 3.

Proof. As in the proof of Theorem 2, we denote $\bar{Y} = \text{vec}(Y)$, $\bar{B} = \text{vec}(\hat{B})$, and $\bar{E} = \text{vec}(E)$. We consider the following derivation conditioned on an event \mathcal{C}_0 that satisfies (C.4)–(C.5), which further satisfies $P(\mathcal{C}_0) \geq 1 - k_1 \exp(-k_2 \log(pq))$. And, we write

$$\hat{B}_{Pl} := \arg \min_{B \in \mathbb{R}^{p \times q}} \mathcal{L}_n(B) + \lambda_n \sum_{j=1}^p \sum_{k=1}^q |B_{jk}| \quad (\text{F.1})$$

Since \hat{B}_{Pl} is the minimizer of the problem (F.1), we have

$$\begin{aligned} \mathcal{L}_n(B) - \mathcal{L}_n(B_*) &\leq \lambda_n \|\bar{B}_*\|_1 - \lambda_n \|\bar{B}_{Pl}\|_1 \\ &= \lambda_n \|\bar{B}_{*S}\|_1 - \lambda_n \|\bar{B}_{Pl;S}\|_1 - \lambda_n \|\bar{B}_{Pl;S^c}\|_1 \\ &\leq \lambda_n \|\tilde{\Delta}_S\|_1 - \lambda_n \|\tilde{\Delta}_{S^c}\|_1 \end{aligned} \quad (\text{F.2})$$

by triangle inequality and \bar{B}_{*S^c} , where $\tilde{\Delta} = \bar{B}_{Pl} - \bar{B}_*$. We now study the term $\mathcal{L}_n(B) - \mathcal{L}_n(B_*)$. Since $\bar{Y} = \bar{X}\bar{B}_* + \bar{E}$, we have

$$\begin{aligned} \mathcal{L}_n(B) - \mathcal{L}_n(B_*) &= \frac{1}{n} (\bar{Y} - \bar{X}\bar{B}_{Pl})^T (\Omega_n \otimes I_n) (\bar{Y} - \bar{X}\bar{B}_{Pl}) - \frac{1}{n} (\bar{Y} - \bar{X}\bar{B}_*)^T (\Omega_n \otimes I_n) (\bar{Y} - \bar{X}\bar{B}_*) \\ &= \frac{1}{n} (\bar{X}\tilde{\Delta})^T (\Omega_n \otimes I_n) (\bar{X}\tilde{\Delta}) \\ &\quad + \frac{2}{n} (\bar{X}\tilde{\Delta})^T (\Omega_n \otimes I_n) \bar{E}. \end{aligned} \quad (\text{F.3})$$

Recall that

$$v(\eta^2, \theta) = \frac{1}{\eta^2(1 + (q-1)\theta)}. \quad (\text{F.4})$$

By assumption (C3), we get

$$\begin{aligned} \frac{1}{n} (\bar{X}\tilde{\Delta})^T (\Omega_n \otimes I_n) (\bar{X}\tilde{\Delta}) &\geq \kappa v(\eta_n^2, \theta_n) \|\tilde{\Delta}\|_2^2 \\ &= \kappa v(\eta_*^2, \theta_*) \|\tilde{\Delta}\|_2^2 + \kappa v(\eta_*^2, \theta_*) \left(\frac{v(\eta_n^2, \theta_n)}{v(\eta_*^2, \theta_*)} - 1 \right) \|\tilde{\Delta}\|_2^2 \\ &\geq \kappa v(\eta_*^2, \theta_*) \|\tilde{\Delta}\|_2^2 - \kappa v(\eta_*^2, \theta_*) \left| \frac{v(\eta_n^2, \theta_n)}{v(\eta_*^2, \theta_*)} - 1 \right| \|\tilde{\Delta}\|_2^2 \\ &= \kappa v(\eta_*^2, \theta_*) \left(1 - \left| \frac{v(\eta_n^2, \theta_n)}{v(\eta_*^2, \theta_*)} - 1 \right| \right) \|\tilde{\Delta}\|_2^2 \\ &\geq \frac{1}{2} \kappa v(\eta_*^2, \theta_*) \|\tilde{\Delta}\|_2^2. \end{aligned} \quad (\text{F.5})$$

On the other hand, we have

$$\begin{aligned} \frac{1}{n}(\bar{X}\tilde{\Delta})^T(\Omega_n \otimes I_n)\bar{E} &\geq -\frac{1}{n}\|\tilde{\Delta}\|_1 \|\bar{X}^T(\Omega_n \otimes I_n)\bar{E}\|_\infty \\ &= -\frac{1}{n}\|\tilde{\Delta}\|_1 \|\bar{X}^T\bar{R}\|_\infty, \end{aligned} \quad (\text{F.6})$$

where $(\Omega_n \otimes I_n)\bar{E} = \bar{R}$; $\bar{R} := \text{vec}(R)$, $R \in \mathbb{R}^{n \times q}$, and R_i 's are iid from $N(0, \Omega_n \Sigma_* \Omega_n)$, for $i = 1, \dots, n$. Thus, when $\lambda_n \geq 4\|\bar{X}^T\bar{R}\|_\infty/n$, we get

$$\frac{2}{n}(\bar{X}\tilde{\Delta})^T(\Omega_n \otimes I_n)\bar{E} \geq -\frac{\lambda_n}{2}\|\tilde{\Delta}\|_1. \quad (\text{F.7})$$

Combining (F.2)–(F.7) implies

$$\frac{1}{2}\kappa v(\eta_*^2, \theta_*)\|\tilde{\Delta}\|_2^2 - \frac{\lambda_n}{2}\|\tilde{\Delta}\|_1 \leq \lambda_n\|\tilde{\Delta}_S\|_1 - \lambda_n\|\tilde{\Delta}_{S^c}\|_1,$$

which in turn yields

$$\begin{aligned} \frac{1}{2}\kappa v(\eta_*^2, \theta_*)\|\tilde{\Delta}\|_2^2 &\leq \frac{3\lambda_n}{2}\|\tilde{\Delta}_S\|_1 - \frac{\lambda_n}{2}\|\tilde{\Delta}_{S^c}\|_1 \\ &\leq \frac{3\lambda_n}{2}\sqrt{s}\|\tilde{\Delta}\|_2, \end{aligned}$$

and further

$$\|\tilde{\Delta}\|_2 \leq \frac{3\lambda_n}{\kappa v_*(\eta_*^2, \theta_*)}\sqrt{s}. \quad (\text{F.8})$$

Note that $R_{\cdot j}$ has iid normal entries with mean zero and variance r_n , where

$$\begin{aligned} r_n &\equiv r_n(\eta_*^2, \theta_*, \eta_n^2, \theta_n) \\ &:= \left[(1 - \theta_*) \frac{1 + (q - 2)\theta_n}{1 + (q - 1)\theta_n} - (\theta_n - \theta_*) \frac{1 - \theta_n}{(1 + (q - 1)\theta_n)^2} \right] \frac{\eta_*^2}{(\eta_n^2)^2} \frac{1}{(1 - \theta_n)^2}. \end{aligned} \quad (\text{F.9})$$

On \mathcal{C}_0 , by (C.5), r_n satisfies

$$\begin{aligned} (\eta_*^2)^2(1 - \theta_*)^2 r_n &\leq [(1 - \theta_*) + |\theta_n - \theta_*|] \frac{(\eta_*^3)^3 (1 - \theta_*)^2}{(\eta_n^2)^2 (1 - \theta_n)^2} \\ &\leq 2\eta_*^2(1 - \theta_*). \end{aligned}$$

As in the proof of Theorem 2, we define the events

$$\mathcal{C}_j = \left\{ \frac{1}{n} \|X^T R_{\cdot j}\|_\infty \leq \sqrt{d_n \frac{t + 2 \log p}{n}} \right\},$$

$$\mathcal{C} = \cap_{j=1}^q \mathcal{C}_j,$$

where $d_n := \frac{2}{\eta_*^2(1-\theta_*)}$. Since $\mathbb{P}(\mathcal{C}_j^c | \mathcal{C}_0) \leq 2 \exp(-t/2)$ by Lemma 6.2 of Bühlmann and Van De Geer [2] and Assumption (C1)–(C2), and (C4), we have

$$\mathbb{P}(\mathcal{C} | \mathcal{C}_0) = \mathbb{P}(\cap_{j=1}^q \mathcal{C}_j | \mathcal{C}_0) \geq 1 - \sum_{j=1}^q \mathbb{P}(\mathcal{C}_j^c | \mathcal{C}_0) \geq 1 - 2q \exp(-t/2).$$

Recall that $\lambda_n = 8\sqrt{d_n \log(pq)/n}$. Thus, again letting $t = 4 \log q + 2 \log p$, we have

$$\mathbb{P}(\lambda_n \geq 4 \|\bar{X}^T \bar{R}\|_\infty | \mathcal{C}_0) \geq 1 - 2 \exp(-\log(pq)),$$

which in turn yields,

$$\begin{aligned} \mathbb{P}(\lambda_n \geq 4 \|\bar{X}^T \bar{R}\|_\infty) &\geq (1 - 2 \exp(-\log(pq)))(1 - k_1 \exp(-k_2 \log(pq))) \\ &\geq 1 - (2 + k_1) \exp(-\log(pq)), \end{aligned} \tag{F.10}$$

due to Assumption (C4). Combining (F.10) and (F.8) completes the proof with $c_4 = k_1 + 2$, $c_5 = 1$, $c_6 = 24\sqrt{2}$. \square

Appendix G. Simulations for comparison of tuning parameter selection procedure

In this section, we conduct simulations that support the tuning parameter selection procedures introduced in Section 6. Throughout this section, we follow the same data generating procedure used in Section 7 (see (16) and the following paragraph).

Appendix G.1. Selection procedures comparison for MRCS, ap.MRCS

We set $s_1 = s_2 = 0.1$ and $\eta_i = 1$ for all $i \in \{1, \dots, q\}$, $(p, q) \in \{(20, 50), (50, 20)\}$. For MRCS-Or, MRCS (which is excluded in $(p, q) = (50, 20)$), and ap.MRCS, we compared the approximate Gaussian validation likelihood minimization [GVLM] to the validation prediction error minimization [VPEM], where the validation prediction error is computed by $\sum_{k=1}^K \|Y_k - X_k \hat{B}_{-k}\|_F^2$ (see Section 6 for the definition of K , B_{-k} , Y_k and X_k). For both procedures, we select each tuning parameter with 5 fold cross validation from $\lambda \in \Lambda$, where $\Lambda = \{10^{-4+0.5k} : k = 0, 1, \dots, 14\}$.

As shown in Figure G.1a and G.1b, VPEM struggled especially with large θ values. As opposed to VPEM, GVLM did not suffer the same issue. TPR does not show any difference between VPEM and GVLM but all estimator improves as θ increases (see Figure G.1d. However, with respect to TNR, GVLM has better TNR results than VPEM (see Figure G.1c).

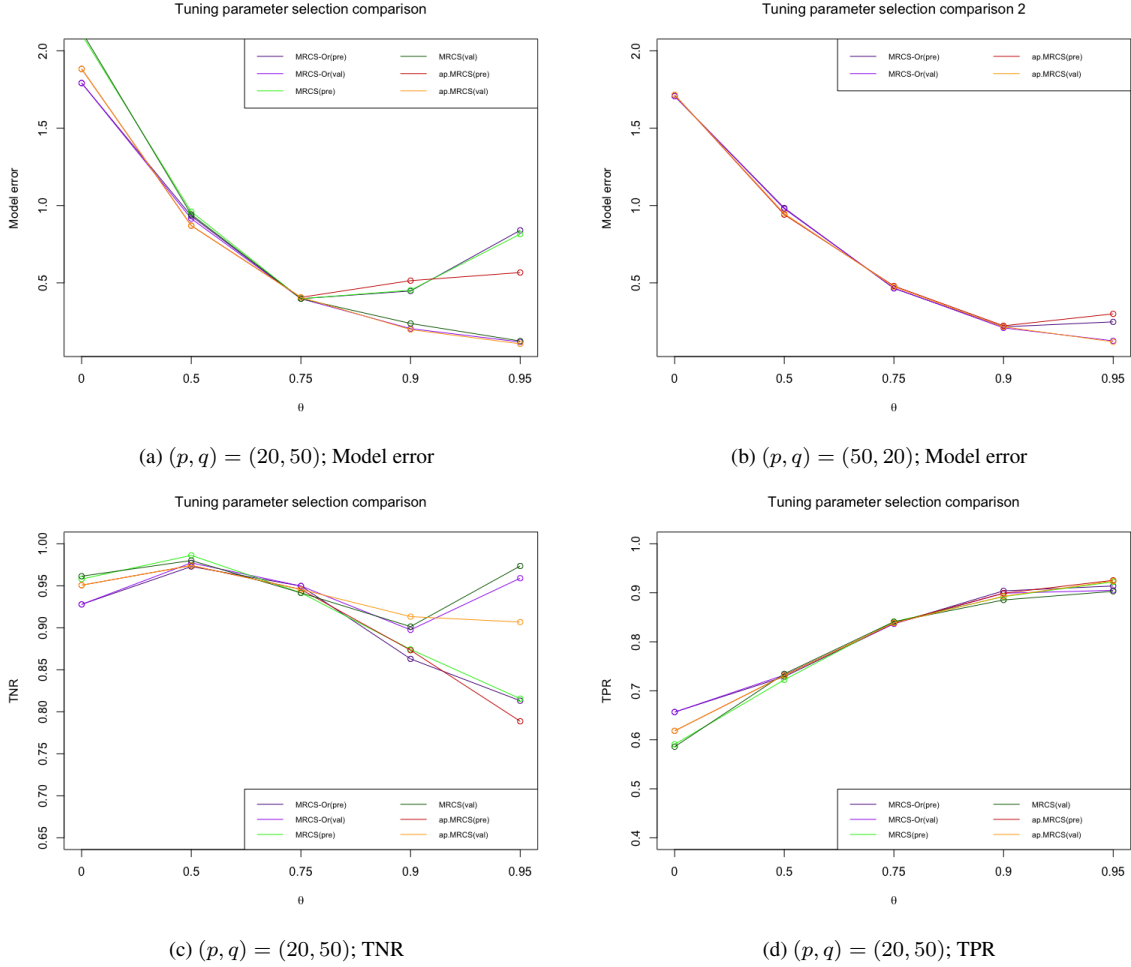


Figure G.1: Comparison of tuning parameter selection procedures: The setting is from Section 7.1 where $s_1 = s_2 = 0.1$, $\eta = 1$, $\theta \in \{0, 0.5, 0.75, 0.9, 0.95\}$, $(p, q) = (20, 50)$ or $(50, 20)$, $n = 50$. “pre” stands for the prediction loss [VPEM], and “val” denotes the approximate Gaussian validation likelihood used for cross validation [GVLM]. We graphed the model error, $\text{tr}[(\hat{B} - B)^T \Sigma_X (\hat{B} - B)]$, TNR and TPR of each procedure with varying θ . The results are based on 50 independent replications.

Appendix G.2. Selection procedures comparison for MRGCS, ap.MRGCS

In addition to the tuning parameter selection procedure (15), one might also consider using the estimated parameters from the output of ap.MRGCS, which is given by

$$\hat{\lambda} = \arg \min_{\lambda \in \Lambda} \sum_{k=1}^K \text{tr} \left\{ n^{-1} (Y_k - X_k \hat{B}_{-k})' (Y_k - X_k \hat{B}_{-k}) \hat{\Sigma}_{-k}^{-1} \right\},$$

where

$$\hat{\Sigma}_{-k} = \text{diag}(\{\hat{\eta}_{-k,i}\}_{i=1}^q) \left[(1 - \hat{\theta}_{-k}) I_q + \hat{\theta}_{-k} \mathbf{1}_q \mathbf{1}_q' \right] \text{diag}(\{\hat{\eta}_{-k,i}\}_{i=1}^q).$$

In the preceding displays, $\hat{\eta}_{-k,i}, \hat{\theta}_{-k}$ are computed from Step 1 of Algorithm 4.1 based on the subsample that excludes the k th fold. However, as noted in Section 6, we still suggest using (15) for the optimal tuning parameter selection procedure for MRGCS and ap.MRGCS. We validate this proposal through the following simulations.

We still use the same setting as in Section Appendix G.1 except that we used (22) and (23) for η_i 's for each $(p, q) = (50, 20), (20, 50)$. We compared the two approximate Gaussian validation likelihood loss criteria (for each ap.MRCS and ap.MRGCS output) to VPEM for MRCS-Or, MRGCS (it is excluded in $(p, q) = (50, 20)$), and ap.MRGCS.

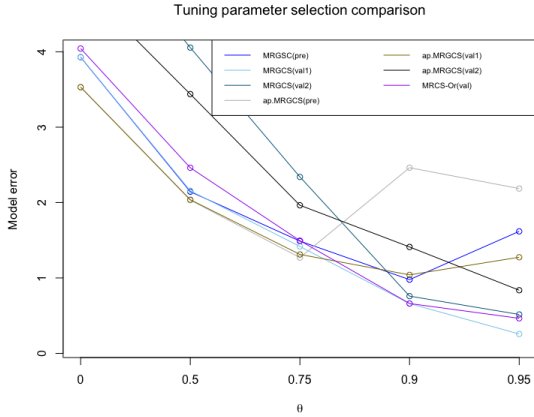
In Figure G.2a and G.2b, the output of ap.MRGCS used in GVLM was even unstable compared with its VPEM. Generally, the ap.MRCS output outperformed the others for both MRGCS and ap.MRGCS. In TPR (see Figure G.2d), all procedure improves as θ increases, but the output of ap.MRCS showed better TPR than that of ap.MRGCS. As opposed to TPR, ap.MRGCS output showed better TNR (see Figure G.2c). This indicates that ap.MRGCS output tends to provide a sparse solution. However, using ap.MRCS output is preferred after considering all model error, TNR, and TPR.

Appendix H. Additional simulations

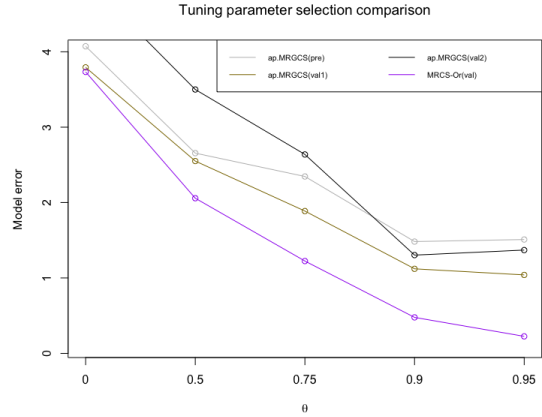
Appendix H.1. Supplement to Setting I: Low-dimensional simulation

We follow the same simulation setup as in (16)–(18) (see Section 7.1) except that we use $p = q = 20$. The complete results are in Figure H.3–H.6.

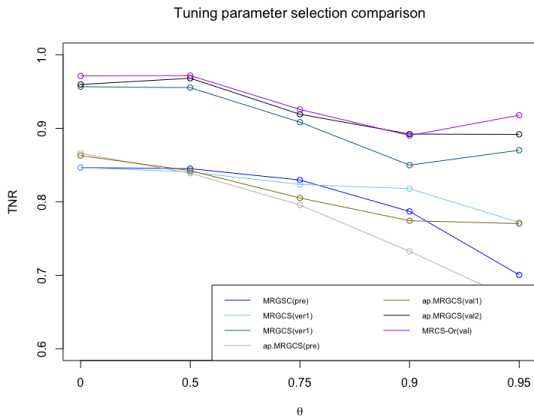
Generally, all our equicorrelation based estimators outperformed lasso estimators as well as MRCE and ap.MRCE. As θ increases, all our estimators improve. ap.MRGCS slightly suffered $(s_1, s_2) = (0.5, 0.1)$. This is also a common phenomenon in other simulations regardless of p, q (see Section 7.1, 7.2, and Appendix H.2). Among the competitors, MRCS and ap.MRCS were the best non-oracle methods. MRCE and ap.MRCE performed decently as $s_1 s_2$ increases, especially, when $(s_1, s_2) = (0.5, 1)$. MRCE and ap.MRCE were the worst two methods in TNR. All joint optimization methods improve in TPR as θ gets increased.



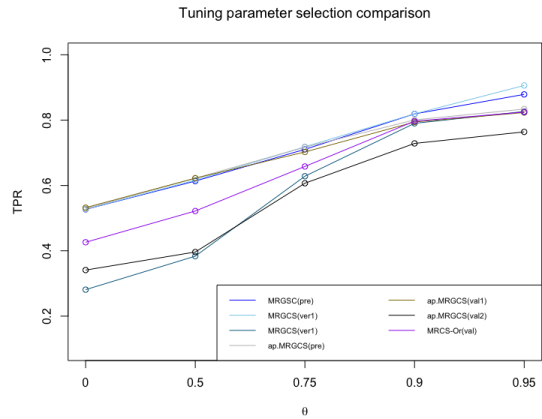
(a) $(p, q) = (20, 50)$; Model error



(b) $(p, q) = (50, 20)$; Model error



(c) $(p, q) = (20, 50)$; TNR



(d) $(p, q) = (20, 50)$; TPR

Figure G.2: Comparison of tuning parameter selection procedures: The setting is from Section 7.2 where $s_1 = s_2 = 0.1$, $\theta \in \{0, 0.5, 0.75, 0.9, 0.95\}$, $(p, q) = (20, 50)$ or $(50, 20)$, $n = 50$ (see Section 7.2 for the corresponding η_i values). “pre” stands for the prediction loss, “val1” denotes the approximate Gaussian validation likelihood procedure using ap.MRCS-based covariance, and “val2” denotes the approximate Gaussian validation likelihood procedure using ap.MRGSC-based covariance. We graphed model error, TNR and TPR of each procedure while varying θ . The results are based on 50 independent replications.

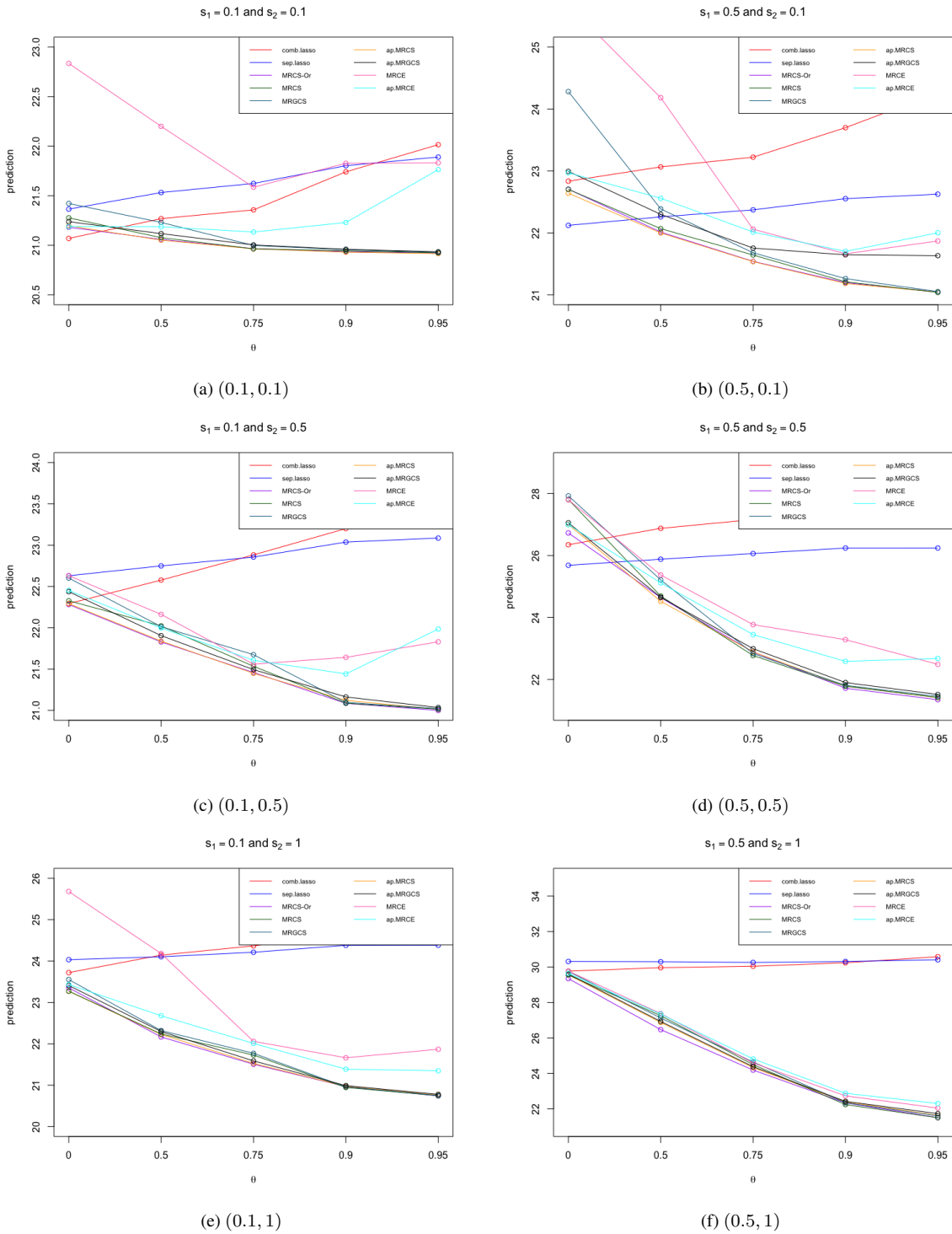


Figure H.3: Prediction plots: Two numbers in each bracket stand for (s_1, s_2) when $(p, q) = (20, 20)$.

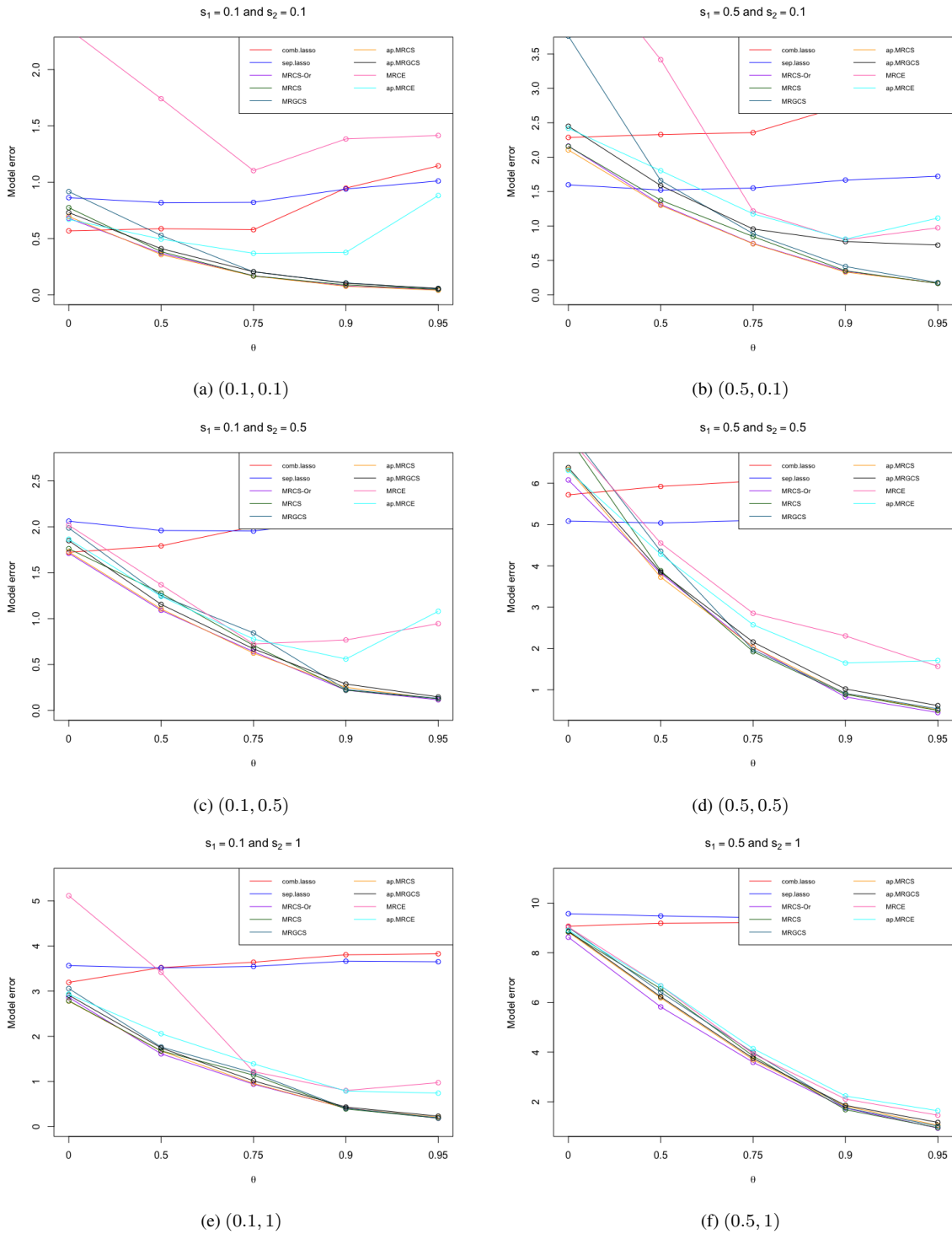


Figure H.4: Model error plots: Two numbers in each bracket stand for (s_1, s_2) when $(p, q) = (20, 20)$.

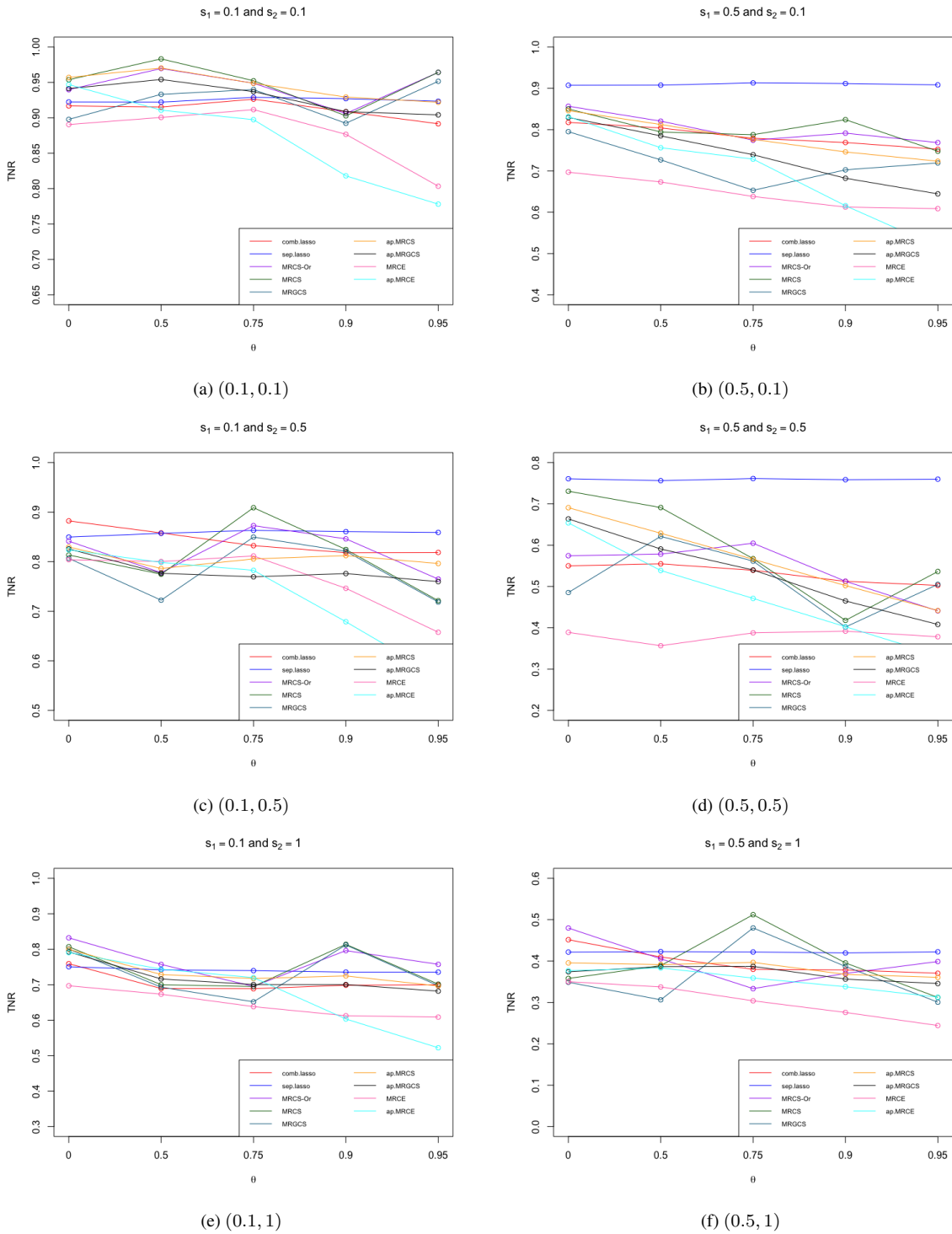


Figure H.5: TNR plots: Two numbers in each bracket stand for (s_1, s_2) when $(p, q) = (20, 20)$.

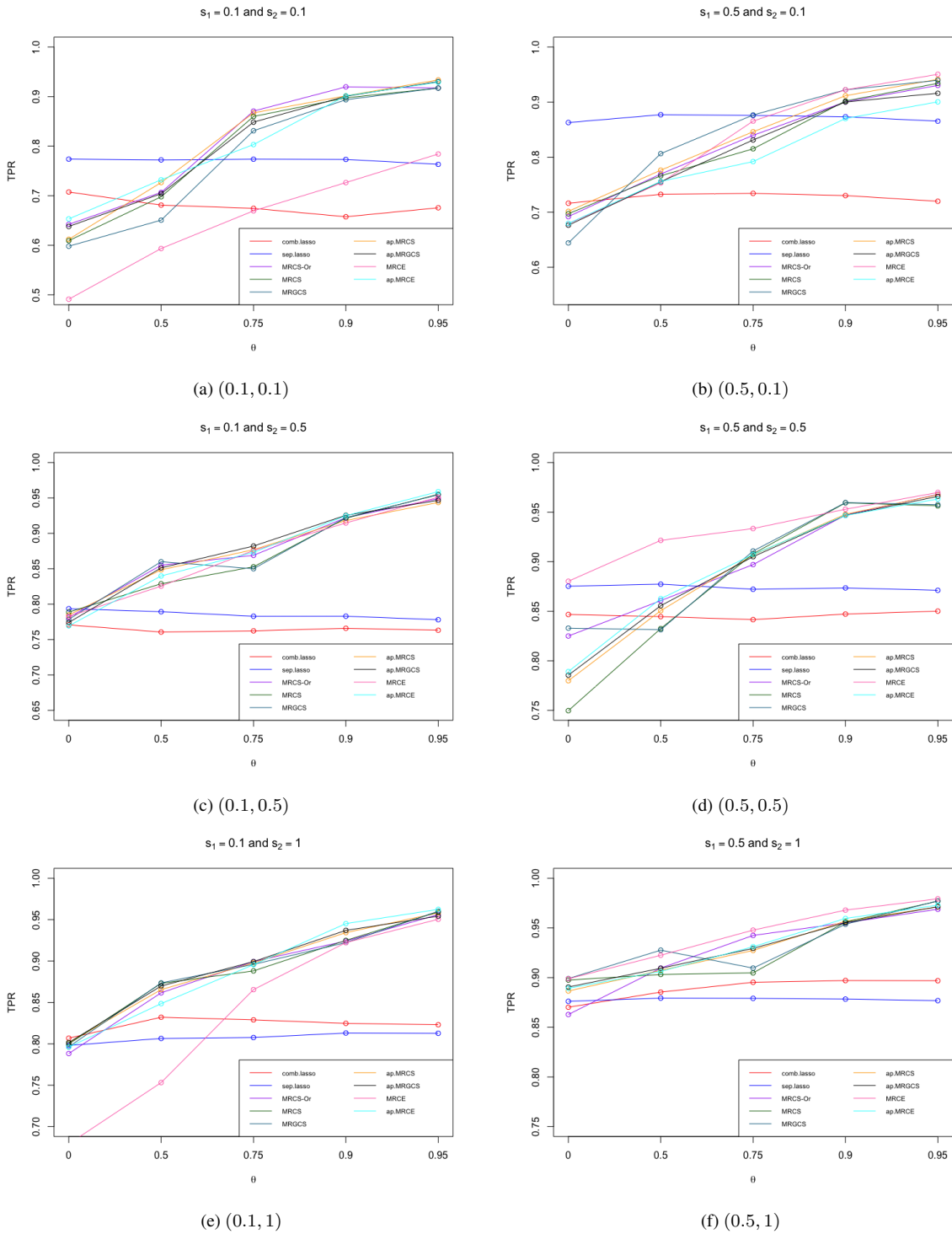


Figure H.6: TPR plots: Two numbers in each bracket stand for (s_1, s_2) when $(p, q) = (20, 20)$.

Appendix H.2. Supplement to Setting II: Equicorrelation of Σ_ with Heterogeneous and symmetrically distributed η_i 's*

We follow the same simulation setup as in Section 7.2 except that we used the following symmetric marginal variances:

$$\begin{aligned} \eta_1, \dots, \eta_5 &= 1/\sqrt{3}, \eta_6, \dots, \eta_{10} = 1/\sqrt{2}, \eta_{11}, \dots, \eta_{15} = 1/\sqrt[4]{3}, \eta_{16}, \dots, \eta_{20} = 1/\sqrt[4]{2}, \\ \eta_{21}, \dots, \eta_{30} &= 1, \eta_{31}, \dots, \eta_{35} = \sqrt[4]{2}, \eta_{36}, \dots, \eta_{40} = \sqrt[4]{3}, \eta_{41}, \dots, \eta_{45} = \sqrt{2}, \eta_{46}, \dots, \eta_{50} = \sqrt{3}, \end{aligned} \quad (\text{H.1})$$

when $(p, q) = (20, 50)$, and

$$\begin{aligned} \eta_1, \dots, \eta_4 &= 1/\sqrt{3}, \eta_5, \dots, \eta_8 = 1/\sqrt{2}, \eta_9, \dots, \eta_{12} = 1, \\ \eta_{13}, \dots, \eta_{16} &= \sqrt{2}, \eta_{17}, \dots, \eta_{20} = \sqrt{3}, \end{aligned} \quad (\text{H.2})$$

when $(p, q) = (50, 20)$. Lastly, when $(p, q) = (80, 80)$, we considered

$$\begin{aligned} \eta_1, \dots, \eta_{10} &= 1/\sqrt{3}, \eta_{11}, \dots, \eta_{20} = 1/\sqrt{2}, \eta_{21}, \dots, \eta_{30} = 1/\sqrt[4]{3}, \eta_{31}, \dots, \eta_{40} = 1/\sqrt[4]{2} \\ \eta_{41}, \dots, \eta_{50} &= \sqrt[4]{2}, \eta_{51}, \dots, \eta_{60} = \sqrt[4]{3}, \eta_{61}, \dots, \eta_{70} = \sqrt{2}, \eta_{71}, \dots, \eta_{80} = \sqrt{3}. \end{aligned} \quad (\text{H.3})$$

Appendix H.2.1. Results when $(p, q) = (20, 50)$

The complete results are in Figure H.7–H.10. MRGCS was the best non-oracle and ap.MRGCS was the second-best. In addition, MRCS and ap.MRCS performed well, even if they assume compound symmetry. This may be due to the symmetrically distributed variances, η_i ($i \in \{1, \dots, q\}$), which are likely to smooth out the heterogeneous variance effect. ap.MRCE performed substantially worse than our equicorrelation based estimators. TNR of ap.MRCE was also significantly worse than the others.

Appendix H.2.2. Results when $(p, q) = (50, 20)$

The complete results are in Figure H.11–H.14. The results are similar to those in Section 7.2.2. ap.MRGCS still struggled with $(s_1, s_2) = (0.5, 0.1)$, but it was the best non-oracle estimator among the non-oracle procedures. In general, ap.MRGCS and ap.MRCS outperformed the others.

Appendix H.2.3. Results when $(p, q) = (80, 80)$

The complete results are in Figure H.15–H.18. The results are similar to those in Section 7.2.3, except that ap.MRCE showed substantially poor performance compared with our methods. ap.MRGCS again struggled with $(s_1, s_2) = (0.5, 0.1)$, and it was even outperformed by separate lasso at all θ values. However, except for this case, ap.MRGCS and ap.MRCS showed the best non-oracle performance.

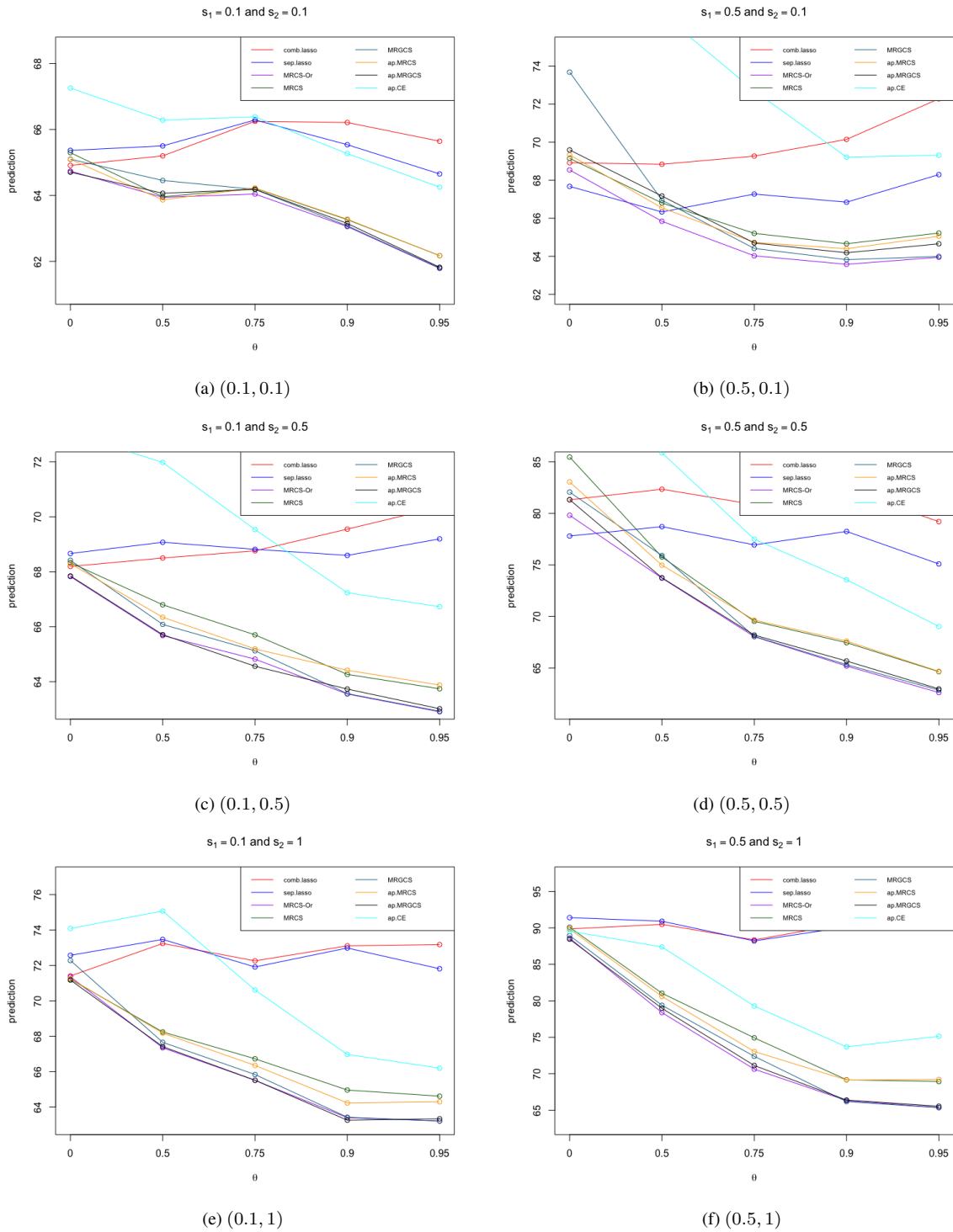


Figure H.7: Prediction plots: Two numbers in each bracket stand for (s_1, s_2) when $(p, q) = (20, 50)$.

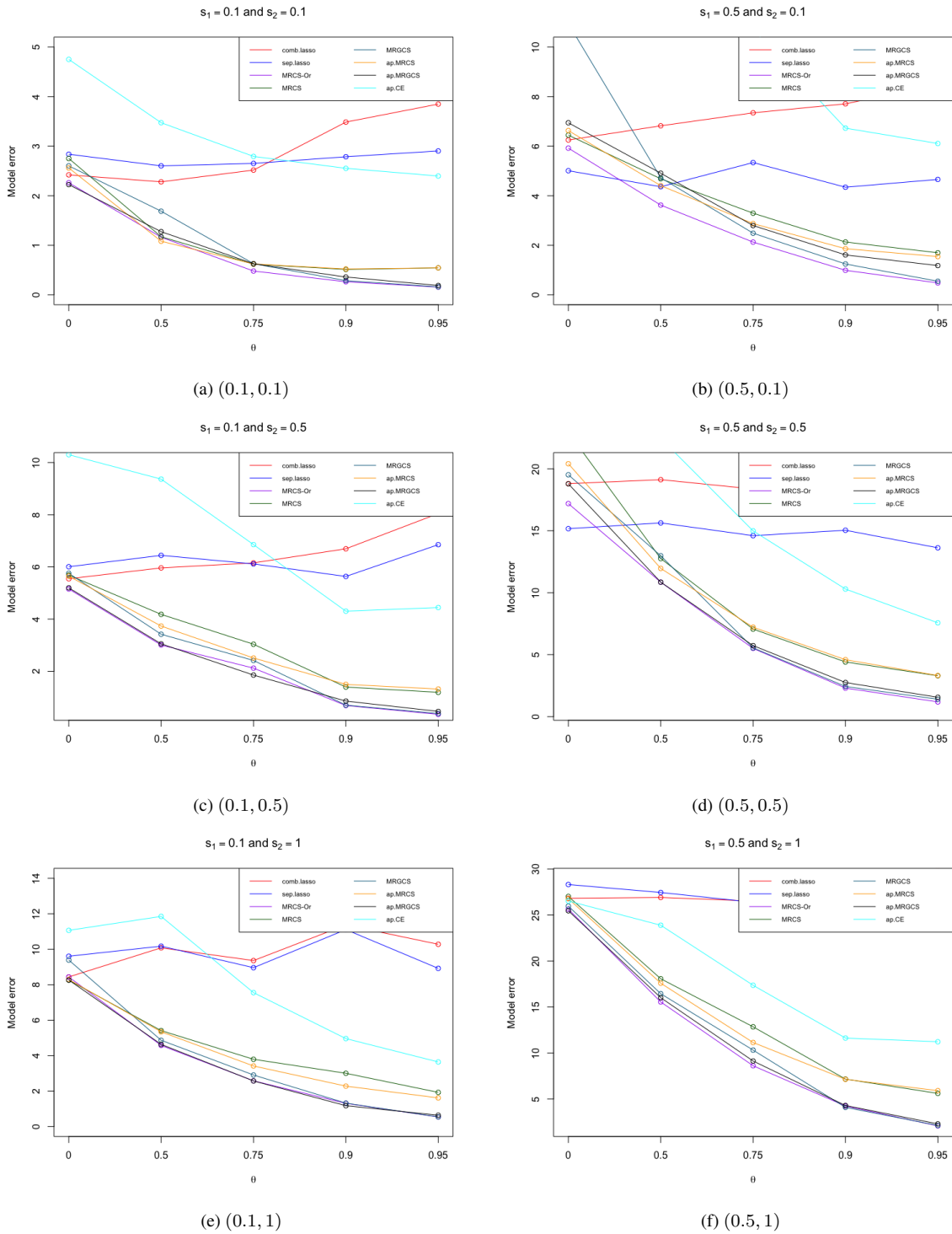


Figure H.8: Model error plots: Two numbers in each bracket stand for (s_1, s_2) when $(p, q) = (20, 50)$.

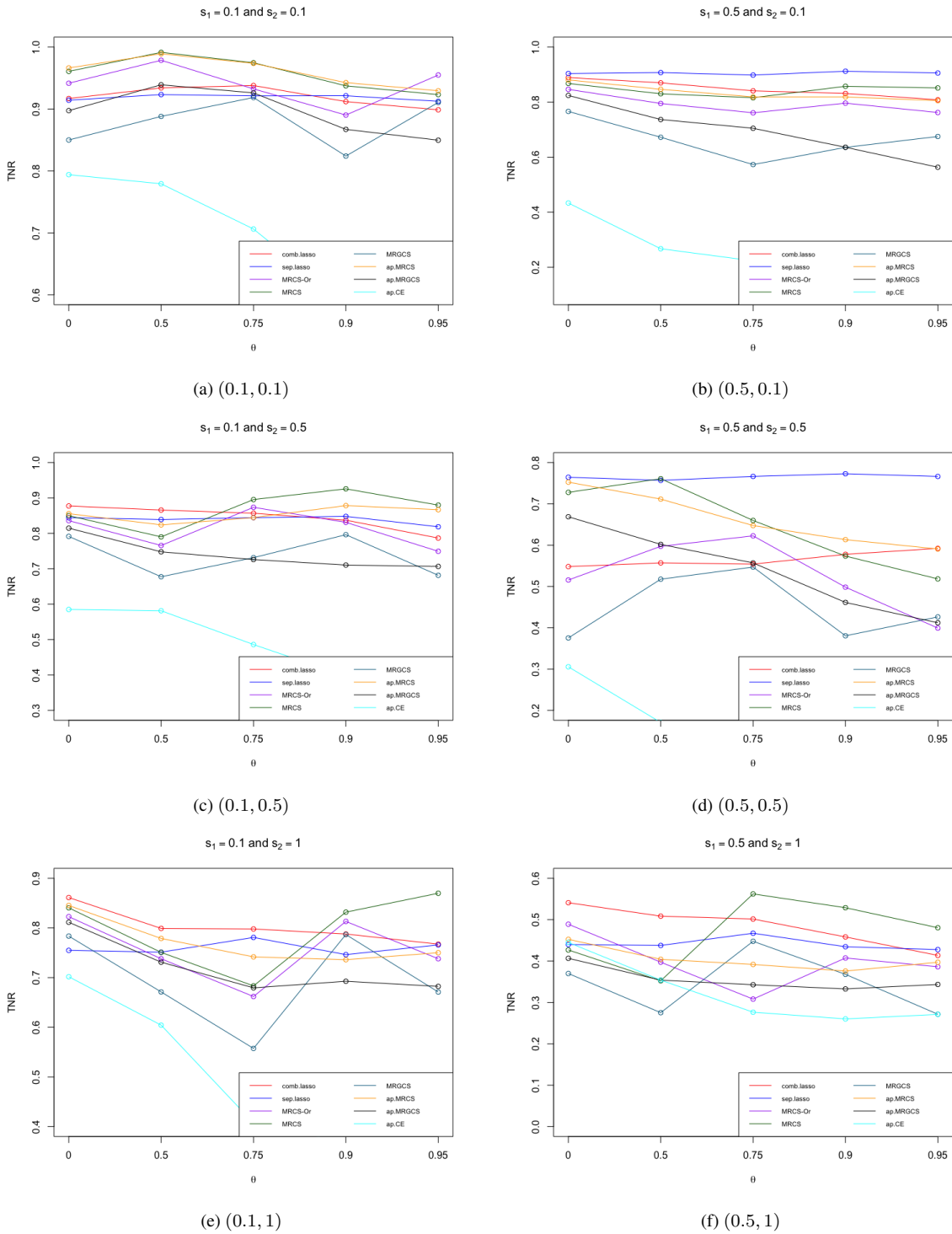


Figure H.9: TNR plots: Two numbers in each bracket stand for (s_1, s_2) when $(p, q) = (20, 50)$.

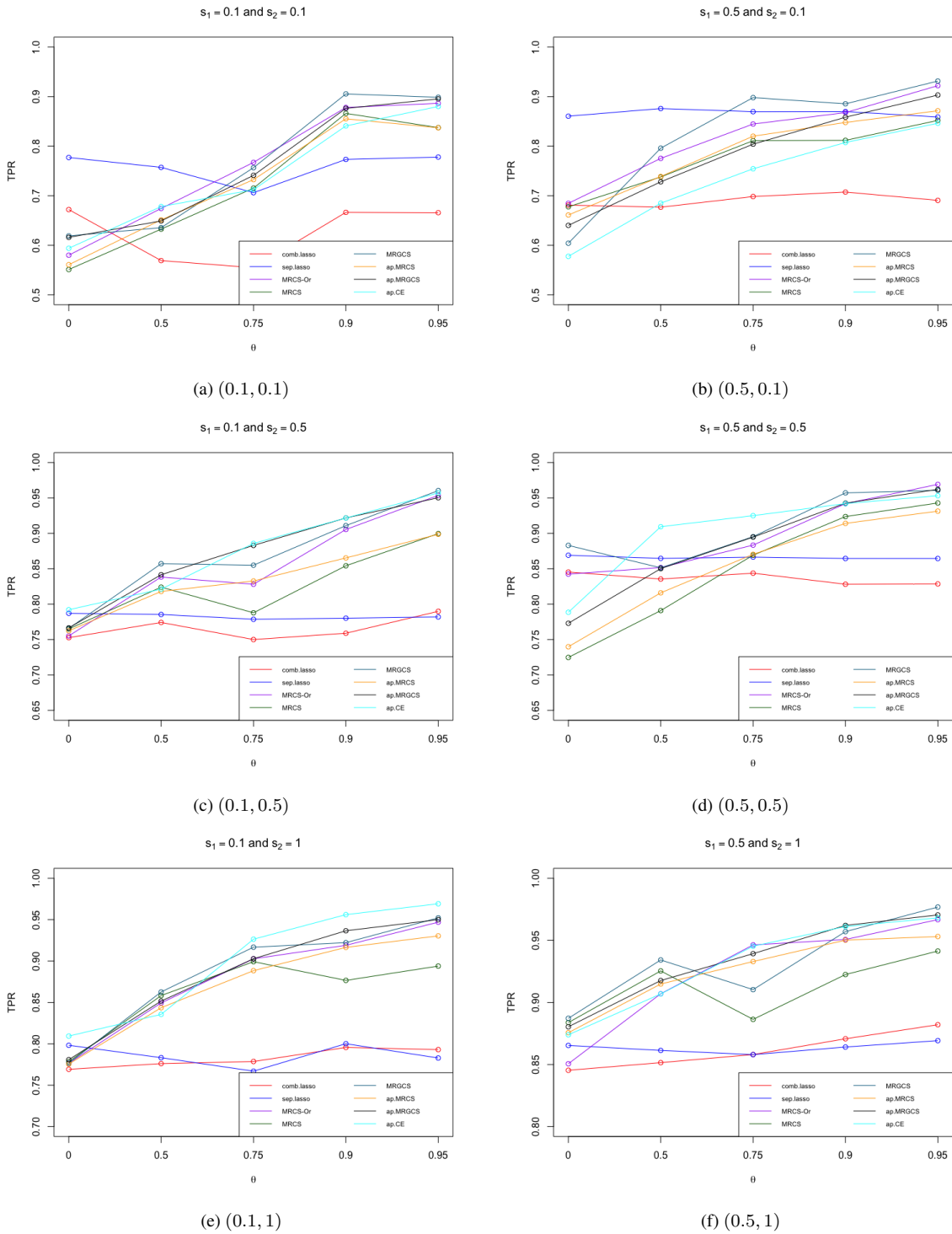


Figure H.10: TPR plots: Two numbers in each bracket stand for (s_1, s_2) when $(p, q) = (20, 50)$.

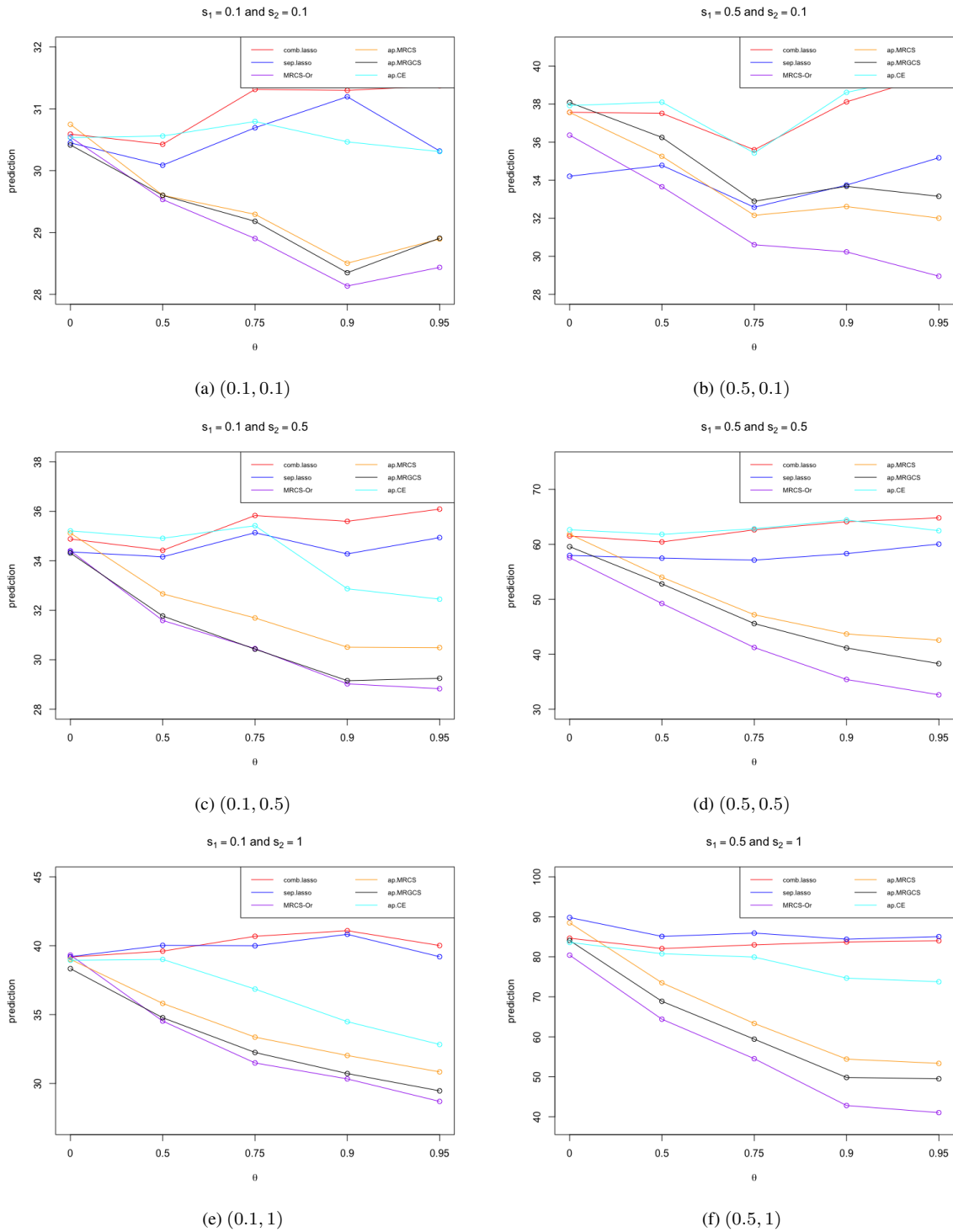


Figure H.11: Prediction plots: Two numbers in each bracket stand for (s_1, s_2) when $(p, q) = (50, 20)$.

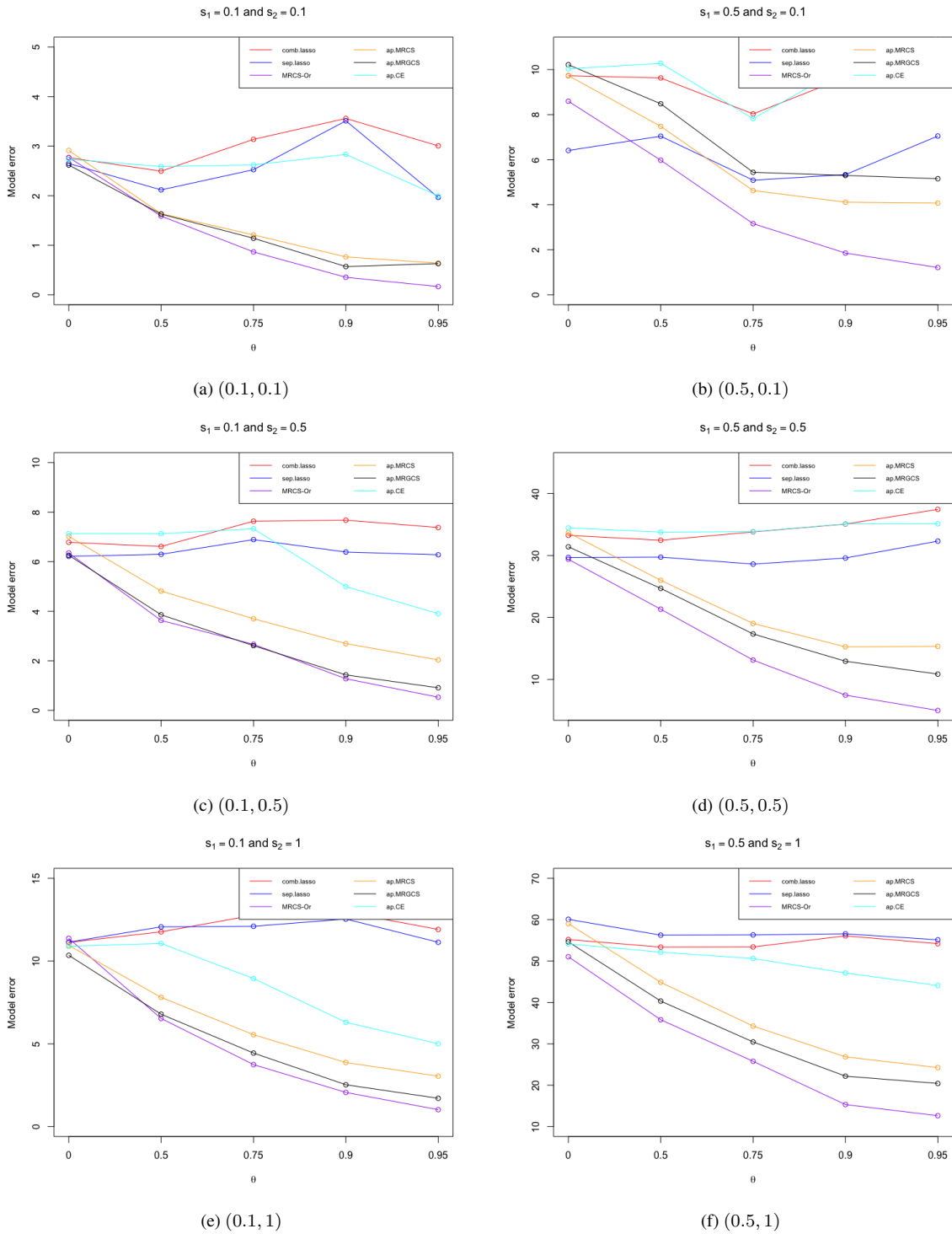


Figure H.12: Model error plots: Two numbers in each bracket stand for (s_1, s_2) when $(p, q) = (50, 20)$.

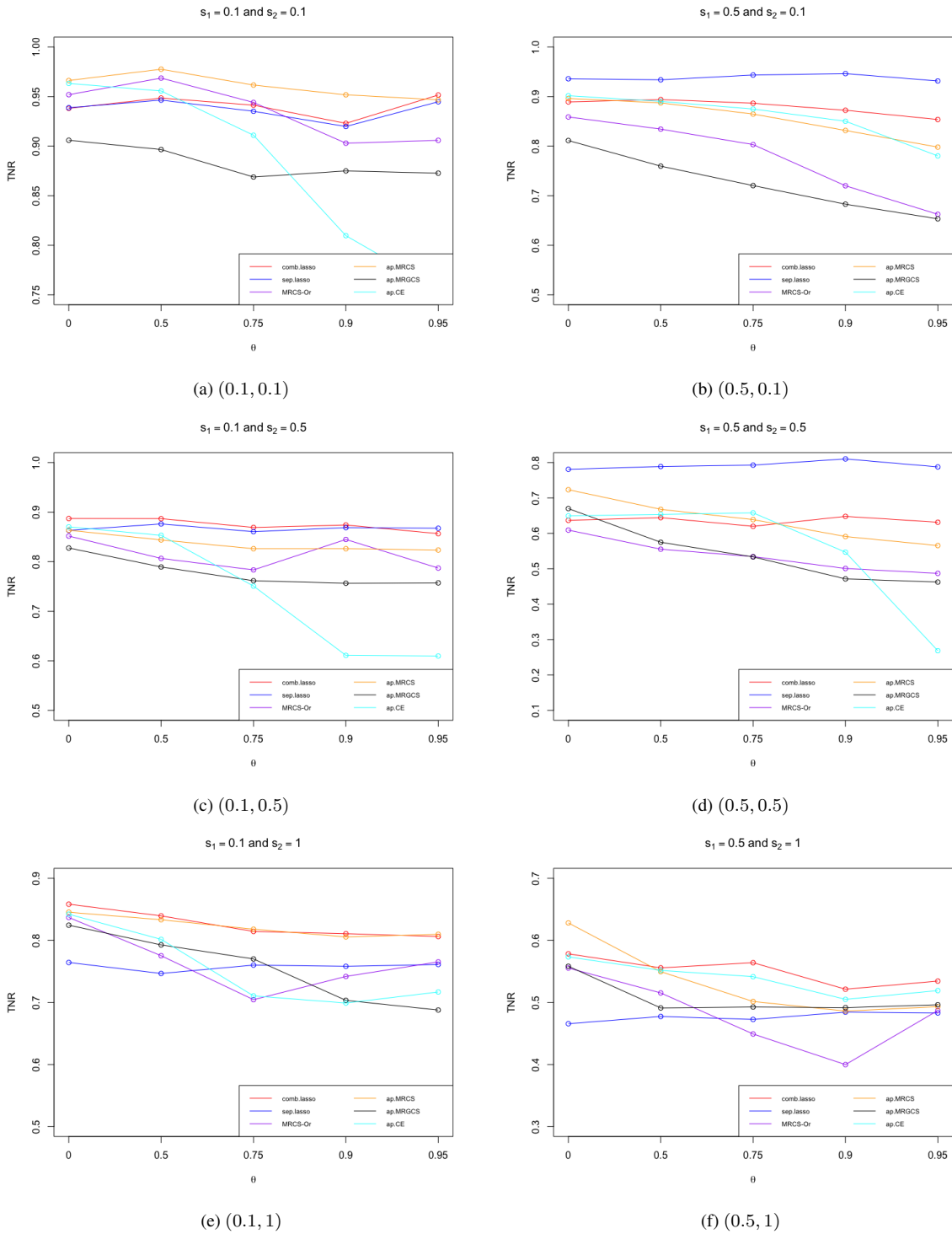


Figure H.13: TNR plots: Two numbers in each bracket stand for (s_1, s_2) when $(p, q) = (50, 20)$.

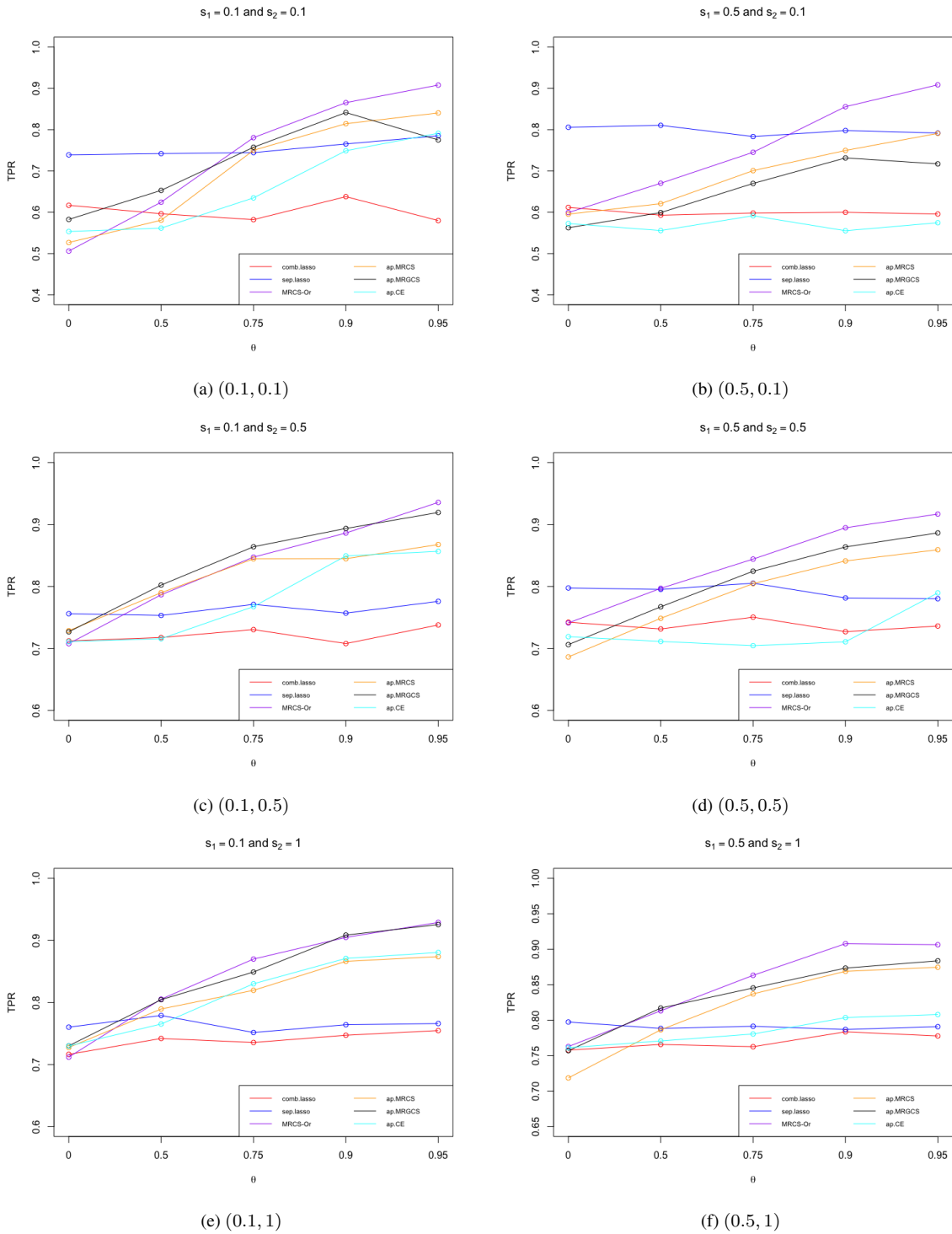
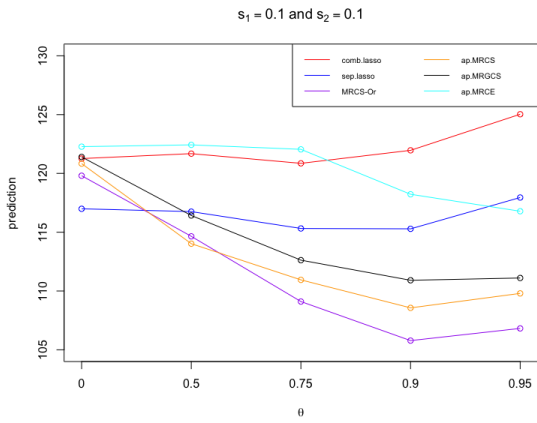
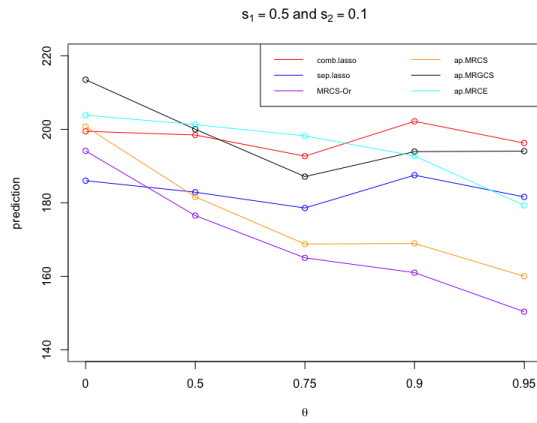


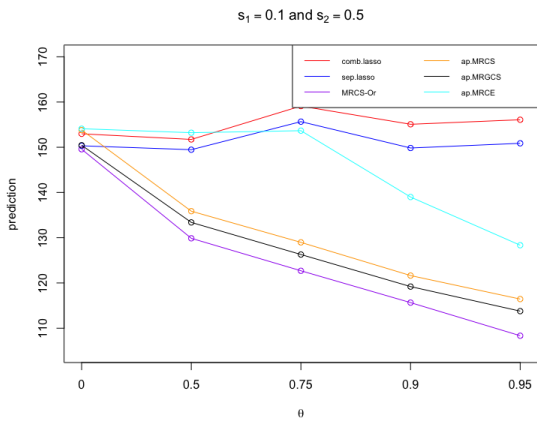
Figure H.14: TPR plots: Two numbers in each bracket stand for (s_1, s_2) when $(p, q) = (50, 20)$.



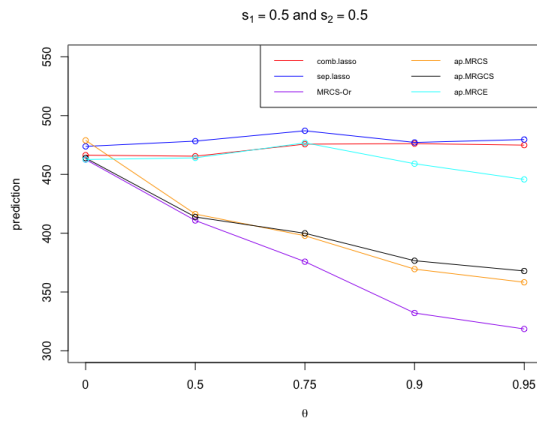
(a) (0.1, 0.1)



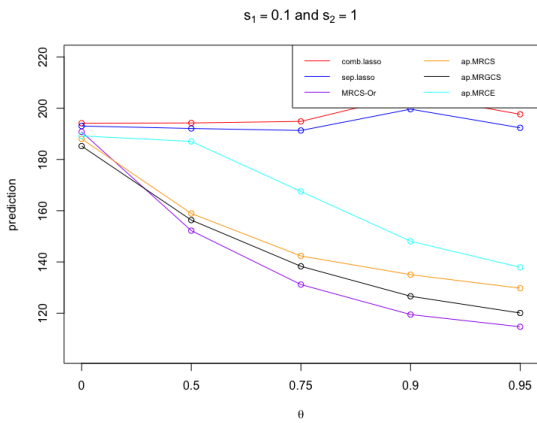
(b) (0.5, 0.1)



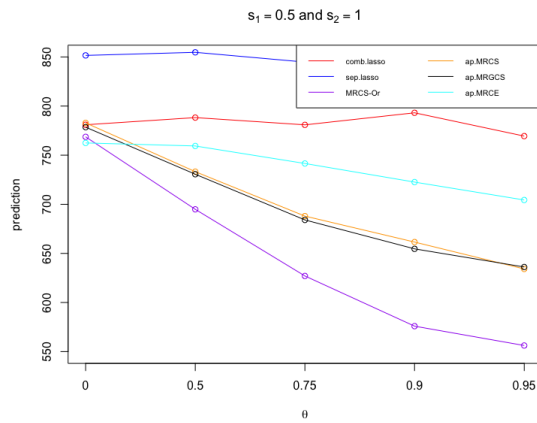
(c) (0.1, 0.5)



(d) (0.5, 0.5)



(e) (0.1, 1)



(f) (0.5, 1)

Figure H.15: Prediction plots: Two numbers in each bracket stand for (s_1, s_2) when $(p, q) = (80, 80)$.

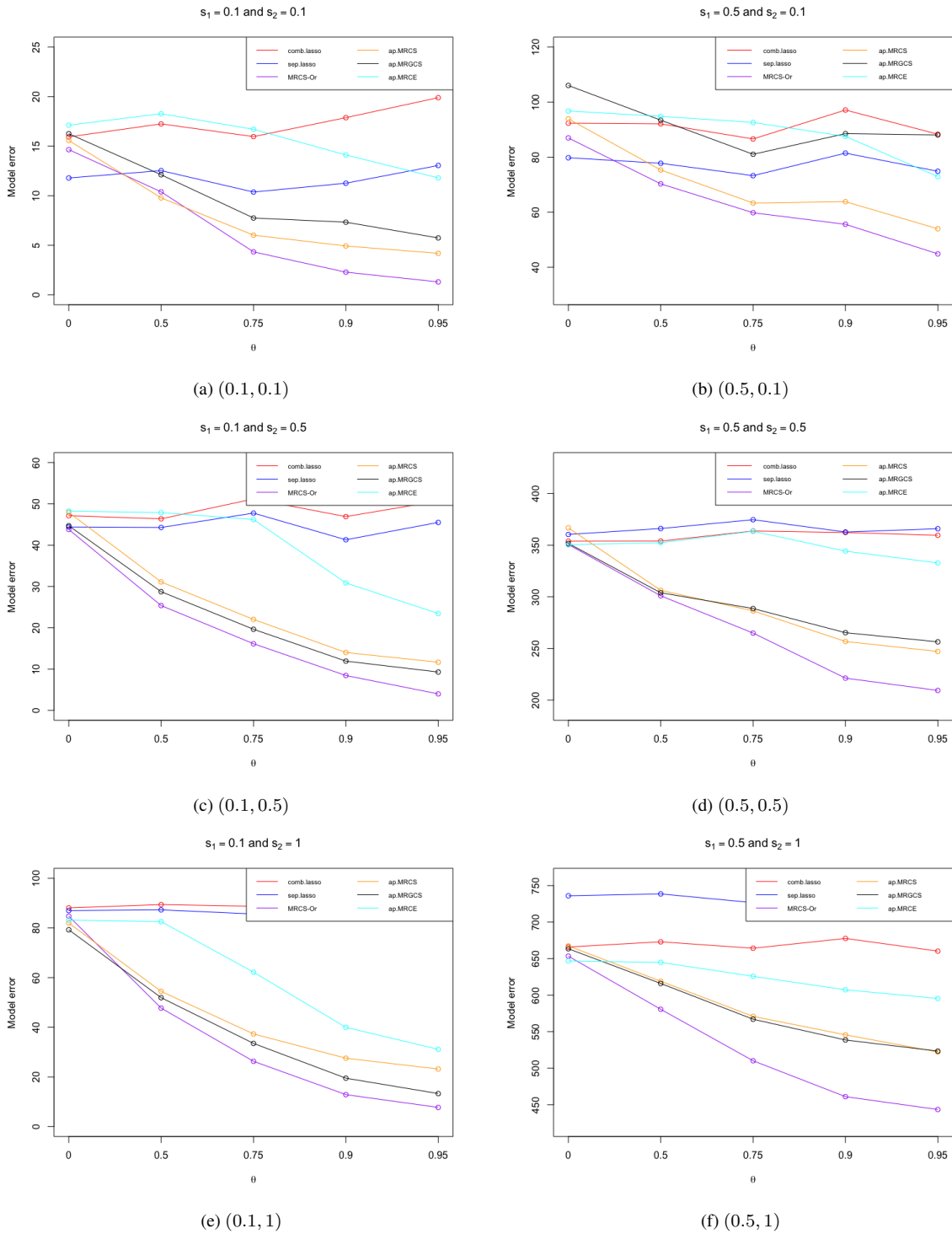


Figure H.16: Model error plots: Two numbers in each bracket stand for (s_1, s_2) when $(p, q) = (80, 80)$.

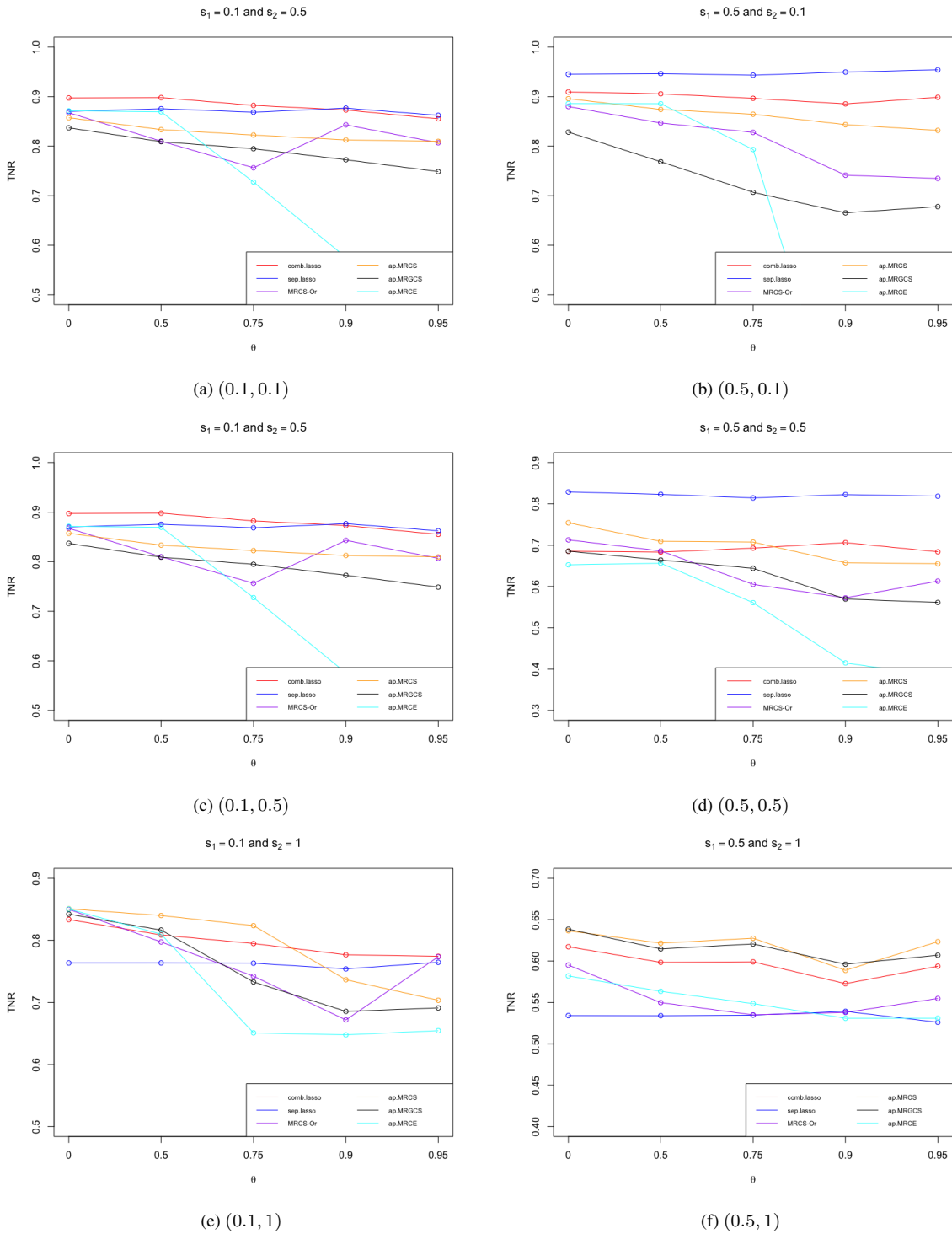


Figure H.17: TNR plots: Two numbers in each bracket stand for (s_1, s_2) when $(p, q) = (80, 80)$.

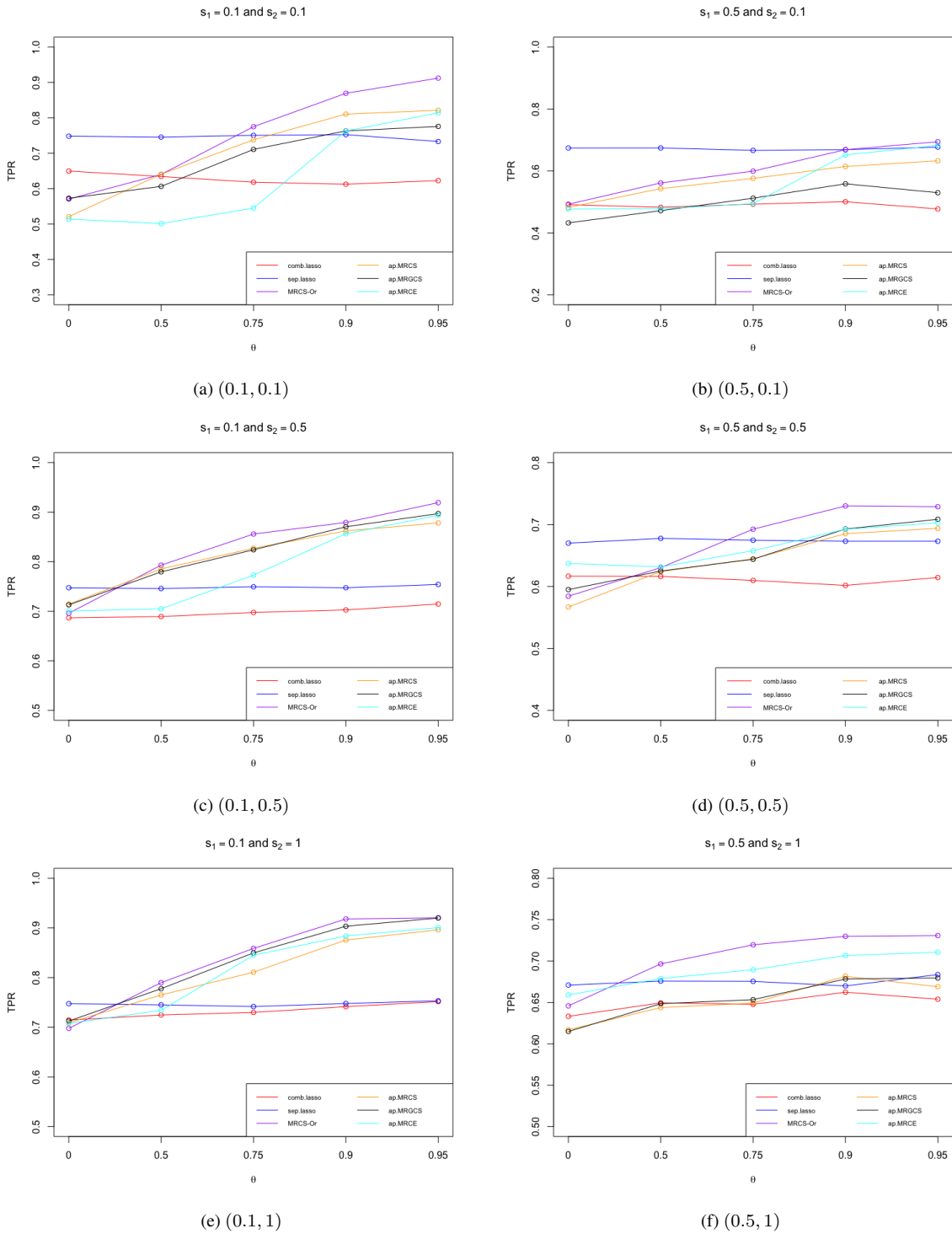


Figure H.18: TPR plots: Two numbers in each bracket stand for (s_1, s_2) when $(p, q) = (80, 80)$.

Appendix H.3. Additional simulations to Section 8.2

We use the same data generating process in Section 8.2 (see (25)) except that we consider different procedure for generating the diagonal matrix D in (25). In this section, we generated diagonals of D through iid draws from a chi-square distribution, which leads to a diagonally dominant Σ_* . The following is the condition numbers for each setting:

- When $(p, q) = (20, 50)$
 - D constructed upon iid $\chi^2(1)$ draws: 1336.829 / 420.5613 / 449.145 (setting A2 / B2 / C2 according to $w = 1/0.5/0.05$)
 - D constructed upon iid $\chi^2(3)$ draws: 71.66033 / 134.6858 / 394.8582 (setting D2 / E2 / F2 according to $w = 1/0.5/0.05$)
- When $(p, q) = (50, 20)$
 - D constructed upon iid $\chi^2(1)$ draws: 832.5564 / 184.3252 / 180.9868 (setting G2 / H2 / I2 according to $w = 1/0.5/0.05$)
 - D constructed upon iid $\chi^2(3)$ draws: 45.09728 / 48.67809 / 149.5864 (setting J2 / K2 / L2 according to $w = 1/0.5/0.05$)

Again, we note that a $q \times q$ compound symmetry matrix with $q = 50$ (resp. $q = 20$) and $\theta = 0.9$ has condition number 451 (resp. 181).

The complete results are in Table H.3–H.6, and they are similar to the results in Section 8.2. We use the same sub-setting notation from A2 to L2 as in Section 8.2. The oracle estimator was generally the best, except for G2-3, J2-3, K2-3, where the sparsity is violated and the ridge methods performed the best. However, even when the corruption level is high, our equicorrelation based estimators generally showed comparable performance to lasso methods and frequently were the best non-oracle methods, when B_* has sparsity. MRCS and ap.MRCS still showed competitive performance to MRGCS and ap.MRGCS.

Appendix I. Tables and figures

| Prediction error comparison table: Setting A2-F2 | | | | | | | | | | | |
|--|------------------------|------------------------|-------------------------------|-------------------------------|------------------------|------------------------|------------------------|------------------------------|-------------------------------|-----------------------------|------------------------|
| Design | OLS | LAS | LASP | c.ridge | s.ridge | ap.MRCE | MRCs-Or | MRCS | ap.MRCS | MRGCS | ap.MRGCS |
| A2-1 | 105.0715 (0.90149) | 78.79229 (0.35488) | 76.45057 (0.39873) | 84.4663 (0.40967) | 79.51207 (0.4522) | 90.18449 (0.49417) | 72.06984 (0.36046) | 84.04781 (0.47639) | 80.67247 (0.4649) | 81.59314 (0.47639) | 80.86959 (0.4649) |
| A2-2 | 104.62121 (0.76294) | 87.5176 (0.42496) | 90.19142 (0.47697) | 94.172 (0.47873) | 95.97215 (0.47486) | 87.86725 (0.44036) | 80.38446 (0.37276) | 87.58095 (0.43506) | 87.33436 (0.42998) | 87.81213 (0.43506) | 87.35972 (0.42998) |
| A2-3 | 105.02951 (0.76602) | 99.98116 (0.68208) | 103.14988 (0.71519) | 98.95046 (0.69429) | 100.2181 (0.67904) | 99.4692 (0.66999) | 96.4327 (0.63352) | 102.9058 (0.70861) | 101.93695 (0.64167) | 103.28047 (0.70861) | 102.08946 (0.64167) |
| B2-1 | 75.65611 (0.90073) | 56.90228 (0.35437) | 55.39336 (0.40303) | 62.02734 (0.39724) | 58.17915 (0.42282) | 63.11375 (0.47894) | 50.72981 (0.29174) | 56.4124 (0.45323) | 55.45088 (0.29716) | 58.04484 (0.45323) | 55.66515 (0.29716) |
| B2-2 | 73.78413 (0.88268) | 64.02048 (0.48114) | 64.55626 (0.4924) | 68.72112 (0.56445) | 69.41612 (0.56592) | 63.25231 (0.45225) | 55.59376 (0.31204) | 60.41139 (0.3497) | 60.19168 (0.39223) | 59.97346 (0.3497) | 60.34828 (0.39223) |
| B2-3 | 75.05742 (0.72402) | 71.5248 (0.64157) | 72.97053 (0.6741) | 70.28107 (0.59533) | 71.39136 (0.62579) | 70.17108 (0.58586) | 67.49098 (0.53642) | 70.89491 (0.64858) | 69.86035 (0.61208) | 70.5892 (0.64858) | 69.88786 (0.61208) |
| C2-1 | 45.69949 (1.11297) | 35.36147 (0.41784) | 33.49663 (0.39197) | 38.78865 (0.50628) | 35.49974 (0.47922) | 33.03231 (0.34002) | 28.54844 (0.27932) | 28.90827 (0.28021) | 28.94331 (0.28293) | 28.95225 (0.28021) | 29.13247 (0.28293) |
| C2-2 | 47.33275 (1.17134) | 40.75669 (0.62639) | 41.27053 (0.65807) | 44.88513 (0.77086) | 45.12465 (0.78301) | 35.05755 (0.51665) | 30.34744 (0.36232) | 30.4403 (0.35979) | 30.43892 (0.36076) | 30.5317 (0.35979) | 30.52386 (0.36076) |
| C2-3 | 48.03612 (1.2146) | 43.98291 (0.81084) | 44.6328 (0.80776) | 43.81589 (0.76541) | 44.13011 (0.78705) | 40.61786 (0.64727) | 37.09105 (0.5055) | 38.21206 (1.10625) | 37.59434 (0.90502) | 40.20935 (1.10625) | 39.438 (0.90502) |
| D2-1 | 276.13188 (1.88367) | 198.59586 (0.77651) | 197.13256 (0.95993) | 206.97201 (0.80589) | 200.13757 (0.93312) | 216.46769 (1.02253) | 190.67826 (0.63568) | 199.93753 (0.76923) | 199.54058 (0.84938) | 200.67057 (0.76923) | 200.14572 (0.84938) |
| D2-2 | 281.52534 (2.44137) | 225.09303 (1.02092) | 229.32895 (1.1545) | 229.17669 (0.96211) | 234.8962 (1.15356) | 225.714 (1.04621) | 214.27238 (0.881) | 220.43282 (1.00556) | 220.36244 (0.99778) | 222.32033 (1.00556) | 221.14247 (0.99778) |
| D2-3 | 273.4428 (1.85887) | 250.22042 (0.91029) | 260.06209 (0.91327) | 244.35205 (0.95593) | 249.28644 (1.0345) | 249.79425 (0.86324) | 242.98559 (0.80546) | 263.89819 (1.49318) | 257.34857 (1.10038) | 264.38402 (1.49318) | 257.61919 (1.10038) |
| E2-1 | 160.90386 (1.12376) | 120.88791 (0.65809) | 116.45597 (0.70934) | 126.2724 (0.75072) | 119.84545 (0.76023) | 133.08762 (0.79213) | 112.5294 (0.55642) | 120.74961 (0.59281) | 119.28996 (0.62913) | 119.2998 (0.59281) | 119.62929 (0.62913) |
| E2-2 | 161.12426 (1.23431) | 130.2945 (0.64501) | 135.11699 (0.75366) | 138.43316 (0.67923) | 141.62628 (0.74148) | 133.91633 (0.71979) | 123.78783 (0.60883) | 128.16975 (0.59831) | 128.14594 (0.59708) | 128.93577 (0.59831) | 128.53518 (0.59708) |
| E2-3 | 159.54963 (1.17964) | 151.26322 (0.85091) | 155.36816 (0.87853) | 147.18217 (0.71254) | 150.72091 (0.76721) | 150.27369 (0.77189) | 145.08906 (0.71307) | 154.4475 (1.16565) | 151.46421 (0.86897) | 155.31105 (1.16565) | 152.08549 (0.86897) |
| F2-1 | 54.84875 (1.11701) | 42.29454 (0.5066) | 40.23873 (0.46356) | 46.04544 (0.53677) | 42.35683 (0.50129) | 41.81673 (0.37382) | 35.38748 (0.32448) | 35.80085 (0.32965) | 35.92453 (0.33705) | 35.95849 (0.32965) | 36.22753 (0.33705) |
| F2-2 | 54.82139 (1.12467) | 48.73603 (0.72249) | 49.24973 (0.73747) | 53.24709 (0.89498) | 53.9335 (0.93141) | 44.51893 (0.54087) | 38.45547 (0.33838) | 38.96842 (0.33371) | 38.82818 (0.32464) | 39.23644 (0.33371) | 39.00763 (0.32464) |
| F2-3 | 54.87582 (1.12495) | 53.39429 (0.77594) | 54.09649 (0.77092) | 52.83553 (0.73876) | 53.33211 (0.75908) | 50.14688 (0.6493) | 46.50683 (0.57486) | 48.06138 (0.83316) | 47.15296 (0.6785) | 48.65246 (0.83316) | 47.27893 (0.6785) |

Table H.3: The prediction error comparison table for each simulation setting in Section [Appendix H.3](#) when $(p, q) = (20, 50)$. The values are the mean squared prediction errors averaged over 50 independent replications. The numbers in parentheses are normalized sample standard deviations. The column labels are defined in Section [7](#) and [8.1](#). The labels 1, 2, 3 indicate the sparsity levels $(s_1, s_2) = (0.5, 0.5), (0.5, 1), (1, 1)$, respectively. Boldface indicates the best non-oracle model. The oracle estimator is on the seventh column.

| Model error comparison table: Setting A2-F2 | | | | | | | | | | | |
|---|------------------------|-----------------------|------------------------------|------------------------------|-----------------------|-----------------------|-----------------------|-----------------------------|------------------------------|-----------------------------|-----------------------|
| Design | OLS | LAS | LASP | c.ridge | s.ridge | ap.MRCE | MRCs-Or | MRCs | ap.MRCs | MRGCS | ap.MRGCS |
| A2-1 | 42.39295 (0.70089) | 17.26117 (0.27595) | 14.91861 (0.32457) | 22.86371 (0.33958) | 17.90237 (0.37709) | 28.43493 (0.39772) | 10.51511 (0.27767) | 22.33984 (0.51384) | 19.11891 (0.34702) | 20.02997 (0.4011) | 19.31545 (0.39004) |
| A2-2 | 42.23756 (0.73002) | 25.71624 (0.37409) | 28.42492 (0.43187) | 32.30901 (0.41279) | 34.23738 (0.43208) | 26.05191 (0.38233) | 18.57594 (0.29277) | 25.7862 (0.37367) | 25.53783 (0.3739) | 26.0215 (0.3611) | 25.56082 (0.36155) |
| A2-3 | 42.65128 (0.71445) | 37.52372 (0.48534) | 40.67412 (0.52458) | 36.61466 (0.51837) | 37.76556 (0.49354) | 37.04592 (0.47818) | 33.97818 (0.41658) | 40.38988 (0.46421) | 39.4397 (0.45246) | 40.77066 (0.53596) | 39.60936 (0.45182) |
| B2-1 | 31.14934 (0.68511) | 13.29088 (0.2843) | 11.69225 (0.30887) | 18.37806 (0.31959) | 14.47773 (0.34524) | 19.42273 (0.4285) | 7.12205 (0.22313) | 12.78614 (0.34926) | 11.82619 (0.27888) | 14.38179 (0.35786) | 12.05595 (0.25494) |
| B2-2 | 29.65723 (0.77201) | 20.09906 (0.34665) | 20.58149 (0.35734) | 24.75082 (0.39576) | 25.46399 (0.39688) | 19.28519 (0.32426) | 11.8882 (0.19258) | 16.59847 (0.32694) | 16.41701 (0.27514) | 16.2451 (0.22163) | 16.59242 (0.28141) |
| B2-3 | 30.39852 (0.52269) | 27.37935 (0.50579) | 28.80194 (0.5272) | 26.13305 (0.4656) | 27.22649 (0.48522) | 26.15787 (0.48074) | 23.36803 (0.3862) | 26.77497 (0.49644) | 25.7945 (0.46687) | 26.45568 (0.50936) | 25.79595 (0.46745) |
| C2-1 | 18.96585 (0.92727) | 9.03644 (0.39136) | 7.02547 (0.36382) | 12.40961 (0.47395) | 9.00063 (0.42804) | 6.50119 (0.18319) | 1.80521 (0.03815) | 2.17131 (0.03409) | 2.18127 (0.06256) | 2.22184 (0.03649) | 2.38911 (0.06656) |
| C2-2 | 19.15577 (1.02716) | 13.80474 (0.54388) | 14.26366 (0.57717) | 17.88023 (0.6924) | 18.15454 (0.70646) | 8.10232 (0.3728) | 3.37173 (0.08005) | 3.43928 (0.07848) | 3.43806 (0.07352) | 3.54561 (0.07175) | 3.53265 (0.07201) |
| C2-3 | 20.26237 (1.07382) | 17.76817 (0.75564) | 18.39034 (0.74578) | 17.55728 (0.72232) | 17.91135 (0.72971) | 14.07746 (0.582) | 10.28052 (0.38326) | 11.27033 (0.40731) | 10.69155 (0.39051) | 13.05092 (1.01575) | 12.43701 (0.80875) |
| D2-1 | 111.27776 (1.66321) | 36.45598 (0.61624) | 34.84428 (0.74871) | 44.65856 (0.57515) | 37.88761 (0.71301) | 54.20788 (0.72843) | 28.62152 (0.4955) | 37.81118 (0.57045) | 37.31678 (0.59651) | 38.51193 (0.55557) | 37.937 (0.63313) |
| D2-2 | 116.09085 (2.1362) | 61.49551 (0.90658) | 65.82194 (1.04345) | 65.64489 (0.83411) | 71.40972 (0.9927) | 62.11997 (0.93692) | 50.92173 (0.76843) | 56.98089 (0.85082) | 56.88708 (0.84472) | 58.8232 (0.89514) | 57.63959 (0.8681) |
| D2-3 | 110.87053 (1.73308) | 87.1054 (0.90066) | 96.81336 (1.00135) | 81.29844 (0.9457) | 86.20105 (0.99948) | 86.89881 (0.8451) | 80.02526 (0.792) | 101.0393 (1.31973) | 94.41737 (1.08012) | 101.20467 (1.50165) | 94.77628 (1.11487) |
| E2-1 | 66.26434 (0.84762) | 26.82913 (0.4813) | 22.55788 (0.55399) | 32.1563 (0.54483) | 25.91308 (0.57146) | 38.70073 (0.60633) | 18.46266 (0.31511) | 26.49327 (0.57516) | 25.10216 (0.46719) | 25.19701 (0.36249) | 25.40263 (0.4608) |
| E2-2 | 66.73458 (1.2566) | 36.02501 (0.48539) | 40.82276 (0.60869) | 43.92905 (0.51081) | 47.15565 (0.58005) | 39.59048 (0.57995) | 29.6172 (0.40664) | 33.85957 (0.43007) | 33.84195 (0.42747) | 34.64423 (0.42874) | 34.24579 (0.42352) |
| E2-3 | 64.83845 (1.02699) | 57.19454 (0.77782) | 61.22643 (0.79812) | 53.00983 (0.59635) | 56.59714 (0.70367) | 56.07241 (0.64918) | 50.89877 (0.60097) | 59.98199 (0.79877) | 57.08262 (0.72041) | 60.85837 (1.03405) | 57.61517 (0.73279) |
| F2-1 | 22.1054 (0.999) | 10.10014 (0.41701) | 8.16875 (0.35764) | 13.75242 (0.43543) | 10.18145 (0.39115) | 9.58014 (0.22971) | 3.33699 (0.08664) | 3.75176 (0.08877) | 3.84514 (0.10269) | 3.91707 (0.09189) | 4.14802 (0.10806) |
| F2-2 | 22.3724 (1.08322) | 15.31959 (0.48125) | 15.84472 (0.5439) | 19.50745 (0.62453) | 20.20755 (0.66363) | 11.55726 (0.41419) | 5.88562 (0.1019) | 6.37313 (0.13122) | 6.22846 (0.12121) | 6.64052 (0.13676) | 6.38857 (0.11985) |
| F2-3 | 22.04484 (0.92716) | 20.40432 (0.68318) | 21.06828 (0.67232) | 19.82113 (0.61695) | 20.35087 (0.64229) | 17.13677 (0.49477) | 13.42993 (0.28681) | 15.02451 (0.39563) | 13.99176 (0.27427) | 15.63436 (0.63396) | 14.36106 (0.4605) |

Table H.4: The model error comparison table for each simulation setting in Section Appendix H.3 when $(p, q) = (20, 50)$. The values are the mean squared prediction errors averaged over 50 independent replications. The numbers in parentheses are normalized sample standard deviations. The column labels are defined in Section 7 and 8.1. The labels 1, 2, 3 indicate the sparsity levels $(s_1, s_2) = (0.5, 0.5), (0.5, 1), (1, 1)$, respectively. Boldface indicates the best non-oracle model. The oracle estimator is on the seventh column.

| Prediction error comparison table: Setting G2–L2 | | | | | | | | |
|--|-------------------------------|------------------------------|-------------------------------|------------------------|-------------------------------|------------------------|-------------------------------|------------------------|
| θ | LAS | LASP | c.ridge | s.ridge | ap.MRCE | MRCS-Or | ap.MRCS | ap.MRGCS |
| G2-1 | 44.83533 (1.1591) | 43.46363 (1.40537) | 53.05025 (1.24214) | 51.21144 (1.59279) | 44.5823 (0.95241) | 33.9537 (0.89919) | 45.35985 (1.18674) | 45.90278 (1.20162) |
| G2-2 | 64.82553 (0.97176) | 69.44478 (1.0354) | 76.63785 (0.94248) | 81.77781 (1.01504) | 62.50284 (0.92436) | 50.17423 (1.18861) | 64.92464 (1.19798) | 64.32426 (1.06947) |
| G2-3 | 133.45879 (2.66461) | 153.04183 (2.8973) | 109.90867 (1.59821) | 117.93036 (1.74162) | 139.2495 (2.60436) | 146.8506 (8.81637) | 148.6895 (4.86074) | 141.73388 (2.94612) |
| H2-1 | 37.01575 (0.85019) | 35.93307 (0.93848) | 43.34182 (0.91763) | 42.19558 (1.08917) | 36.34143 (0.8625) | 26.23449 (0.55683) | 33.26838 (0.78547) | 33.92596 (0.67365) |
| H2-2 | 50.89406 (0.82046) | 55.2831 (1.03371) | 65.83079 (0.83084) | 69.89328 (0.91223) | 50.21027 (0.75308) | 38.05912 (0.52668) | 46.45042 (0.79867) | 46.91264 (0.80098) |
| H2-3 | 110.38893 (1.66942) | 124.38963 (2.04462) | 93.03523 (1.46699) | 98.32905 (1.57249) | 118.24035 (2.35693) | 92.29068 (2.19205) | 114.19288 (2.7504) | 109.58705 (1.67005) |
| I2-1 | 29.85667 (0.65668) | 28.80508 (0.71843) | 37.88529 (0.88379) | 36.95055 (1.03214) | 29.57164 (0.6902) | 16.49538 (0.23436) | 17.26156 (0.26099) | 17.94684 (0.28855) |
| I2-2 | 40.65305 (0.87366) | 44.66089 (1.02929) | 56.80885 (1.02794) | 60.82274 (1.21179) | 38.92704 (0.85435) | 22.12666 (0.38204) | 24.56793 (0.47369) | 25.33271 (0.49249) |
| I2-3 | 91.69167 (1.96659) | 104.63603 (2.1685) | 78.70372 (1.55065) | 83.83394 (1.54102) | 91.35578 (1.97122) | 60.24393 (1.26672) | 69.3502 (1.20634) | 71.55799 (1.22631) |
| J2-1 | 125.89001 (1.8527) | 126.61688 (2.26474) | 131.36489 (1.8628) | 126.64774 (2.13564) | 125.87506 (1.81853) | 114.49484 (1.95569) | 128.51114 (1.52357) | 129.81748 (1.61378) |
| J2-2 | 170.12318 (1.66048) | 177.52194 (1.91271) | 169.78467 (1.48657) | 180.68469 (1.67556) | 166.90405 (1.56726) | 154.63228 (1.56597) | 165.53654 (1.54722) | 166.10404 (1.64566) |
| J2-3 | 260.05584 (2.41941) | 299.78893 (3.48501) | 223.77021 (1.96252) | 237.8733 (2.01791) | 261.45428 (2.60148) | 257.66007 (3.09796) | 275.7491 (2.90973) | 273.79175 (2.99102) |
| K2-1 | 82.47142 (1.08254) | 81.63699 (1.4018) | 88.23276 (1.24962) | 87.18334 (1.45946) | 84.45061 (1.42602) | 72.24252 (0.88952) | 80.65078 (1.24135) | 81.07492 (1.2521) |
| K2-2 | 107.31975 (1.01603) | 119.784 (1.3951) | 121.33131 (1.04207) | 127.18878 (1.24454) | 107.78692 (0.9779) | 99.23878 (1.03708) | 110.56906 (1.02082) | 111.31289 (1.05706) |
| K2-3 | 191.46974 (1.67299) | 220.4474 (3.43336) | 160.92903 (1.61539) | 169.7814 (1.93251) | 188.32649 (1.82336) | 202.65962 (5.26571) | 187.86521 (2.39414) | 188.03239 (2.28333) |
| L2-1 | 35.42431 (0.69618) | 34.2385 (0.72038) | 43.01718 (0.85946) | 41.86826 (0.98601) | 35.28308 (0.69019) | 23.55794 (0.349) | 25.15583 (0.37057) | 25.66002 (0.36527) |
| L2-2 | 47.33255 (0.96358) | 51.39827 (1.10066) | 62.11514 (0.91844) | 66.57404 (1.01125) | 45.6146 (0.76398) | 30.95948 (0.42458) | 33.07476 (0.44855) | 33.79567 (0.4878) |
| L2-3 | 105.76418 (2.28921) | 121.86037 (2.68535) | 87.06077 (1.50741) | 93.5535 (1.70534) | 109.15378 (2.59976) | 81.73934 (1.34799) | 89.01742 (1.89727) | 90.88147 (1.89529) |

Table H.5: The prediction error comparison table for each simulation setting in Section [Appendix H.3](#) when $(p, q) = (50, 20)$. The values are the mean squared prediction errors averaged over 50 independent replications. The numbers in parentheses are normalized sample standard deviations. The column labels are defined in Section [7](#) and [8.1](#). The labels 1, 2, 3 indicate the sparsity levels $(s_1, s_2) = (0.5, 0.5), (0.5, 1), (1, 1)$, respectively. Boldface indicates the best non-oracle model. The oracle estimator is on the sixth column.

| Model error comparison table: Setting G2–L2 | | | | | | | | |
|---|-----------------------------|------------------------------|-------------------------------|------------------------|------------------------------|------------------------|------------------------------|------------------------|
| θ | LAS | LASP | c.ridge | s.ridge | ap.MRCE | MRCS-Or | ap.MRCS | ap.MRGCS |
| G2-1 | 25.14384 (1.13407) | 23.78569 (1.34304) | 33.1064 (1.21714) | 31.34058 (1.54674) | 24.88036 (0.93052) | 14.60273 (0.87037) | 25.71716 (1.17192) | 26.31923 (1.1905) |
| G2-2 | 44.61278 (0.89817) | 49.3369 (1.00043) | 56.27542 (0.88576) | 61.35783 (0.9877) | 42.29644 (0.84892) | 30.55962 (1.12392) | 44.81787 (1.12645) | 44.19587 (0.98705) |
| G2-3 | 111.11682 (2.5884) | 130.52844 (2.77553) | 88.65276 (1.5735) | 96.53391 (1.66283) | 116.89217 (2.61566) | 124.53132 (8.5668) | 126.1663 (4.80341) | 119.10135 (2.87938) |
| H2-1 | 21.95861 (0.823) | 20.9488 (0.89498) | 28.21326 (0.88127) | 27.16125 (1.05464) | 21.27333 (0.82758) | 11.35252 (0.51332) | 18.2892 (0.7277) | 18.86563 (0.60315) |
| H2-2 | 36.05095 (0.79906) | 40.32027 (0.97442) | 50.7382 (0.76463) | 54.92287 (0.85724) | 35.24728 (0.70676) | 23.29013 (0.49518) | 31.44054 (0.72526) | 31.91841 (0.74804) |
| H2-3 | 93.96859 (1.50734) | 107.78664 (1.8749) | 77.1775 (1.25161) | 82.15628 (1.3589) | 101.65402 (2.16544) | 76.4224 (2.11463) | 97.8597 (2.62389) | 93.25851 (1.44925) |
| I2-1 | 19.13619 (0.62648) | 18.07609 (0.67067) | 26.87164 (0.80152) | 26.03099 (0.9598) | 18.79242 (0.63511) | 5.87354 (0.20828) | 6.64095 (0.21676) | 7.32643 (0.24041) |
| I2-2 | 28.87246 (0.75068) | 32.92022 (0.89493) | 44.66045 (0.86671) | 48.68481 (1.08192) | 27.18182 (0.71677) | 10.96406 (0.29269) | 13.25166 (0.3523) | 14.0125 (0.37053) |
| I2-3 | 80.00193 (1.85136) | 92.9246 (2.02994) | 67.27094 (1.44039) | 72.27628 (1.42068) | 79.58536 (1.82847) | 48.6636 (1.04336) | 57.80099 (1.03631) | 60.1247 (1.09194) |
| J2-1 | 54.98627 (1.73007) | 56.04015 (2.20274) | 60.76481 (1.75115) | 56.25554 (2.0839) | 54.97554 (1.6641) | 44.10214 (1.84991) | 57.56517 (1.43305) | 58.83578 (1.5081) |
| J2-2 | 98.1547 (1.39359) | 105.43109 (1.76736) | 98.07573 (1.14373) | 108.58913 (1.45523) | 94.82636 (1.3107) | 82.74791 (1.30263) | 93.74954 (1.25026) | 94.29603 (1.33995) |
| J2-3 | 184.39942 (2.10522) | 223.20874 (2.87413) | 149.23673 (1.55949) | 163.32049 (1.7028) | 185.62347 (2.28317) | 182.5674 (2.94675) | 200.04534 (2.71763) | 197.98187 (2.72995) |
| K2-1 | 41.87521 (1.02633) | 41.08228 (1.4252) | 47.69412 (1.17469) | 46.6846 (1.44253) | 43.84725 (1.28318) | 31.72079 (0.81321) | 40.02228 (1.13387) | 40.49055 (1.16072) |
| K2-2 | 66.0407 (0.87697) | 78.16363 (1.31751) | 80.22467 (0.91312) | 85.91252 (1.16308) | 66.47505 (0.8628) | 58.40079 (0.92193) | 69.28555 (0.90648) | 69.99709 (0.90859) |
| K2-3 | 149.12254 (1.44325) | 177.60716 (3.14376) | 119.57849 (1.33734) | 128.35844 (1.63375) | 146.01533 (1.55979) | 160.09242 (4.91225) | 145.69808 (2.21759) | 145.89654 (2.11809) |
| L2-1 | 21.67108 (0.65689) | 20.48414 (0.67071) | 29.25733 (0.82955) | 28.07226 (0.97772) | 21.52181 (0.65743) | 10.12368 (0.31029) | 11.71929 (0.35248) | 12.19634 (0.34613) |
| L2-2 | 33.68214 (0.84221) | 37.71081 (0.99064) | 48.27169 (0.73503) | 52.5079 (0.88085) | 32.09719 (0.63973) | 17.53978 (0.37087) | 19.71687 (0.40564) | 20.40054 (0.43919) |
| L2-3 | 90.6962 (2.18118) | 106.13995 (2.37254) | 72.41254 (1.32946) | 78.84207 (1.53518) | 93.63538 (2.31693) | 66.93323 (1.25891) | 74.10679 (1.7931) | 75.99779 (1.7611) |

Table H.6: The model error comparison table for each simulation setting in Section Appendix H.3 when $(p, q) = (50, 20)$. The values are the mean squared prediction errors averaged over 50 independent replications. The numbers in parentheses are normalized sample standard deviations. The column labels are defined in Section 7 and 8.1. The labels 1, 2, 3 indicate the sparsity levels $(s_1, s_2) = (0.5, 0.5), (0.5, 1), (1, 1)$, respectively. Boldface indicates the best non-oracle model. The oracle estimator is on the sixth column.

Appendix I.1. Tables for Section 8.2

| Prediction error comparison table: Setting A–F | | | | | | | | | | | |
|--|------------------------|-------------------------------|-------------------------------|-------------------------------|------------------------|------------------------|------------------------|-------------------------------|------------------------------|------------------------|------------------------|
| Design | OLS | LAS | LASP | c.ridge | s.ridge | ap.MRCE | MRCS-Or | MRCS | ap.MRCS | MRGCS | ap.MRGCS |
| A-1 | 421.3023 (3.28586) | 298.42428 (1.32846) | 297.6855 (1.47443) | 306.96871 (1.4173) | 298.78469 (1.39863) | 314.64878 (1.77209) | 265.44132 (1.10646) | 297.93267 (1.34256) | 299.79817 (1.28261) | 299.67561 (1.34256) | 299.8103 (1.28261) |
| A-2 | 421.24545 (2.90543) | 327.56468 (1.25869) | 338.57449 (1.5704) | 333.10994 (1.40993) | 341.87992 (1.48088) | 328.97359 (1.41943) | 295.09134 (1.31911) | 327.90459 (1.48397) | 327.65685 (1.40809) | 330.86734 (1.48397) | 328.64242 (1.40809) |
| A-3 | 423.84581 (2.94269) | 372.56158 (2.0557) | 386.54732 (2.11265) | 360.10005 (1.80145) | 368.7804 (1.99544) | 370.65029 (1.8931) | 347.78963 (1.72325) | 394.76222 (2.70602) | 383.01155 (1.87572) | 393.60105 (2.70602) | 382.69695 (1.87572) |
| B-1 | 238.43803 (1.99238) | 171.61615 (0.77837) | 168.99091 (0.89788) | 178.45972 (0.7475) | 172.44148 (0.86062) | 184.72421 (0.87895) | 151.78365 (0.60891) | 170.77475 (0.59449) | 169.45224 (0.60621) | 171.33406 (0.59449) | 170.15885 (0.60621) |
| B-2 | 231.72801 (2.3423) | 189.36662 (0.83056) | 194.28062 (1.06268) | 197.3021 (0.7944) | 200.55102 (1.06139) | 192.46704 (0.90105) | 167.95685 (0.70579) | 184.63716 (0.80241) | 184.72838 (0.76253) | 185.73553 (0.80241) | 185.13032 (0.76253) |
| B-3 | 234.71038 (1.74771) | 214.87314 (1.44266) | 221.11154 (1.65027) | 207.72906 (1.33315) | 213.15969 (1.42005) | 211.66591 (1.34992) | 202.6108 (1.32292) | 223.0754 (1.70947) | 217.47247 (1.54624) | 222.62461 (1.70947) | 217.58813 (1.54624) |
| C-1 | 61.51457 (1.14936) | 46.67554 (0.41137) | 45.16545 (0.41993) | 51.09038 (0.54318) | 47.56594 (0.50113) | 47.68118 (0.39966) | 39.46289 (0.30375) | 41.24857 (0.31877) | 41.41736 (0.32009) | 41.60935 (0.31877) | 41.83975 (0.32009) |
| C-2 | 63.29166 (1.19927) | 54.5344 (0.64778) | 54.65462 (0.66049) | 58.97623 (0.78077) | 59.39909 (0.74672) | 50.45691 (0.51123) | 43.35193 (0.40627) | 45.68504 (0.44356) | 44.94594 (0.43563) | 46.09739 (0.44356) | 45.12151 (0.43563) |
| C-3 | 64.03305 (1.25486) | 59.30977 (0.81106) | 60.07406 (0.81974) | 58.46108 (0.77287) | 59.34065 (0.79913) | 55.4602 (0.58784) | 52.10512 (0.50461) | 53.49548 (0.626) | 52.51051 (0.57489) | 53.94183 (0.626) | 53.05081 (0.57489) |
| D-1 | 558.74471 (3.73806) | 390.47356 (1.24105) | 388.68335 (1.63307) | 395.06585 (1.34186) | 389.16316 (1.48051) | 409.55343 (1.62612) | 358.98208 (1.28938) | 385.93684 (1.35932) | 386.26484 (1.29872) | 388.81632 (1.35932) | 387.33796 (1.29872) |
| D-2 | 564.13649 (5.0482) | 424.37231 (1.51057) | 442.28868 (1.84653) | 434.68602 (1.44811) | 442.94447 (1.67828) | 430.49058 (1.46774) | 404.62239 (1.47361) | 429.33388 (1.51177) | 427.00528 (1.45592) | 433.22052 (1.51177) | 428.0325 (1.45592) |
| D-3 | 555.82106 (3.90354) | 483.69323 (1.67152) | 495.75362 (1.83794) | 457.10829 (1.40863) | 472.06041 (1.58048) | 478.29561 (1.54378) | 490.9024 (2.3392) | 508.10263 (3.64916) | 488.57275 (1.97457) | 509.09845 (3.64916) | 486.62817 (1.97457) |
| E-1 | 303.01131 (1.99873) | 216.49803 (0.94551) | 215.36076 (1.06092) | 225.8805 (1.06224) | 217.66458 (1.10995) | 235.32617 (1.24057) | 199.25027 (0.86844) | 216.25975 (0.96294) | 215.38208 (0.94547) | 217.45551 (0.96294) | 216.36837 (0.94547) |
| E-2 | 302.62906 (2.11844) | 243.39502 (1.07497) | 246.56048 (1.13222) | 245.26924 (0.98032) | 251.98864 (1.07024) | 241.48383 (1.05926) | 222.12474 (0.96153) | 235.85209 (1.02713) | 236.39031 (1.02652) | 237.44853 (1.02713) | 237.10805 (1.02652) |
| E-3 | 301.59992 (1.97572) | 271.84761 (1.33779) | 283.47367 (1.52899) | 266.58831 (1.29148) | 270.46679 (1.31735) | 271.95514 (1.26651) | 260.94096 (1.21011) | 287.39082 (2.27853) | 278.72921 (1.41849) | 287.5462 (2.27853) | 279.35487 (1.41849) |
| F-1 | 69.1122 (1.13611) | 52.27008 (0.48932) | 50.49189 (0.48904) | 56.974 (0.55182) | 52.88907 (0.53755) | 54.57006 (0.39142) | 45.21246 (0.34061) | 46.98724 (0.41626) | 47.15466 (0.38378) | 47.78788 (0.41626) | 47.60962 (0.38378) |
| F-2 | 69.0662 (1.15143) | 60.86532 (0.75389) | 61.14864 (0.75718) | 65.8587 (0.9132) | 66.55683 (0.91706) | 57.72872 (0.5888) | 49.90487 (0.35281) | 52.93111 (0.41744) | 51.62936 (0.3619) | 52.90665 (0.41744) | 51.90156 (0.3619) |
| F-3 | 68.93688 (1.17405) | 66.90949 (0.784) | 67.81019 (0.79865) | 65.59747 (0.75564) | 66.58424 (0.77268) | 63.20517 (0.6412) | 60.10471 (0.60468) | 62.18728 (0.70581) | 60.80521 (0.68918) | 61.87549 (0.70581) | 60.90517 (0.68918) |

Table I.7: The prediction error comparison table for each simulation setting in Section 8.2 when $(p, q) = (20, 50)$. The values are the mean squared prediction errors averaged over 50 independent replications. The numbers in parentheses are normalized sample standard deviations. The column labels are defined in Section 7 and 8.1. The labels 1, 2, 3 indicate the sparsity levels $(s_1, s_2) = (0.5, 0.5), (0.5, 1), (1, 1)$, respectively. Boldface indicates the best non-oracle model. The oracle estimator is on the seventh column.

| Model error comparison table: Setting A-F | | | | | | | | | | | |
|---|------------------------|------------------------------|------------------------------|-------------------------------|------------------------|------------------------|------------------------|------------------------------|------------------------------|------------------------|------------------------|
| Design | OLS | LAS | LASP | c.ridge | s.ridge | ap.MRCE | MRCS-Or | MRCS | ap.MRCS | MRGCS | ap.MRGCS |
| A-1 | 169.49322 (2.53288) | 49.93963 (0.96146) | 49.35352 (1.13484) | 58.52519 (1.0516) | 50.50883 (1.1362) | 66.30341 (1.39676) | 17.82823 (0.67809) | 49.50422 (0.95861) | 51.40402 (1.11572) | 51.2598 (0.96324) | 51.45167 (1.03735) |
| A-2 | 172.55375 (2.62797) | 78.36706 (0.93968) | 89.33389 (1.04166) | 84.15166 (1.01617) | 92.95695 (1.06284) | 79.69219 (0.96694) | 46.0565 (0.898) | 78.65624 (0.96127) | 78.41338 (0.93359) | 81.62068 (1.04528) | 79.38073 (0.94881) |
| A-3 | 173.05229 (2.7413) | 121.56443 (1.47978) | 135.33523 (1.64689) | 109.53369 (1.13637) | 117.89774 (1.42685) | 120.13303 (1.29742) | 97.57773 (1.43399) | 144.01482 (1.85565) | 132.24879 (1.35438) | 142.4011 (2.52323) | 131.88986 (1.46298) |
| B-1 | 99.23479 (1.57555) | 34.75711 (0.74709) | 31.93273 (0.84364) | 41.61723 (0.66706) | 35.47491 (0.74302) | 47.55133 (0.81709) | 14.7796 (0.50105) | 33.88262 (0.67183) | 32.61942 (0.63723) | 34.36268 (0.5858) | 33.26948 (0.59968) |
| B-2 | 94.38538 (1.9962) | 51.24645 (0.62806) | 55.9567 (0.85358) | 59.05804 (0.59067) | 62.26096 (0.79994) | 54.24585 (0.67322) | 30.57363 (0.50754) | 46.65243 (0.56914) | 46.73351 (0.55903) | 47.7272 (0.61967) | 47.12427 (0.58215) |
| B-3 | 96.1279 (1.54068) | 76.44908 (1.09613) | 82.68874 (1.4136) | 69.60995 (1.04494) | 74.83864 (1.17936) | 73.39833 (1.02504) | 64.36683 (0.96925) | 84.57594 (1.31653) | 79.18676 (1.22334) | 84.35722 (1.55367) | 79.26583 (1.24824) |
| C-1 | 25.47427 (0.95087) | 11.0638 (0.39081) | 9.43837 (0.38988) | 15.46791 (0.50382) | 11.76765 (0.45624) | 11.84424 (0.2639) | 3.45578 (0.10422) | 5.26781 (0.11345) | 5.44013 (0.12778) | 5.61142 (0.13509) | 5.82692 (0.13586) |
| C-2 | 25.71332 (1.05639) | 18.24156 (0.55983) | 18.29504 (0.5722) | 22.6413 (0.6873) | 23.07493 (0.66562) | 14.17451 (0.43169) | 7.0494 (0.13847) | 9.37432 (0.21277) | 8.62192 (0.17155) | 9.77303 (0.21043) | 8.81697 (0.17246) |
| C-3 | 26.83281 (1.11853) | 23.69789 (0.75449) | 24.44588 (0.7476) | 22.85877 (0.69729) | 23.73203 (0.72958) | 19.61069 (0.50636) | 15.97679 (0.38878) | 17.29766 (0.45466) | 16.36872 (0.37332) | 17.72032 (0.49317) | 16.91631 (0.44281) |
| D-1 | 224.83755 (3.33543) | 62.69404 (0.8991) | 60.66062 (1.33599) | 67.14954 (0.98038) | 61.20804 (1.18794) | 81.3977 (1.37702) | 31.40809 (0.95891) | 58.13068 (0.96301) | 58.45669 (0.95851) | 61.09928 (1.04411) | 59.57743 (0.95744) |
| D-2 | 233.11746 (4.37987) | 95.07723 (1.31886) | 112.66173 (1.53547) | 104.91901 (1.26361) | 112.83378 (1.33494) | 101.05026 (1.29215) | 75.24154 (1.27828) | 100.03988 (1.33791) | 97.73367 (1.28075) | 103.84379 (1.32325) | 98.68772 (1.24385) |
| D-3 | 227.17133 (3.47871) | 156.24403 (1.57096) | 167.9195 (1.58083) | 130.21511 (1.24865) | 144.77209 (1.46772) | 151.14687 (1.40266) | 164.11705 (1.97114) | 180.5606 (2.94715) | 161.64299 (1.91862) | 181.52586 (3.59713) | 159.37811 (1.73592) |
| E-1 | 124.24667 (1.55272) | 39.5913 (0.70682) | 38.56105 (0.89482) | 49.04118 (0.72425) | 41.00836 (0.88218) | 57.99386 (0.89817) | 22.35643 (0.55781) | 39.40462 (0.57523) | 38.52094 (0.59058) | 40.51292 (0.65933) | 39.43874 (0.63862) |
| E-2 | 124.17102 (2.17952) | 65.81175 (0.86855) | 68.87426 (0.91018) | 67.56181 (0.71284) | 74.19776 (0.84761) | 64.07924 (0.79321) | 45.13431 (0.70173) | 58.41796 (0.74688) | 58.95914 (0.75938) | 59.98033 (0.76769) | 59.64012 (0.76233) |
| E-3 | 122.85455 (1.69619) | 94.9139 (1.03329) | 106.74197 (1.27066) | 90.07125 (1.05467) | 93.97887 (1.10338) | 95.09407 (0.895) | 83.92015 (0.91605) | 109.96276 (1.31683) | 101.41468 (1.0535) | 110.34212 (2.0455) | 102.06991 (1.10863) |
| F-1 | 27.92716 (1.03375) | 11.73688 (0.38946) | 10.14497 (0.37853) | 16.37945 (0.45912) | 12.42706 (0.43389) | 13.99748 (0.30284) | 4.88248 (0.15396) | 6.60306 (0.18474) | 6.7363 (0.18886) | 7.38975 (0.24697) | 7.14922 (0.18346) |
| F-2 | 28.22102 (1.10901) | 19.13628 (0.51893) | 19.40333 (0.56308) | 23.80962 (0.63592) | 24.51151 (0.64924) | 16.3342 (0.44749) | 9.01109 (0.15183) | 11.98734 (0.23445) | 10.62209 (0.19826) | 11.89068 (0.23925) | 10.85284 (0.20617) |
| F-3 | 27.79606 (0.97823) | 25.51196 (0.68362) | 26.37553 (0.67819) | 24.26311 (0.63958) | 25.26677 (0.65867) | 21.83446 (0.4816) | 18.66392 (0.31219) | 20.67019 (0.43667) | 19.38073 (0.32098) | 20.59742 (0.41504) | 19.55339 (0.34476) |

Table I.8: The model error comparison table for each simulation setting in Section 8.2 when $(p, q) = (20, 50)$. The values are the mean squared prediction errors averaged over 50 independent replications. The numbers in parentheses are normalized sample standard deviations. The column labels are defined in Section 7 and 8.1. The labels 1, 2, 3 indicate the sparsity levels $(s_1, s_2) = (0.5, 0.5), (0.5, 1), (1, 1)$, respectively. Boldface indicates the best non-oracle model. The oracle estimator is on the seventh column.

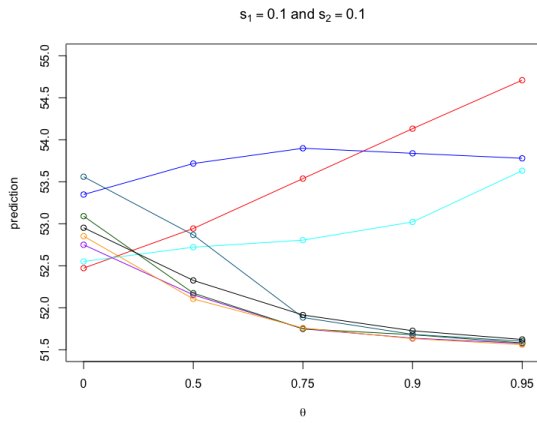
| Prediction error comparison table: Setting G–L | | | | | | | | |
|--|------------------------|------------------------|-------------------------------|-------------------------------|-------------------------------|------------------------|-------------------------------|-------------------------------|
| θ | LAS | LASP | c.ridge | s.ridge | ap.MRCE | MRCS-Or | ap.MRCS | ap.MRGCS |
| G-1 | 216.36174 (2.86649) | 215.52127 (3.70502) | 216.47546 (2.76849) | 211.91985 (3.3165) | 220.51808 (3.39456) | 187.96523 (2.78338) | 222.52834 (3.5455) | 222.66418 (3.41285) |
| G-2 | 263.41619 (1.98844) | 285.02027 (2.71801) | 264.92923 (1.6942) | 276.98381 (2.10046) | 264.15557 (2.09645) | 240.47493 (1.82606) | 262.68599 (1.98103) | 262.68063 (2.0417) |
| G-3 | 395.69762 (3.07959) | 433.34207 (4.7154) | 345.28576 (2.39476) | 359.9579 (2.55413) | 391.58235 (3.56139) | 396.31235 (7.71721) | 396.43227 (3.28527) | 395.78278 (3.34694) |
| H-1 | 126.19852 (1.93327) | 126.8254 (2.26943) | 132.26305 (1.9858) | 127.90539 (2.15603) | 126.01257 (1.61227) | 110.17097 (1.78233) | 128.74505 (1.58099) | 129.11045 (1.52652) |
| H-2 | 173.69427 (1.86647) | 181.23264 (2.30472) | 174.25862 (1.37817) | 184.63054 (1.81405) | 169.0882 (1.73478) | 151.32558 (1.41248) | 168.31328 (1.65608) | 168.1326 (1.63334) |
| H-3 | 261.81695 (3.00509) | 298.17749 (3.82723) | 225.74933 (2.24818) | 241.20864 (2.53746) | 264.54552 (2.63176) | 267.58151 (3.43096) | 276.20571 (2.95179) | 275.65074 (3.07556) |
| I-1 | 41.63441 (0.81513) | 40.1446 (0.75983) | 49.17791 (0.91626) | 48.07737 (1.08256) | 40.77438 (0.78999) | 30.08706 (0.49678) | 33.58747 (0.53835) | 34.25374 (0.54227) |
| I-2 | 57.17378 (0.88511) | 61.94668 (1.08764) | 72.17713 (1.0231) | 77.38905 (1.13609) | 55.84518 (0.85055) | 41.50233 (0.64667) | 45.42631 (0.77073) | 45.84982 (0.75067) |
| I-3 | 118.15544 (2.06356) | 134.63409 (2.70658) | 98.78048 (1.40466) | 103.92663 (1.48789) | 125.73519 (2.45548) | 97.30096 (1.71619) | 112.20106 (1.71757) | 110.56873 (1.82489) |
| J-1 | 200.43829 (2.57578) | 198.97452 (3.29339) | 199.56624 (2.15461) | 195.67974 (2.81587) | 204.83302 (2.65951) | 163.73197 (2.43815) | 203.90903 (2.46013) | 205.80332 (2.44725) |
| J-2 | 246.25816 (1.89352) | 267.34432 (2.70812) | 251.08902 (1.77016) | 262.35167 (2.42688) | 249.31589 (2.13663) | 213.42151 (2.8495) | 245.31119 (1.8859) | 245.24282 (1.87364) |
| J-3 | 371.40413 (3.26637) | 403.65612 (3.70714) | 318.37477 (2.58085) | 334.12819 (3.20183) | 362.58295 (3.10843) | 353.62652 (9.63633) | 370.5129 (2.88689) | 370.72084 (2.76742) |
| K-1 | 123.58749 (1.76113) | 125.00033 (2.37222) | 128.98656 (1.58809) | 124.66788 (1.66317) | 122.2293 (1.65914) | 96.88944 (1.47821) | 122.45039 (1.64529) | 123.40318 (1.76577) |
| K-2 | 163.17932 (1.50443) | 170.86639 (2.16995) | 164.91992 (1.32417) | 175.38938 (1.88923) | 159.10629 (1.45617) | 134.11352 (2.08164) | 157.75598 (1.40035) | 158.11155 (1.43937) |
| K-3 | 246.58744 (2.32164) | 288.1152 (4.69415) | 214.22073 (1.86577) | 228.53336 (2.7029) | 249.75552 (2.63663) | 227.63059 (4.96864) | 258.47333 (3.22339) | 256.43076 (3.05944) |
| L-1 | 41.30739 (0.78605) | 40.14746 (0.91095) | 48.24352 (0.91235) | 47.19567 (1.03426) | 40.32924 (0.74479) | 27.67641 (0.42484) | 32.61238 (0.53586) | 32.8494 (0.4831) |
| L-2 | 54.56206 (0.91428) | 58.65616 (1.06783) | 68.54698 (0.8875) | 74.00147 (1.09136) | 53.09332 (0.76509) | 37.0229 (0.4834) | 41.52311 (0.56277) | 42.38986 (0.58594) |
| L-3 | 114.83236 (2.08432) | 134.3758 (2.43628) | 95.65601 (1.43781) | 102.51199 (1.68005) | 123.16977 (2.70735) | 88.68501 (1.4142) | 106.0427 (1.87293) | 105.54697 (2.03414) |

Table I.9: The prediction error comparison table for each simulation setting in Section 8.2 when $(p, q) = (50, 20)$. The values are the mean squared prediction errors averaged over 50 independent replications. The numbers in parentheses are normalized sample standard deviations. The column labels are defined in Section 7 and 8.1. The labels 1, 2, 3 indicate the sparsity levels $(s_1, s_2) = (0.5, 0.5), (0.5, 1), (1, 1)$, respectively. Boldface indicates the best non-oracle model. The oracle estimator is on the sixth column.

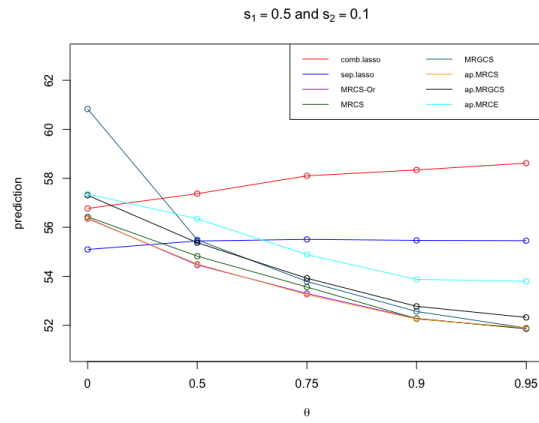
| Model error comparison table: Setting G-L | | | | | | | | |
|---|------------------------|------------------------|-------------------------------|------------------------------|------------------------------|------------------------|------------------------------|-------------------------------|
| θ | LAS | LASP | c.ridge | s.ridge | ap.MRCE | MRCS-Or | ap.MRCS | ap.MRGCS |
| G-1 | 79.22513 (2.6801) | 78.44911 (3.53157) | 79.32835 (2.58437) | 74.85925 (3.13839) | 82.873 (3.19515) | 51.75728 (2.63026) | 84.70892 (3.41663) | 85.10121 (3.24324) |
| G-2 | 128.43497 (1.6269) | 149.90534 (2.69274) | 129.98387 (1.40837) | 141.3373 (1.75774) | 129.36042 (1.68617) | 106.48232 (1.5894) | 127.91495 (1.60924) | 127.78541 (1.68485) |
| G-3 | 255.07622 (2.67378) | 289.50646 (4.11213) | 206.12884 (2.24085) | 219.84926 (2.46772) | 250.77437 (3.12734) | 254.81208 (7.56453) | 256.07743 (2.88895) | 255.29228 (2.94745) |
| H-1 | 53.30905 (1.94869) | 53.94632 (2.3202) | 59.2235 (1.8695) | 55.06309 (2.10927) | 53.11528 (1.58724) | 37.55906 (1.71661) | 55.81225 (1.51831) | 56.12208 (1.49101) |
| H-2 | 100.77962 (1.64842) | 107.93918 (1.99683) | 100.9323 (1.15675) | 110.91099 (1.44178) | 96.05866 (1.51918) | 78.34487 (1.2776) | 95.12575 (1.47348) | 94.95246 (1.4557) |
| H-3 | 186.61943 (2.6937) | 221.7338 (3.31687) | 150.47592 (1.88186) | 166.05064 (2.16387) | 189.81258 (2.41599) | 192.20289 (3.2429) | 201.54967 (2.73932) | 201.03727 (2.8289) |
| I-1 | 24.90288 (0.75135) | 23.50231 (0.73593) | 32.5863 (0.89479) | 31.48974 (1.03914) | 24.09418 (0.74172) | 13.62827 (0.47499) | 17.1114 (0.50828) | 17.767 (0.50074) |
| I-2 | 39.4262 (0.72589) | 44.12001 (0.93035) | 53.81345 (0.84404) | 59.00468 (0.9907) | 37.95985 (0.68486) | 24.13748 (0.53432) | 27.96343 (0.62822) | 28.39407 (0.60723) |
| I-3 | 100.15207 (1.89651) | 116.5759 (2.48215) | 81.16564 (1.31368) | 86.18903 (1.385) | 107.01062 (2.40456) | 79.39258 (1.64254) | 93.80389 (1.49155) | 92.19276 (1.60842) |
| J-1 | 75.66905 (2.34009) | 74.35807 (3.06346) | 75.04052 (1.9716) | 70.96314 (2.64702) | 79.72131 (2.48701) | 39.70002 (2.29301) | 78.60089 (2.25136) | 80.43842 (2.22912) |
| J-2 | 123.05243 (1.45407) | 142.89941 (2.26714) | 126.66689 (1.34028) | 137.30797 (1.84595) | 125.71054 (1.67539) | 89.74062 (2.62063) | 122.1067 (1.47239) | 121.70773 (1.43164) |
| J-3 | 242.40282 (2.46072) | 273.05055 (3.10686) | 190.55096 (1.8896) | 205.75307 (2.32508) | 234.32533 (2.55086) | 226.40655 (9.36907) | 241.93481 (2.29192) | 242.32914 (2.16553) |
| K-1 | 56.05778 (1.6237) | 57.35036 (2.21442) | 61.68682 (1.44577) | 57.58781 (1.61418) | 54.53711 (1.49022) | 29.86232 (1.43188) | 54.58814 (1.52938) | 55.61436 (1.64884) |
| K-2 | 94.47923 (1.23192) | 102.03861 (2.0064) | 97.0119 (0.99208) | 107.00942 (1.61376) | 90.88292 (1.1931) | 66.47393 (1.93766) | 89.82406 (1.18895) | 90.11066 (1.17277) |
| K-3 | 178.01675 (2.00415) | 218.52553 (4.17954) | 146.56115 (1.50611) | 160.68305 (2.29974) | 181.12488 (2.38633) | 159.33957 (4.90595) | 189.23007 (2.93437) | 187.32817 (2.69811) |
| L-1 | 24.8693 (0.72842) | 23.563 (0.823) | 31.86869 (0.89224) | 30.74856 (1.0197) | 23.96931 (0.7297) | 11.59146 (0.37133) | 16.40505 (0.48437) | 16.62412 (0.43348) |
| L-2 | 38.17885 (0.82051) | 42.18953 (0.94958) | 51.93105 (0.73181) | 57.10291 (0.95249) | 36.72201 (0.64068) | 20.95248 (0.43382) | 25.36067 (0.48927) | 26.15182 (0.51303) |
| L-3 | 97.06229 (2.01866) | 115.93181 (2.34998) | 78.21545 (1.33738) | 84.9697 (1.51183) | 105.08442 (2.50173) | 71.35839 (1.43838) | 88.28659 (1.76157) | 88.02542 (1.91513) |

Table I.10: The model error comparison table for each simulation setting in Section 8.2 when $(p, q) = (50, 20)$. The values are the mean squared prediction errors averaged over 50 independent replications. The numbers in parentheses are normalized sample standard deviations. The column labels are defined in Section 7 and 8.1. The labels 1, 2, 3 indicate the sparsity levels $(s_1, s_2) = (0.5, 0.5), (0.5, 1), (1, 1)$, respectively. Boldface indicates the best non-oracle model. The oracle estimator is on the sixth column.

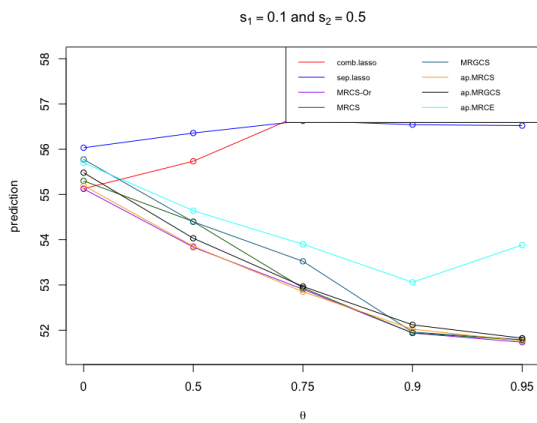
Appendix I.2. Additional plots for Section 7.1



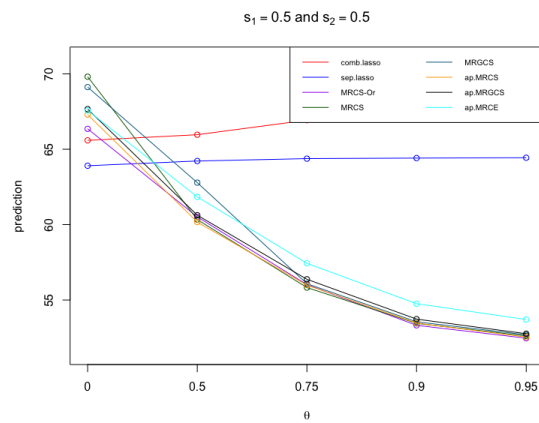
(a) (0.1, 0.1)



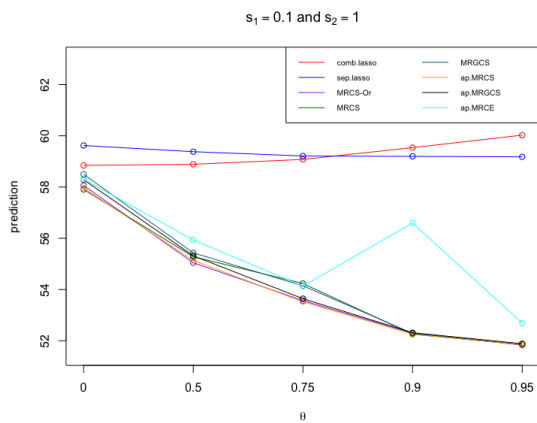
(b) (0.5, 0.1)



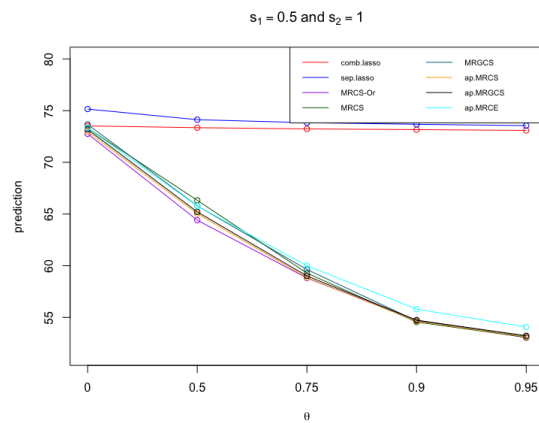
(c) (0.1, 0.5)



(d) (0.5, 0.5)



(e) (0.1, 1)



(f) (0.5, 1)

Figure I.19: Prediction plots: Two numbers in each bracket stand for (s_1, s_2) when $(p, q) = (20, 50)$.

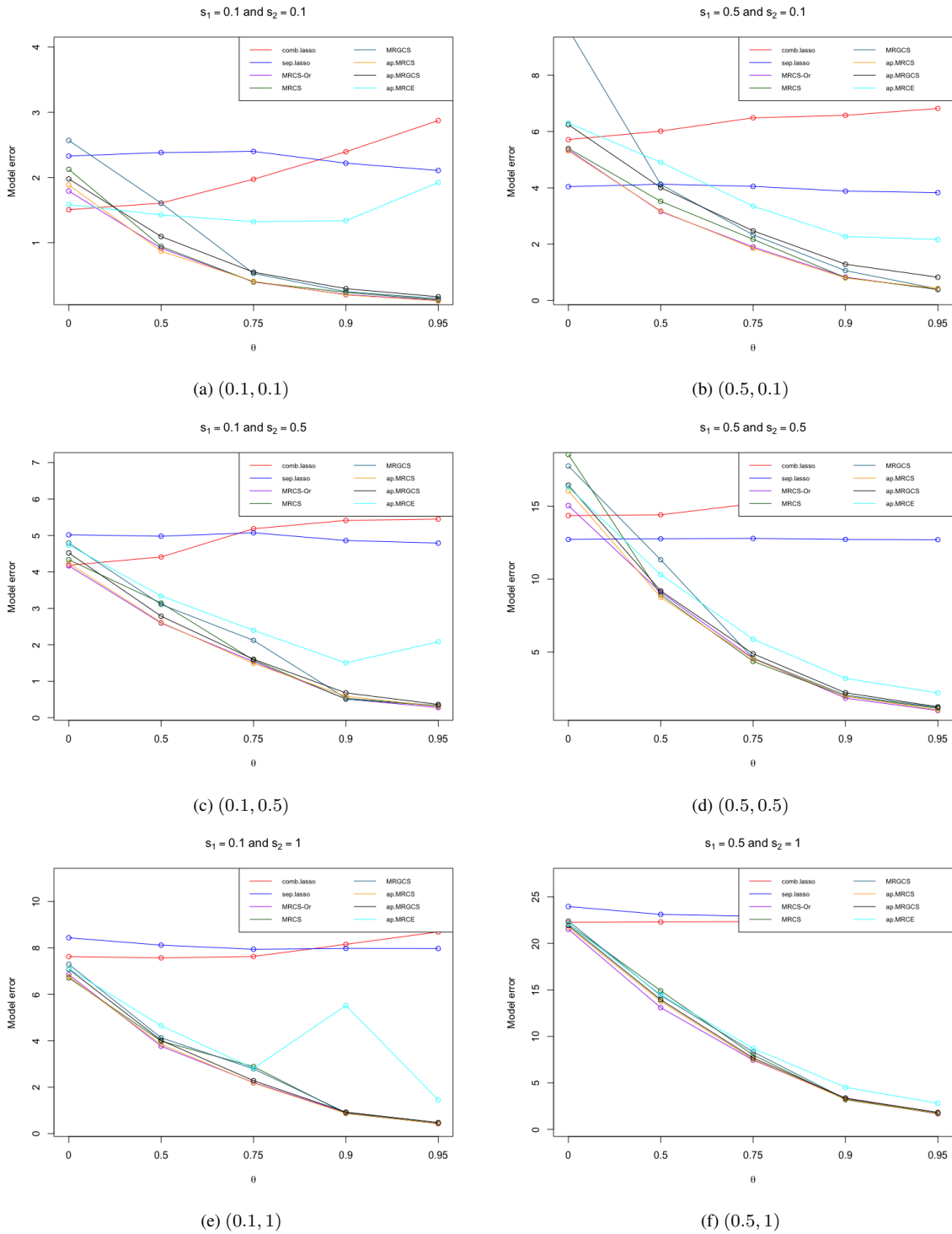


Figure I.20: Model error plots: Two numbers in each bracket stand for (s_1, s_2) when $(p, q) = (20, 50)$.

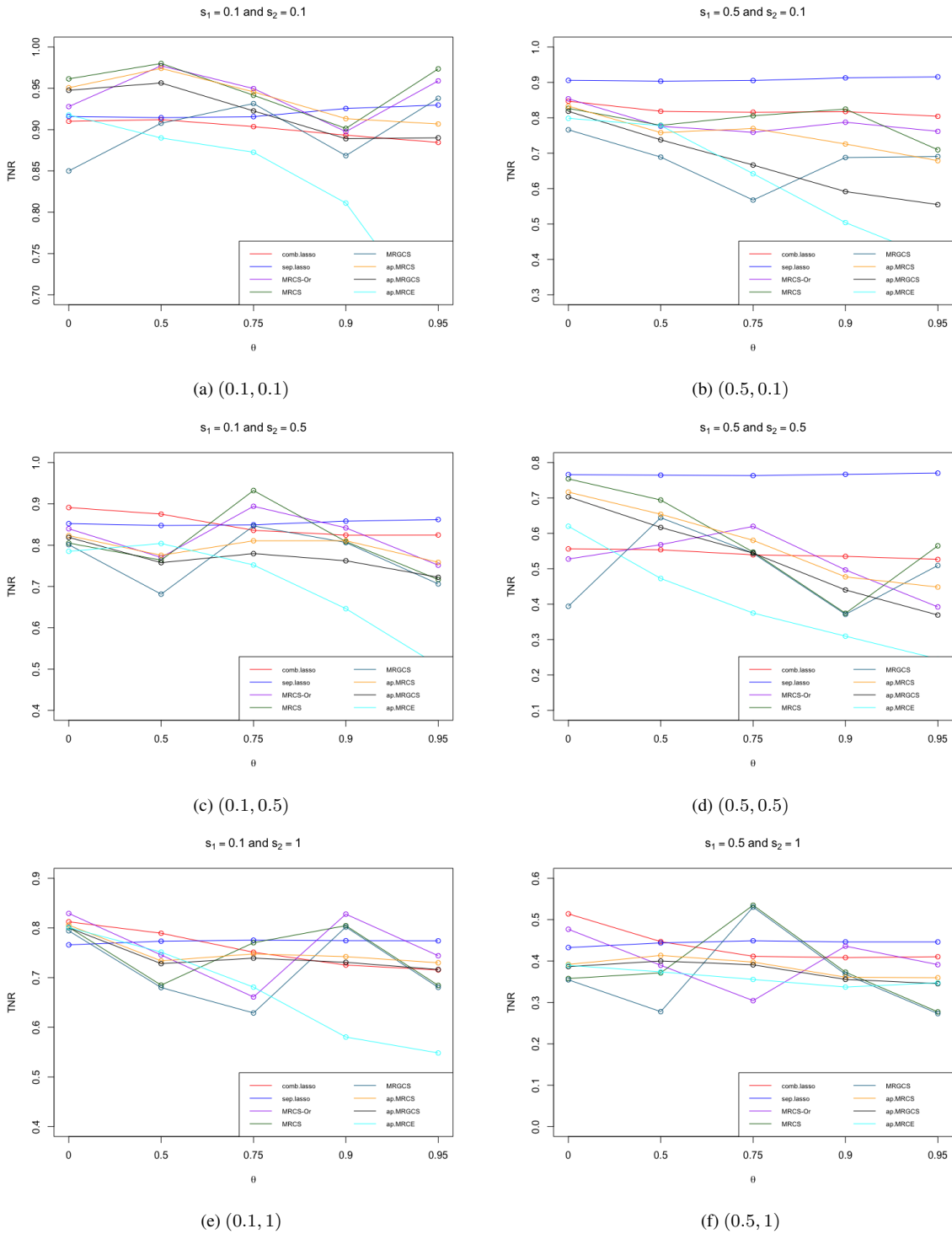


Figure I.21: TNR plots: Two numbers in each bracket stand for (s_1, s_2) when $(p, q) = (20, 50)$.

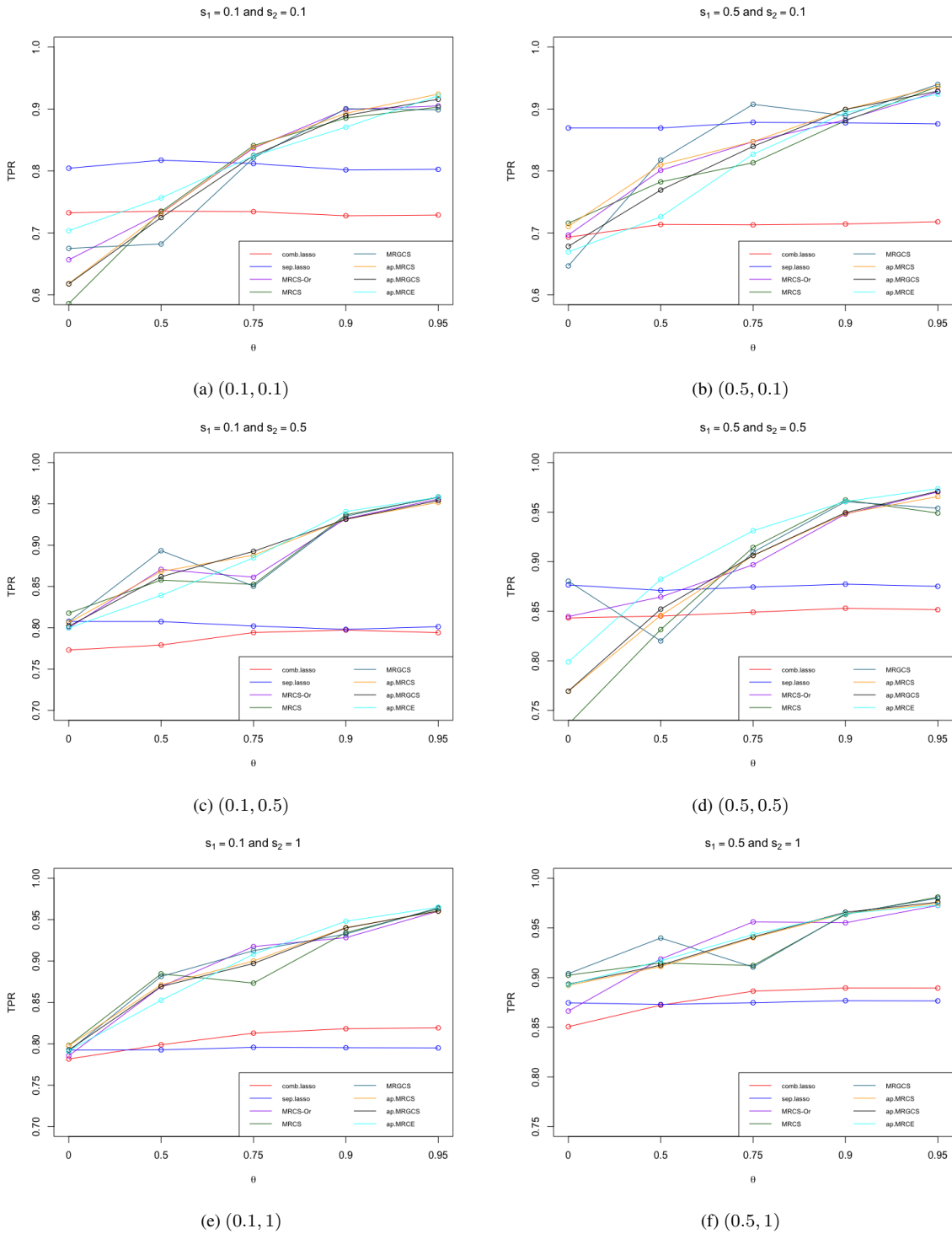


Figure I.22: TPR plots: Two numbers in each bracket stand for (s_1, s_2) when $(p, q) = (20, 50)$.

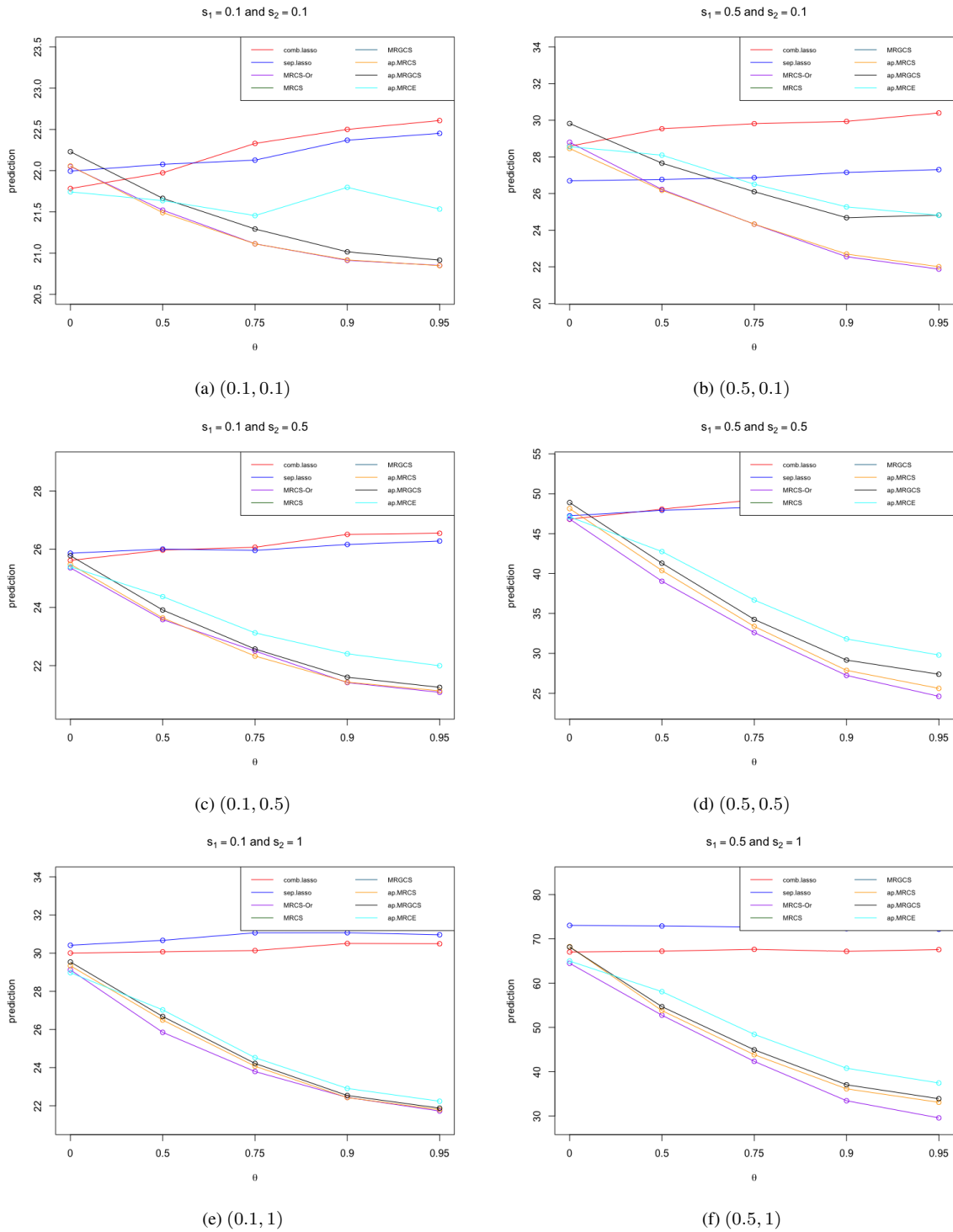


Figure I.23: Prediction plots: Two numbers in each bracket stand for (s_1, s_2) when $(p, q) = (50, 20)$.

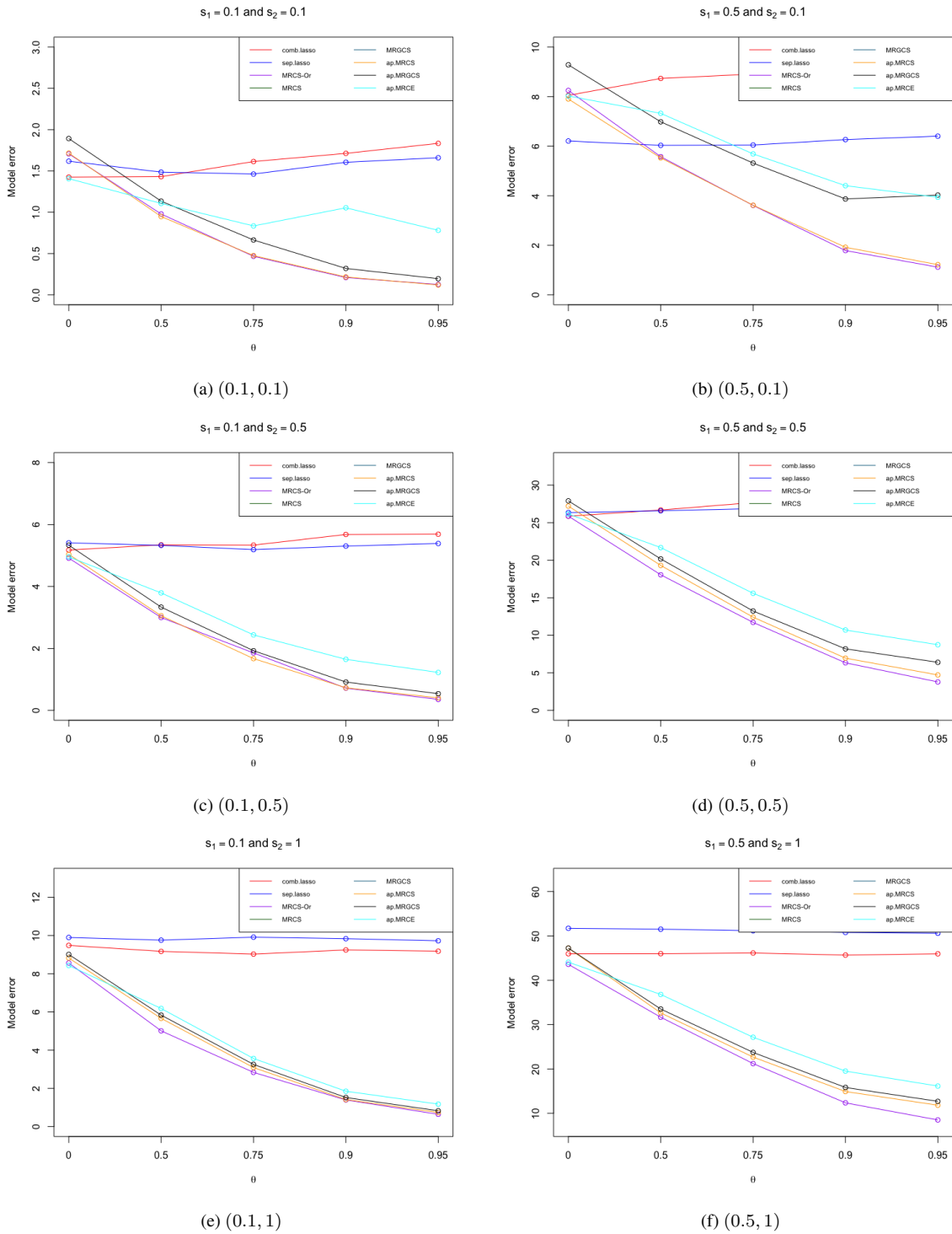


Figure I.24: Model error plots: Two numbers in each bracket stand for (s_1, s_2) when $(p, q) = (50, 20)$.

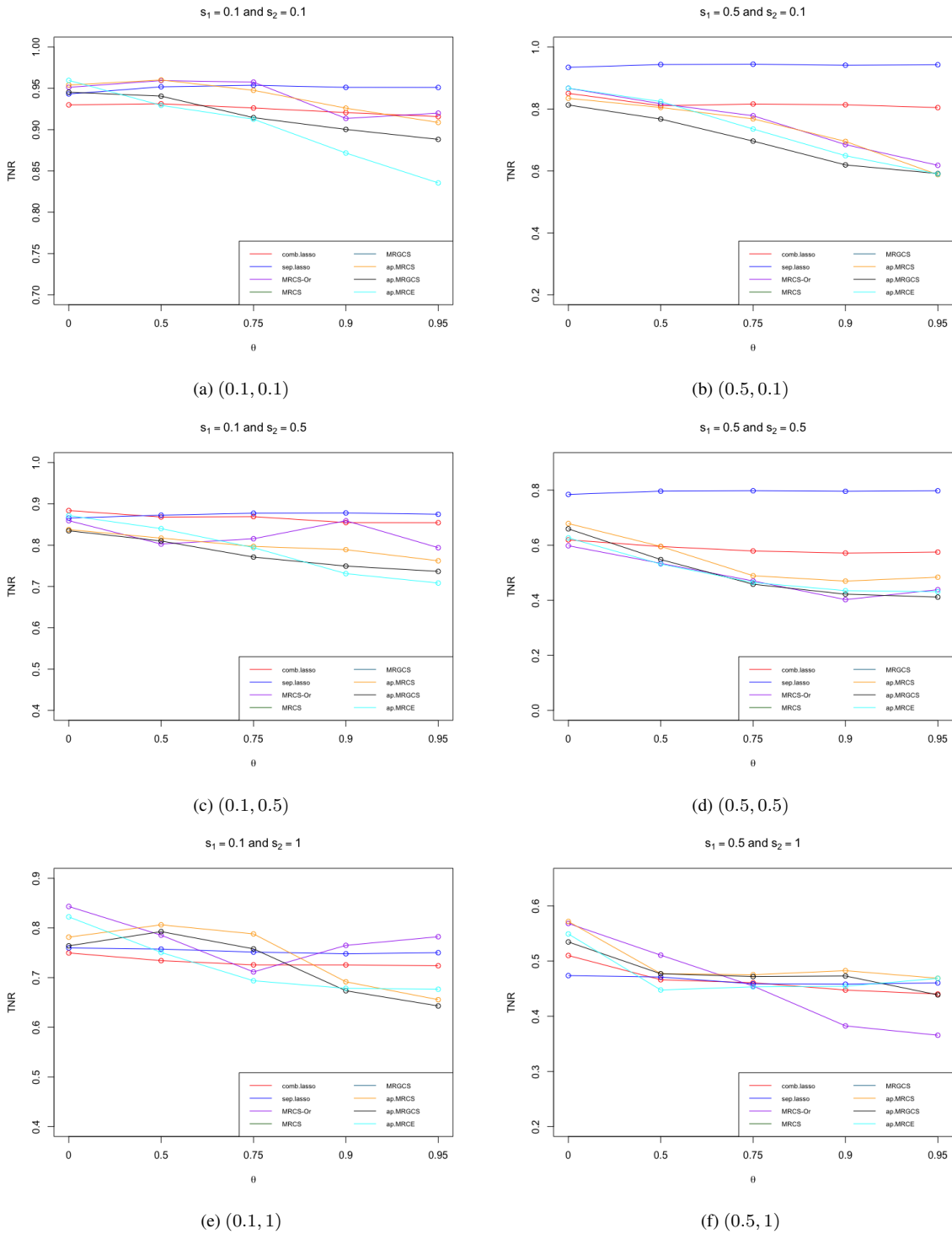


Figure I.25: TNR plots: Two numbers in each bracket stand for (s_1, s_2) when $(p, q) = (50, 20)$.

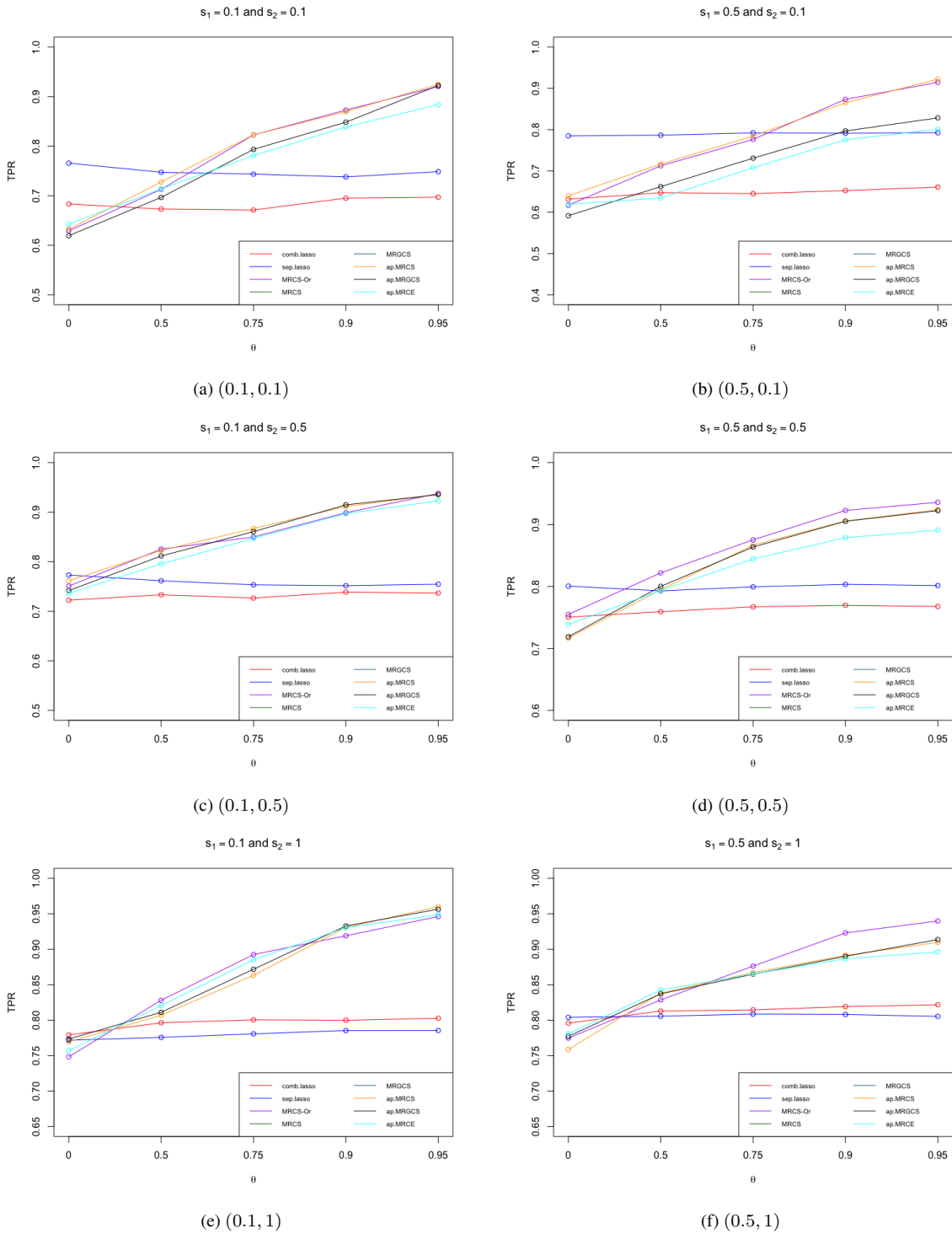


Figure I.26: TPR plots: Two numbers in each bracket stand for (s_1, s_2) when $(p, q) = (50, 20)$.

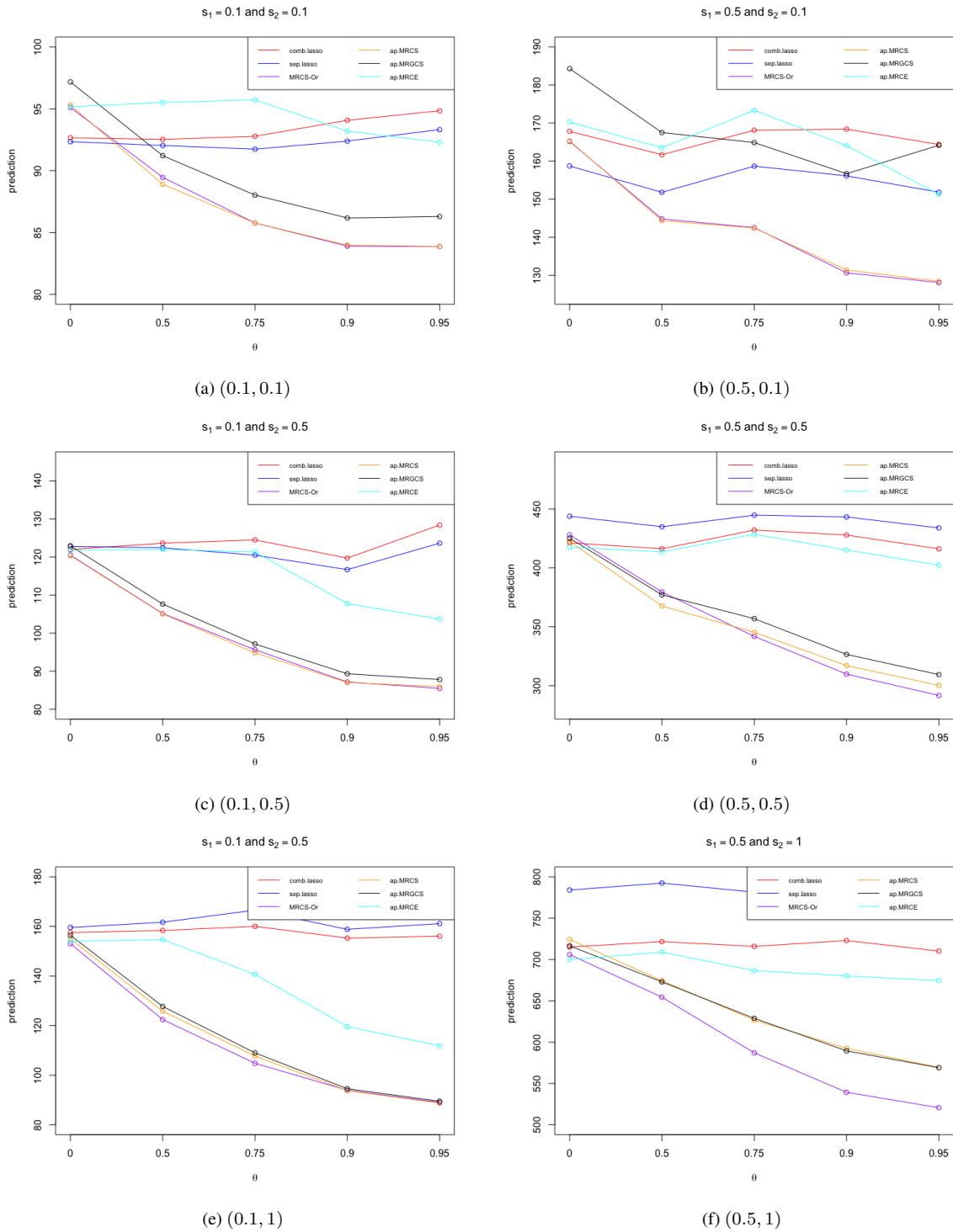
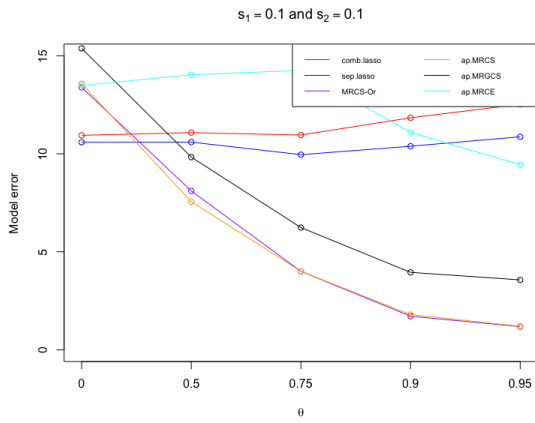
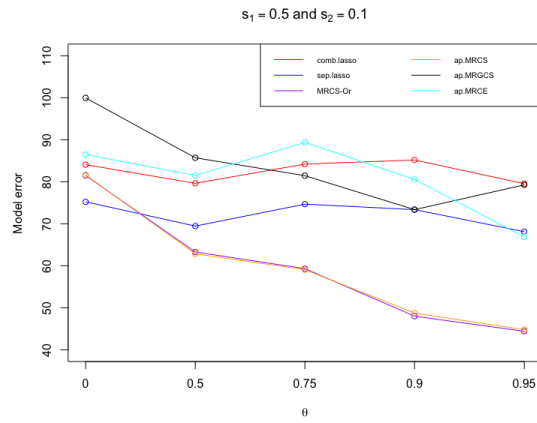


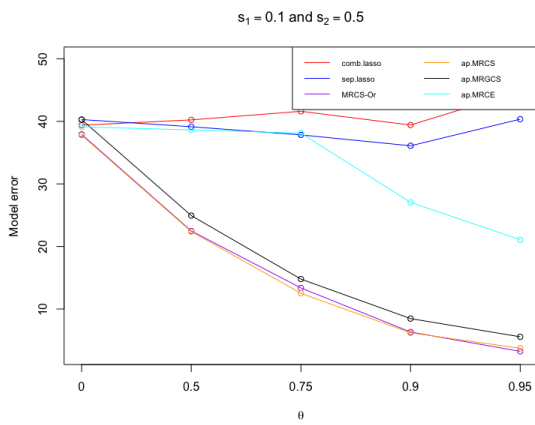
Figure I.27: Prediction plots: Two numbers in each bracket stand for (s_1, s_2) when $(p, q) = (80, 80)$.



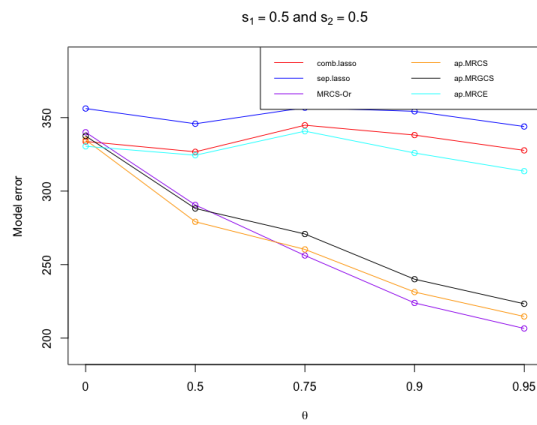
(a) (0.1, 0.1)



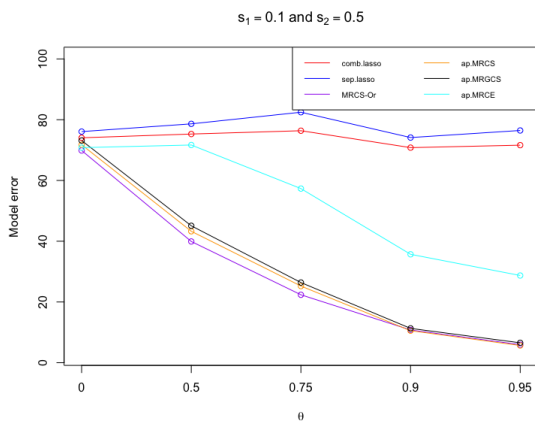
(b) (0.5, 0.1)



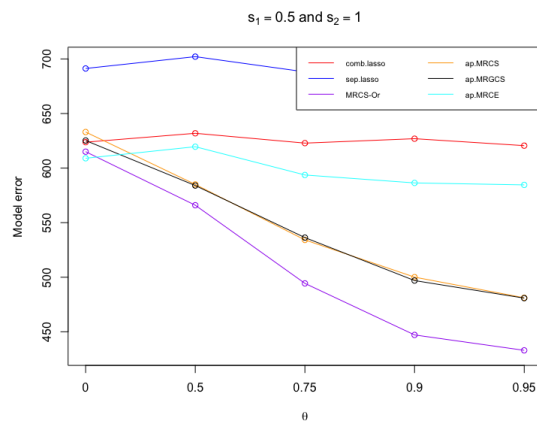
(c) (0.1, 0.5)



(d) (0.5, 0.5)



(e) (0.1, 1)



(f) (0.5, 1)

Figure I.28: Model error plots: Two numbers in each bracket stand for (s_1, s_2) when $(p, q) = (80, 80)$.

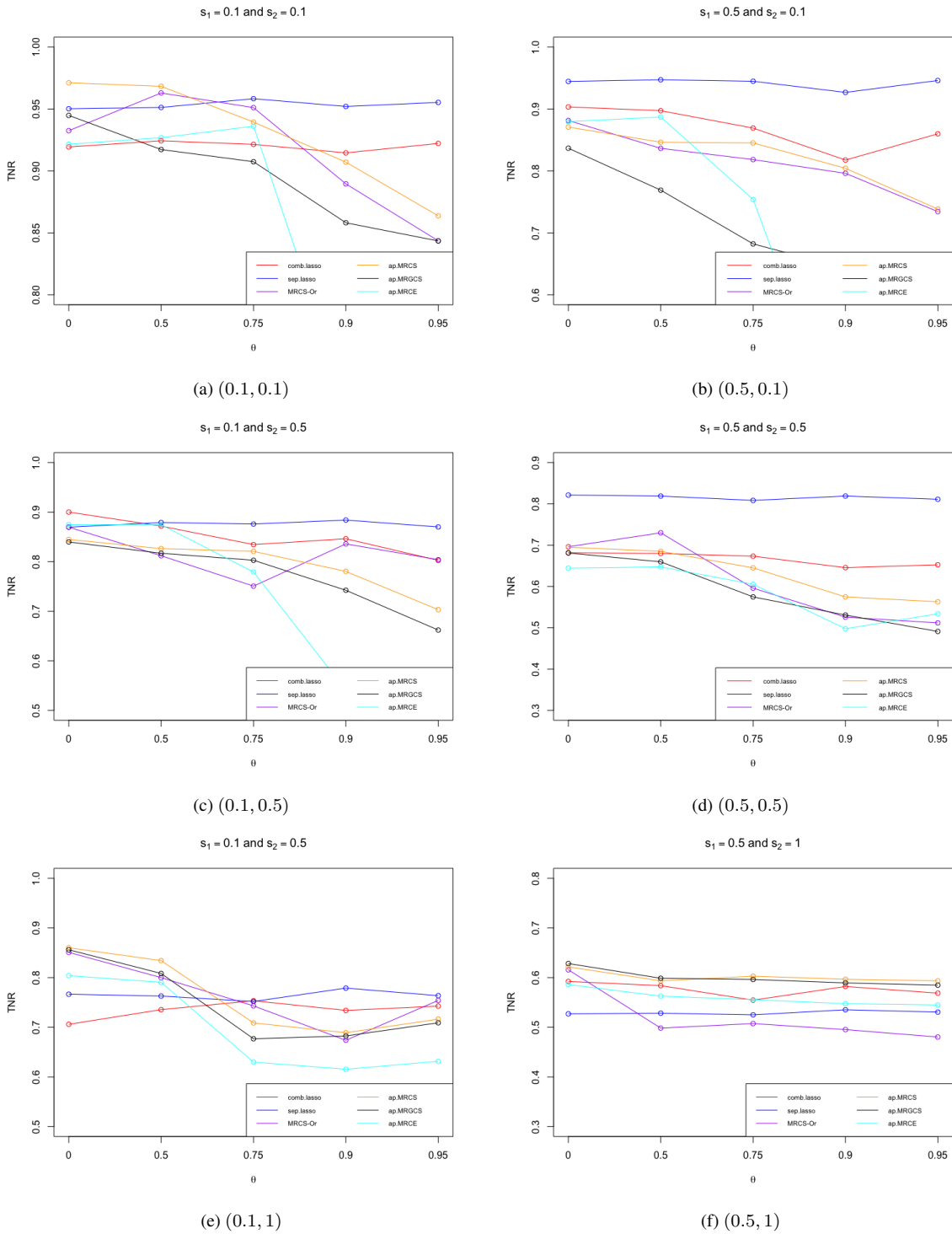


Figure I.29: TNR plots: Two numbers in each bracket stand for (s_1, s_2) when $(p, q) = (80, 80)$.

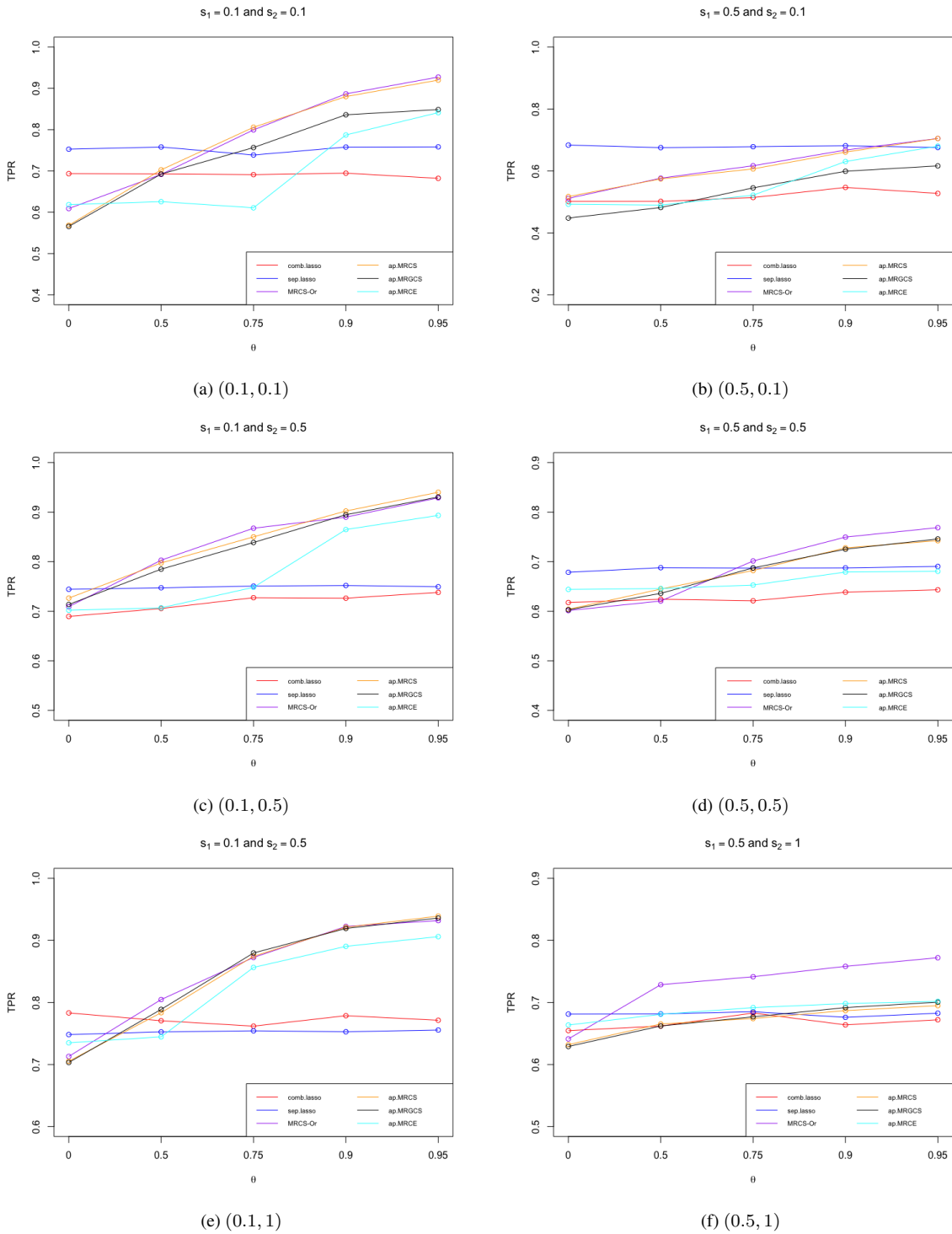


Figure I.30: TPR plots: Two numbers in each bracket stand for (s_1, s_2) when $(p, q) = (80, 80)$.

Appendix I.3. Additional plots for Section 7.2

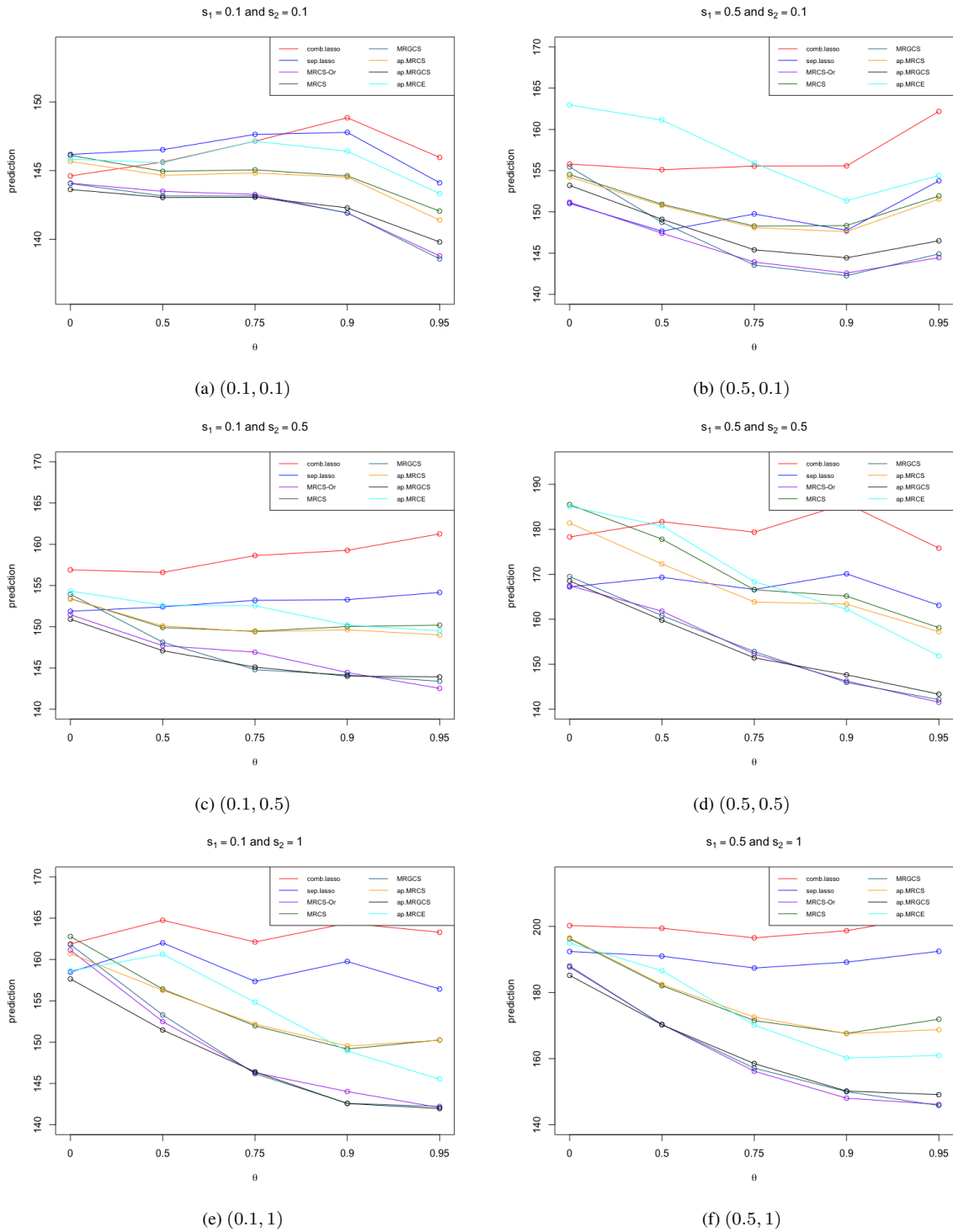


Figure I.31: Prediction plots: Two numbers in each bracket stand for (s_1, s_2) when $(p, q) = (20, 50)$.

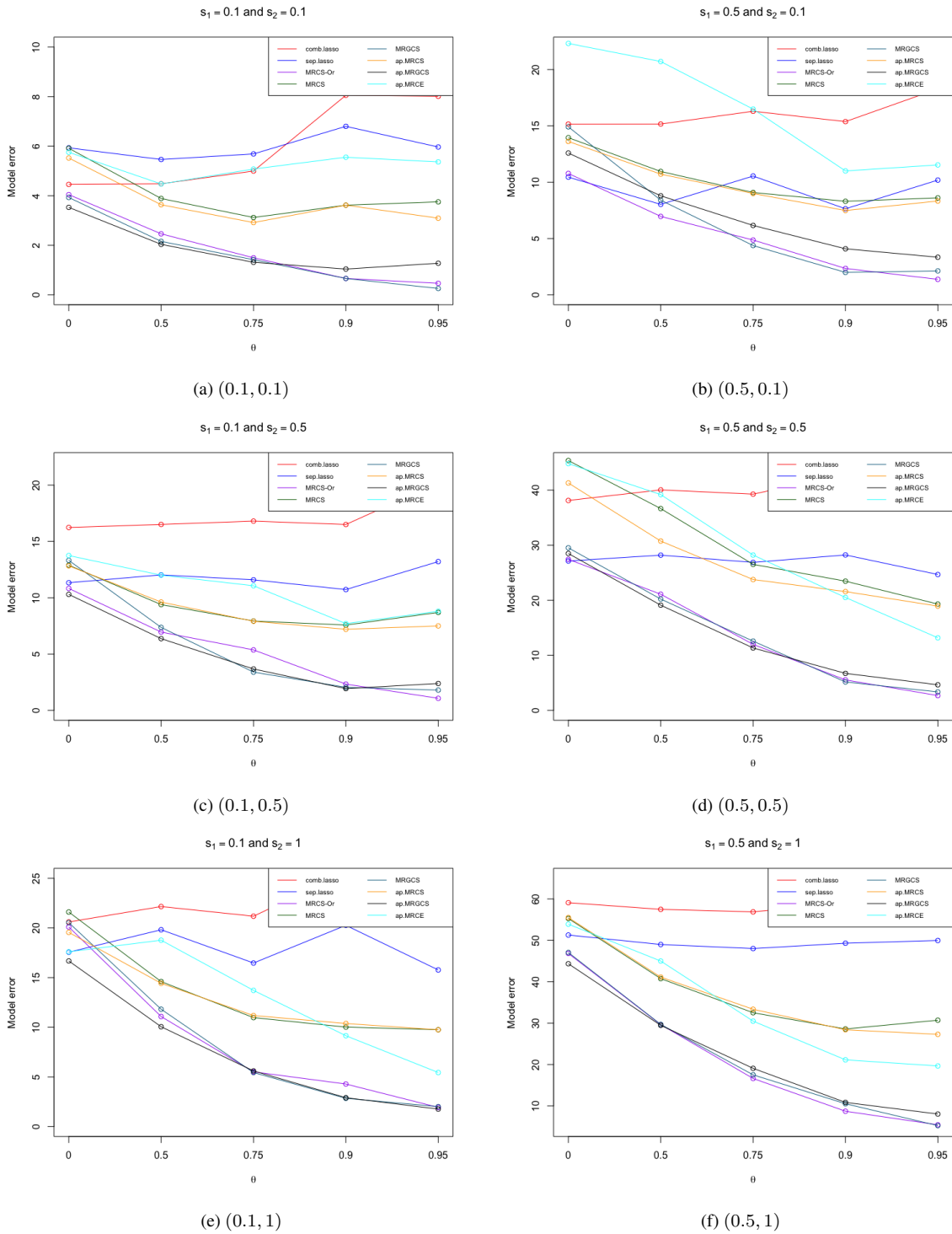


Figure I.32: Model error plots: Two numbers in each bracket stand for (s_1, s_2) when $(p, q) = (20, 50)$.

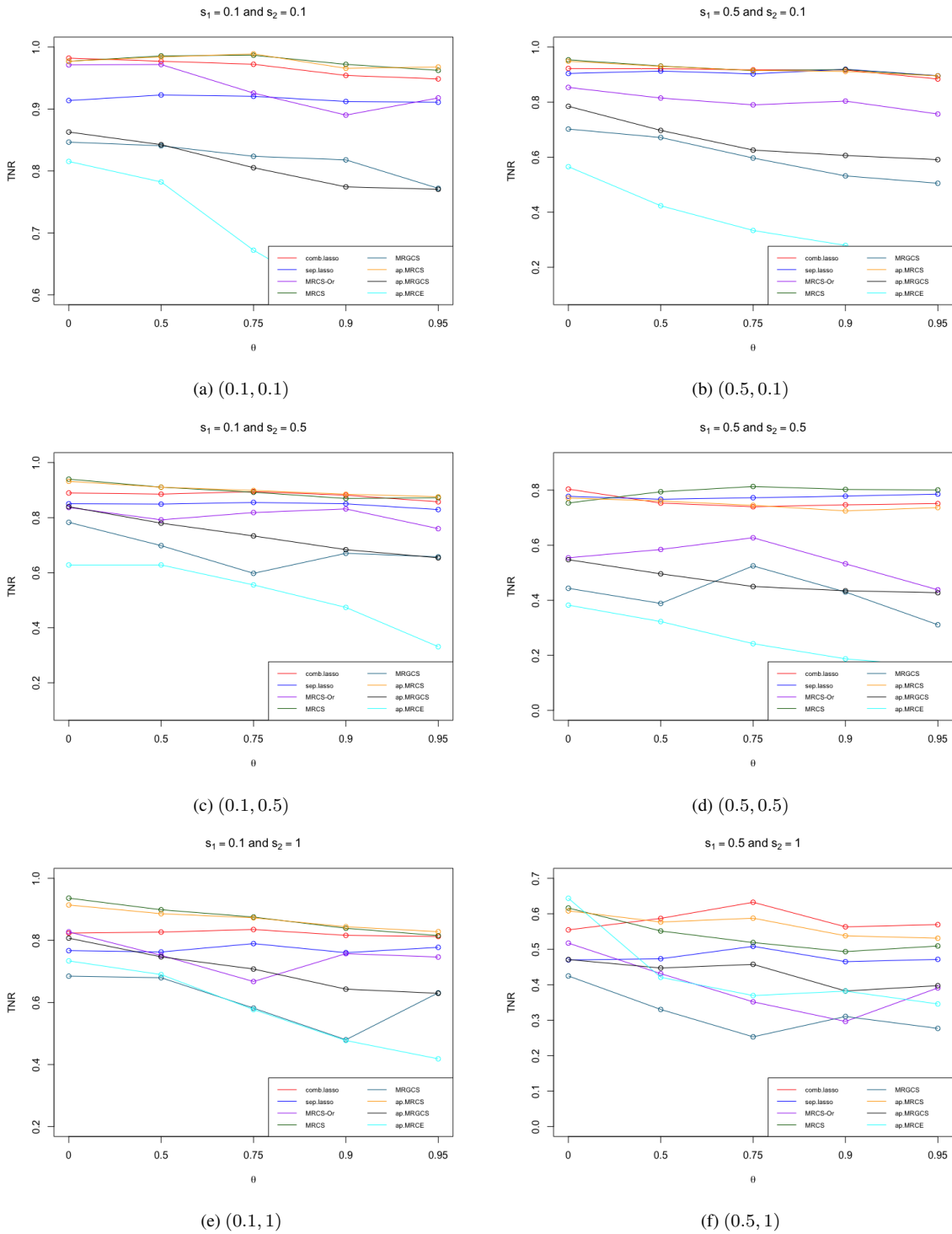


Figure I.33: TNR plots: Two numbers in each bracket stand for (s_1, s_2) when $(p, q) = (20, 50)$.

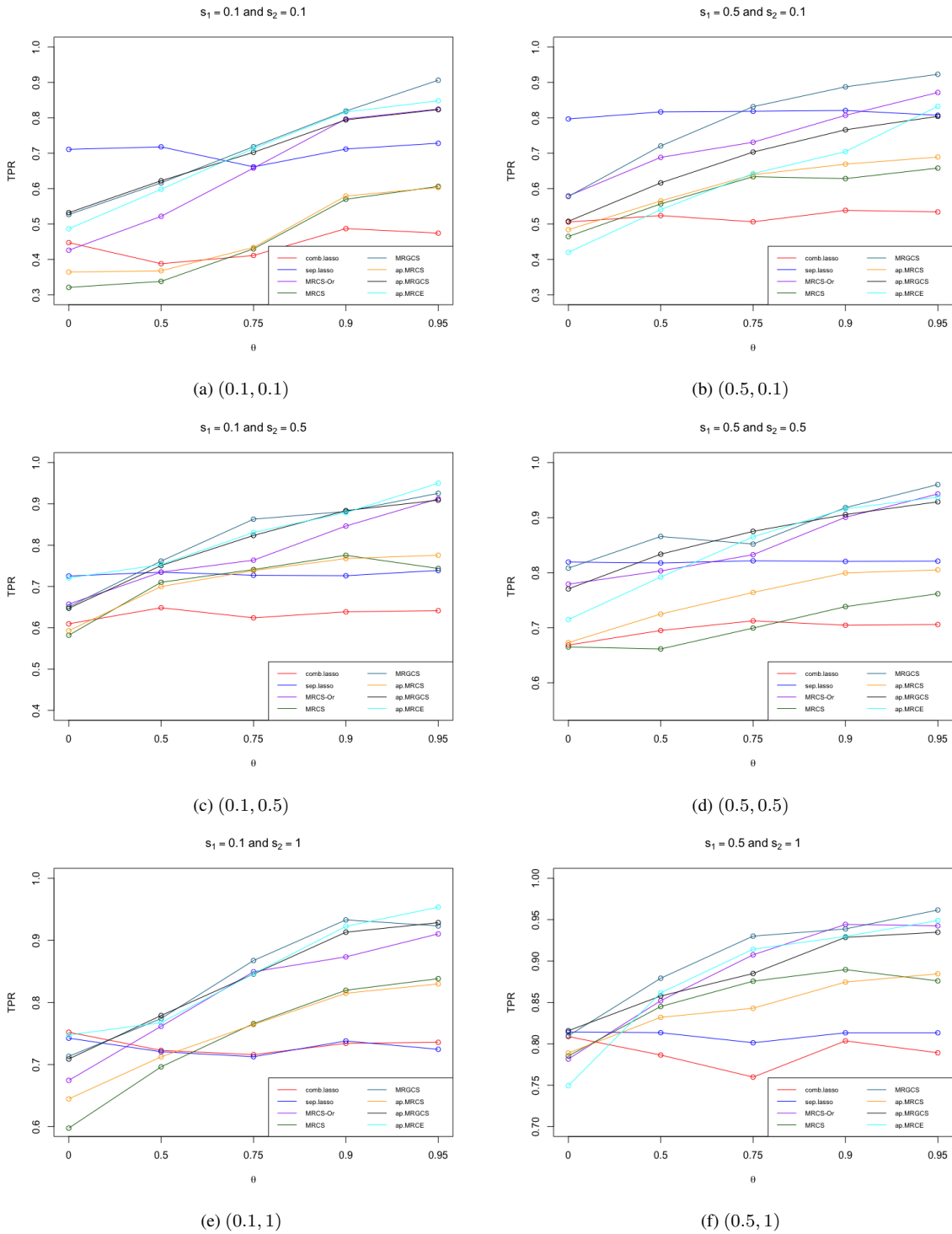


Figure I.34: TPR plots: Two numbers in each bracket stand for (s_1, s_2) when $(p, q) = (20, 50)$.

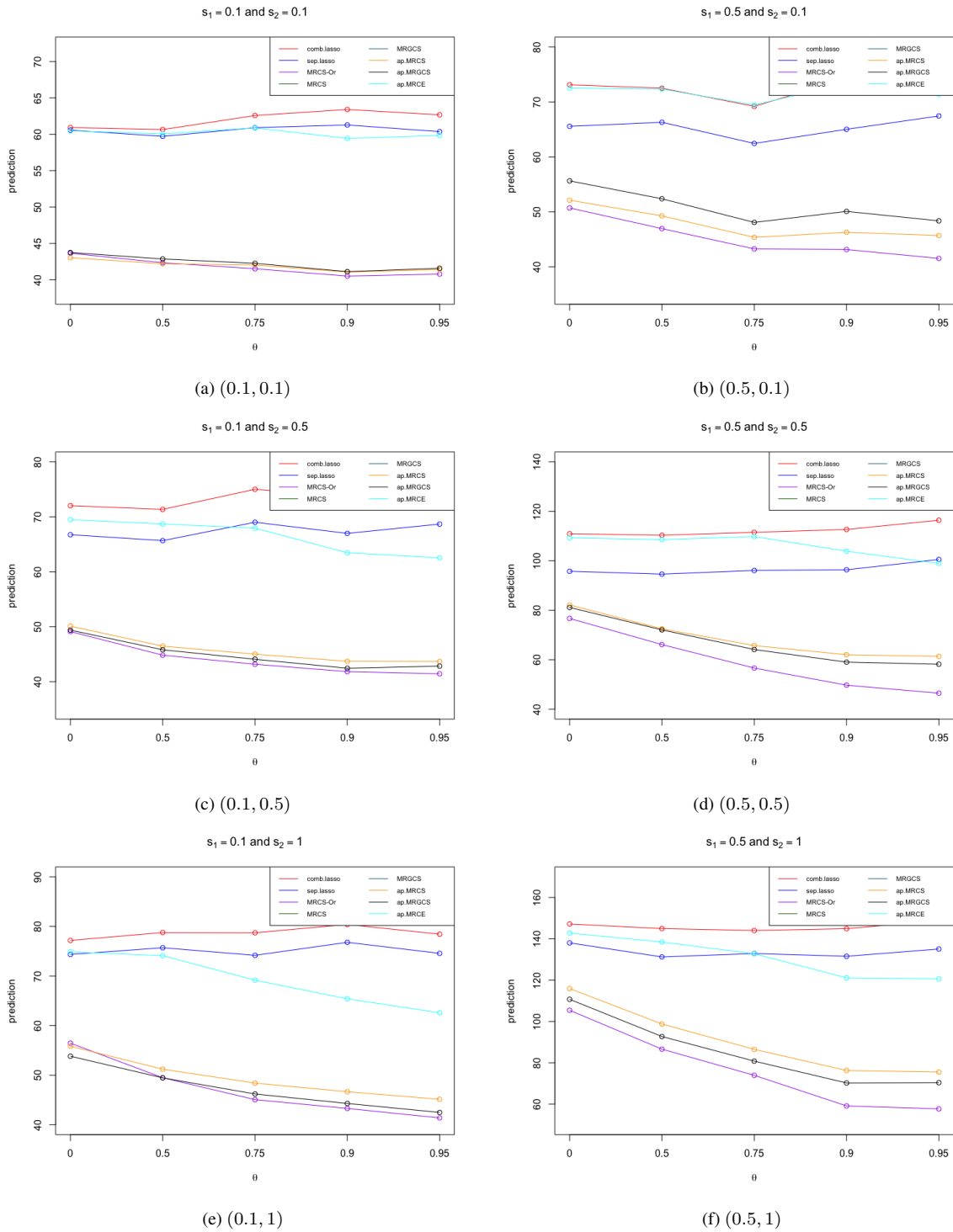


Figure I.35: Prediction plots: Two numbers in each bracket stand for (s_1, s_2) when $(p, q) = (50, 20)$.

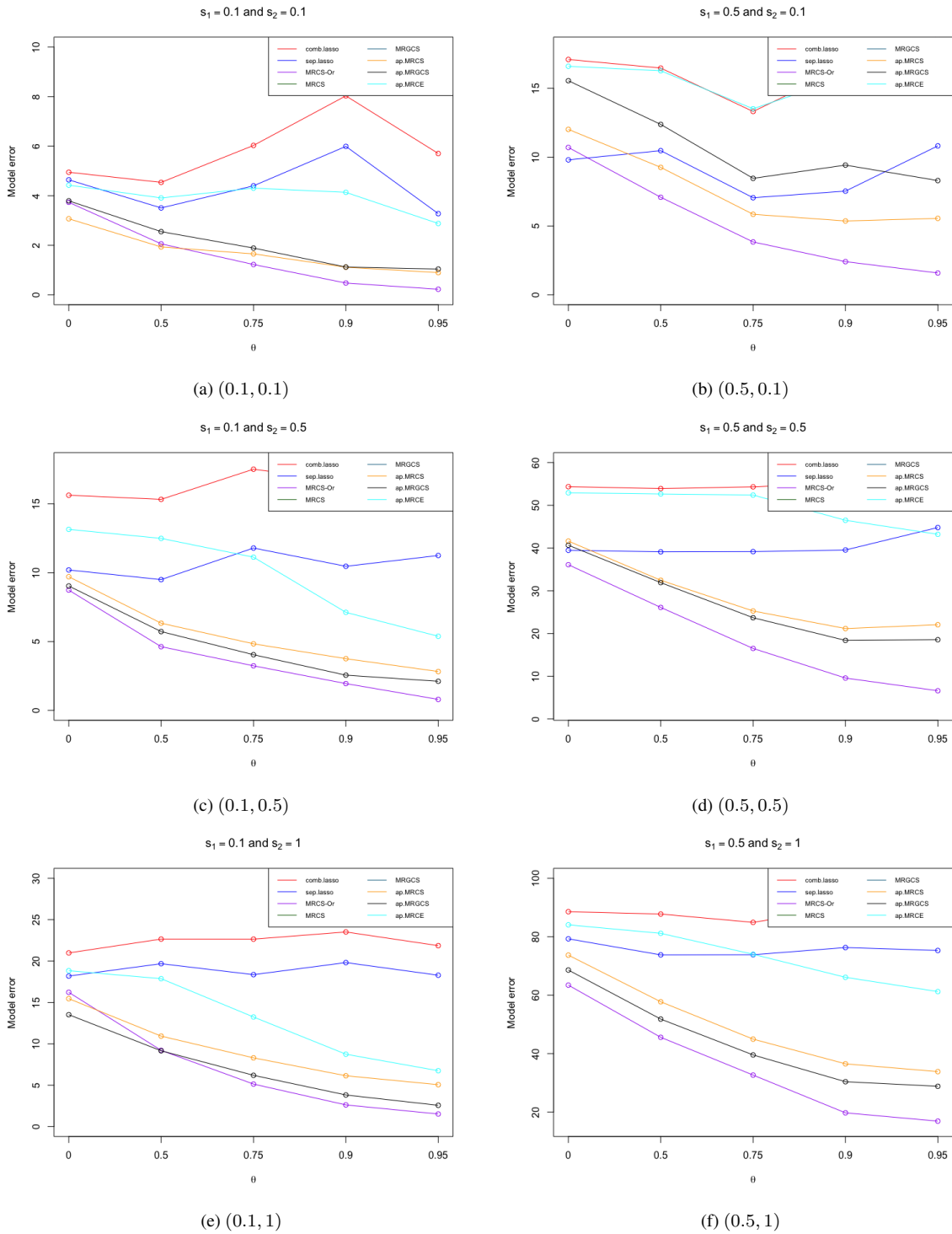


Figure I.36: Model error plots: Two numbers in each bracket stand for (s_1, s_2) when $(p, q) = (50, 20)$.

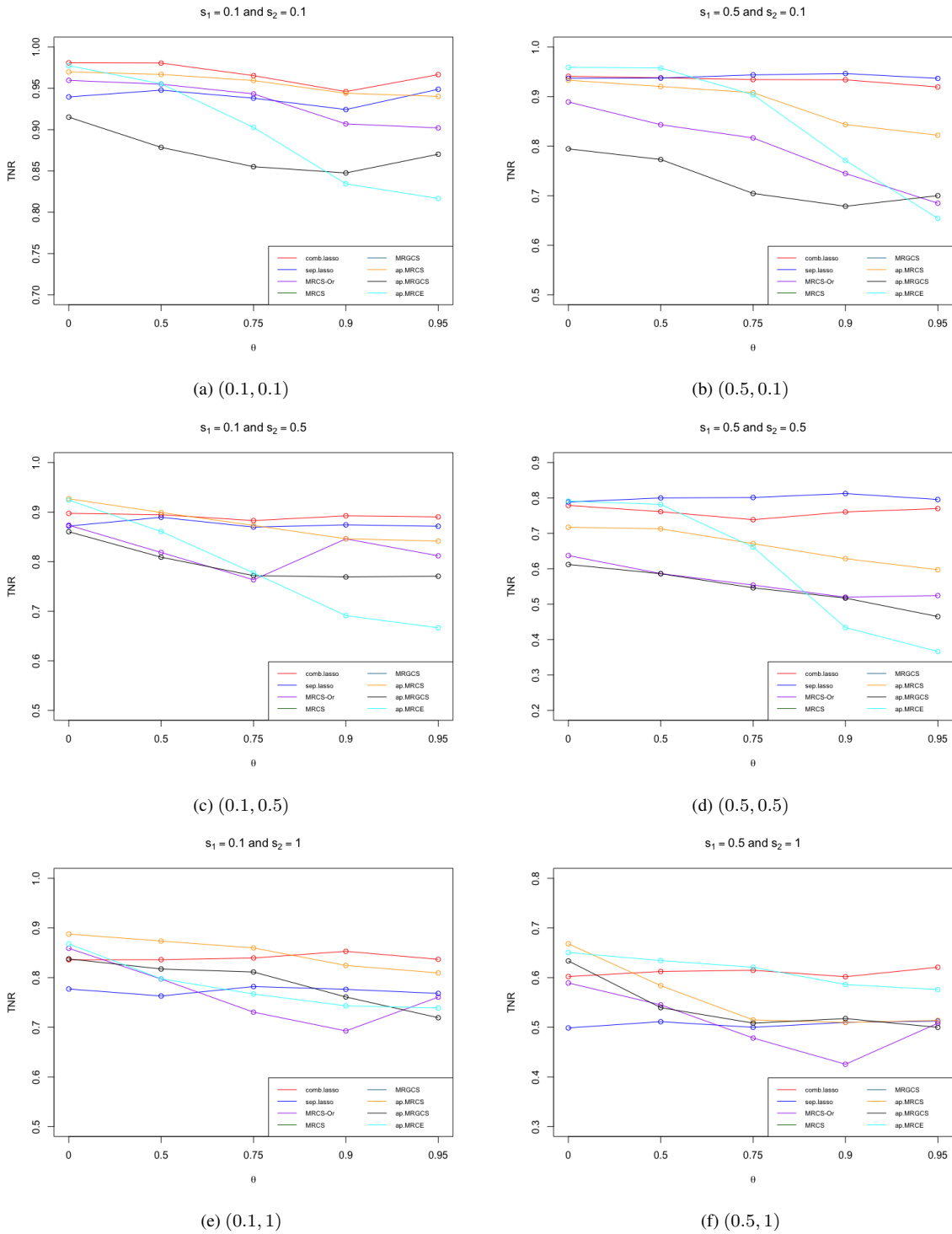


Figure I.37: TNR plots: Two numbers in each bracket stand for (s_1, s_2) when $(p, q) = (50, 20)$.

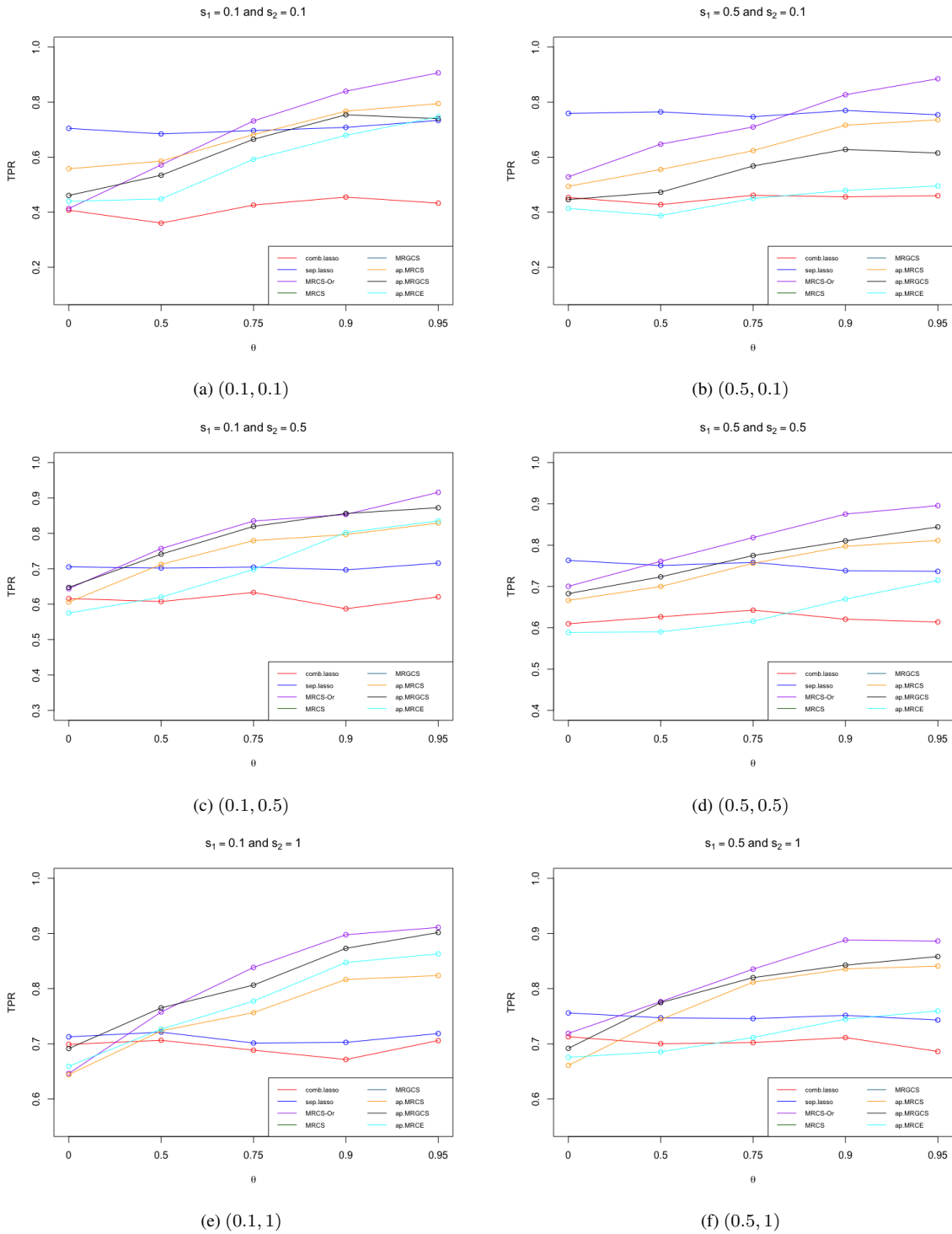


Figure I.38: TPR plots: Two numbers in each bracket stand for (s_1, s_2) when $(p, q) = (50, 20)$.

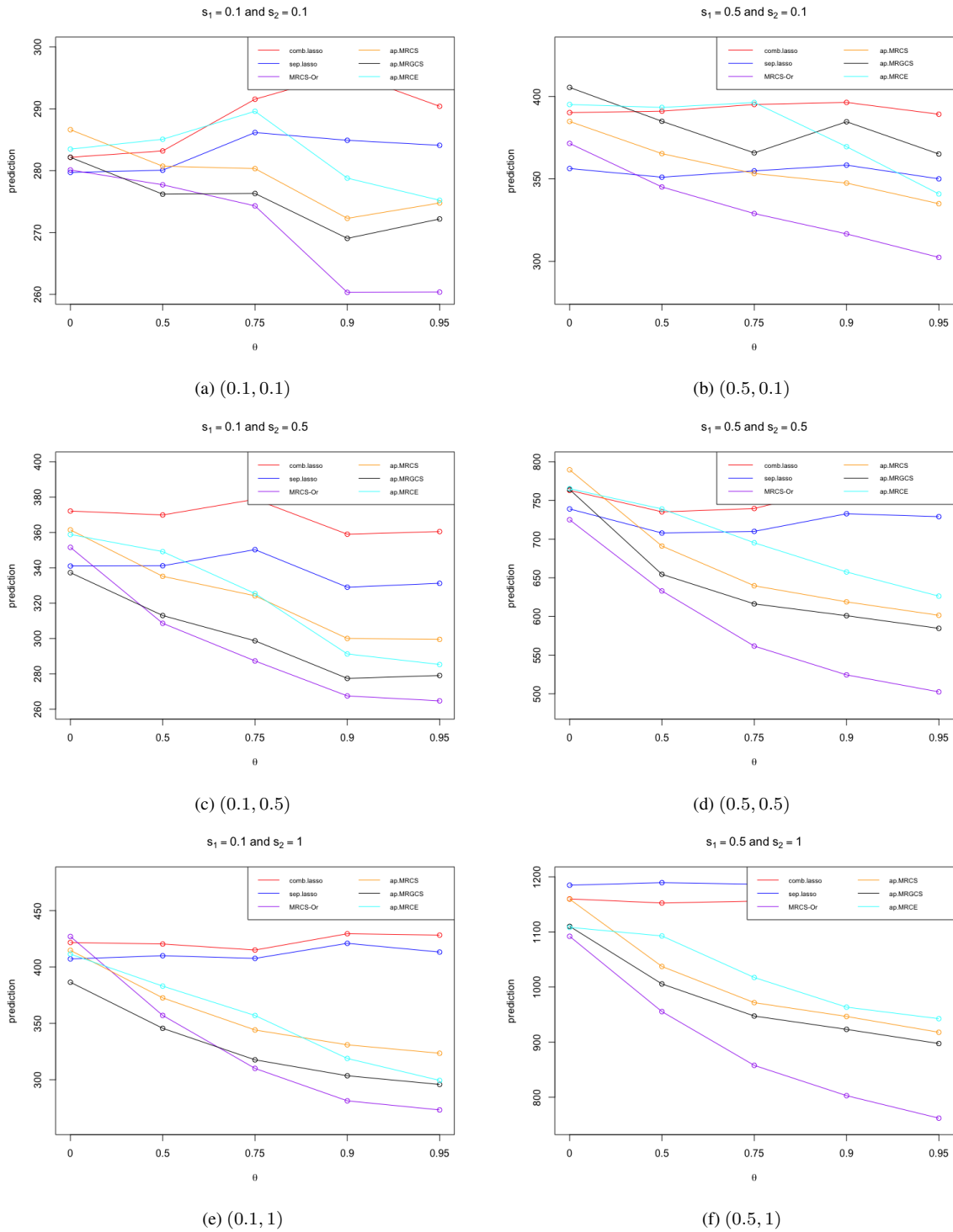


Figure I.39: Prediction plots: Two numbers in each bracket stand for (s_1, s_2) when $(p, q) = (80, 80)$.

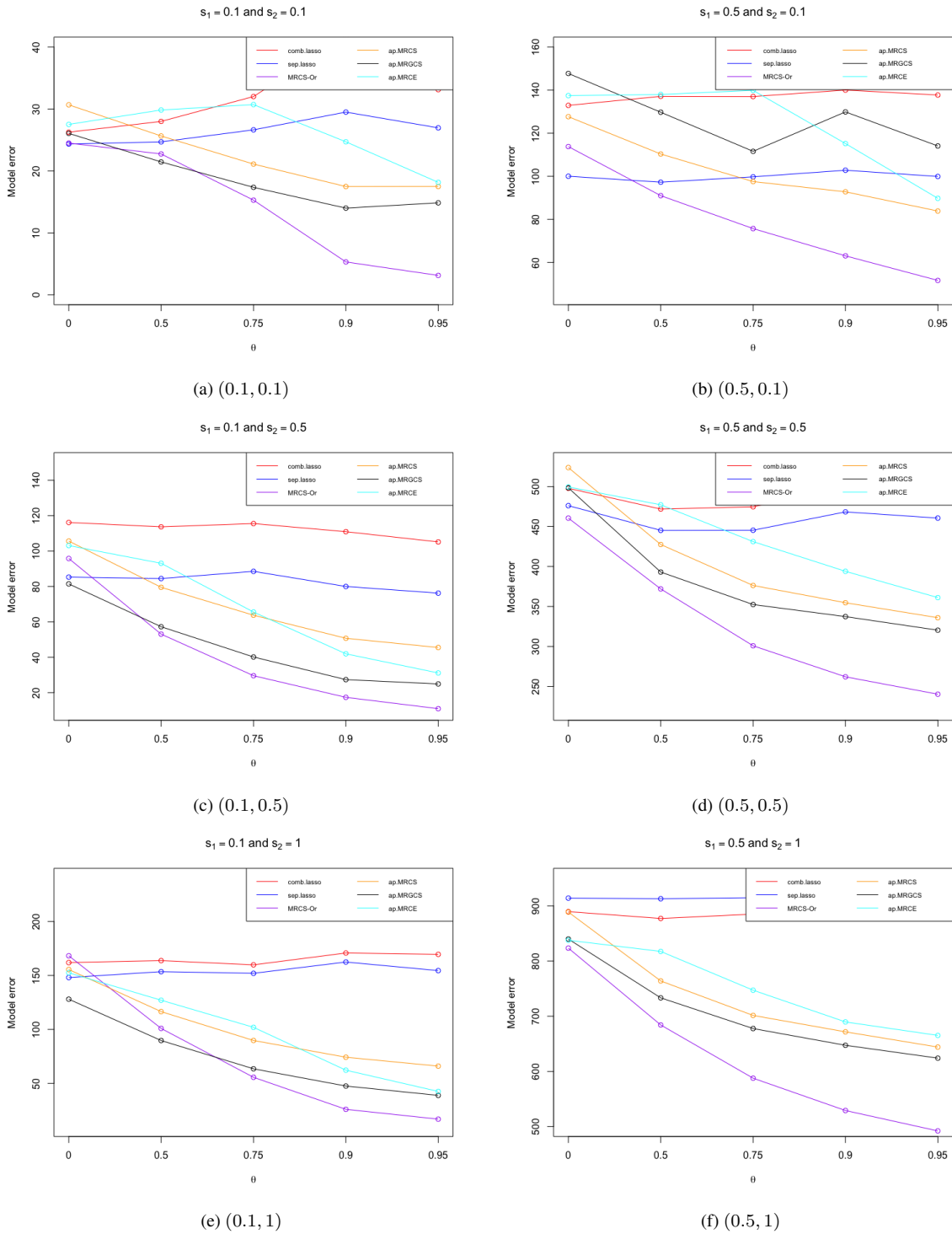


Figure I.40: Model error plots: Two numbers in each bracket stand for (s_1, s_2) when $(p, q) = (80, 80)$.

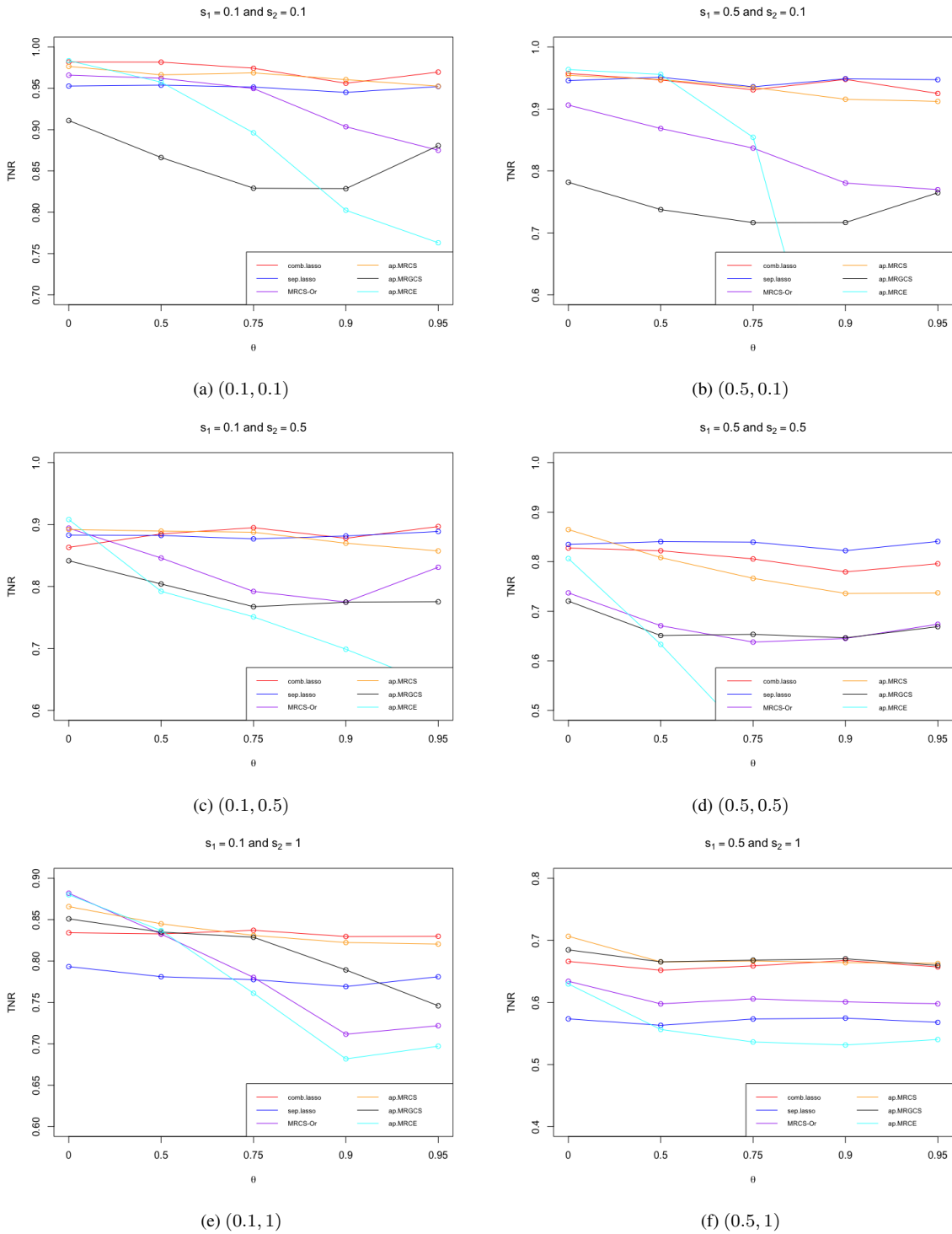


Figure I.41: TNR plots: Two numbers in each bracket stand for (s_1, s_2) when $(p, q) = (80, 80)$.

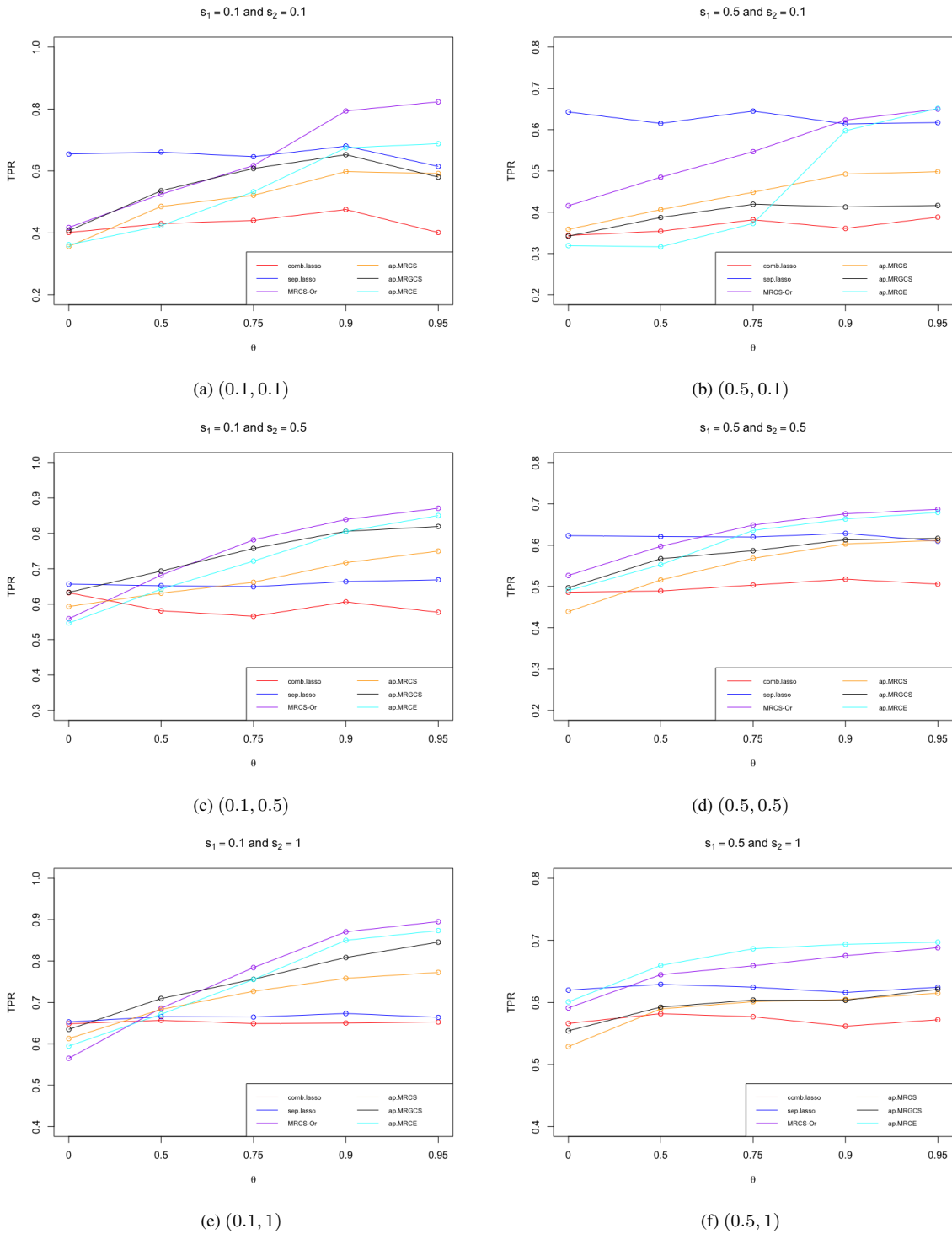


Figure I.42: TPR plots: Two numbers in each bracket stand for (s_1, s_2) when $(p, q) = (80, 80)$.

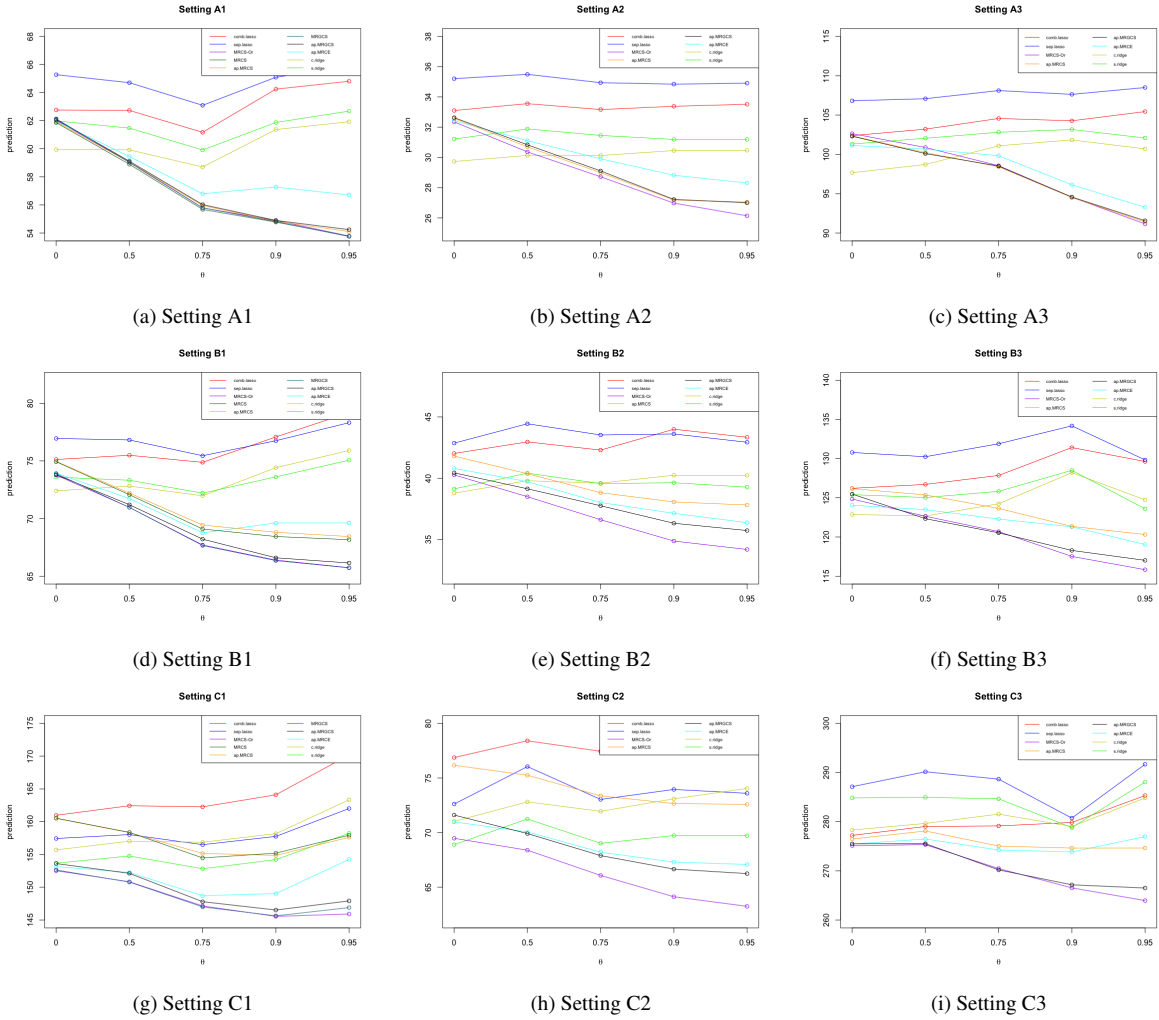
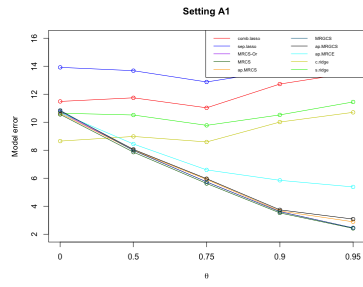
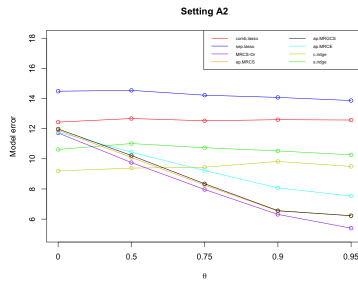


Figure I.43: Prediction plots for each setting in Section 8.1.

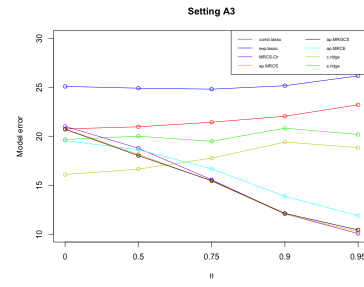
Appendix I.4. Additional plots for Section 8.1



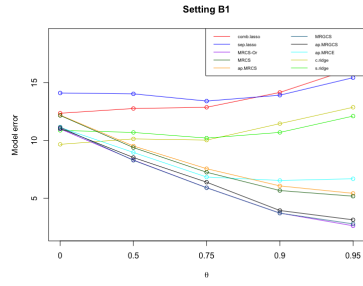
(a) Setting A1



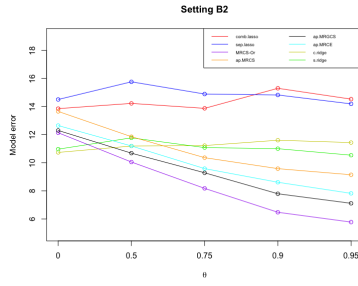
(b) Setting A2



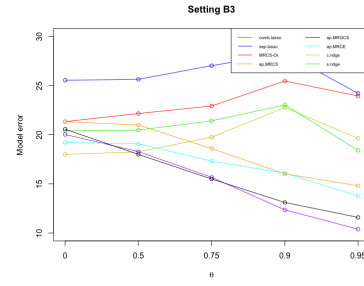
(c) Setting A3



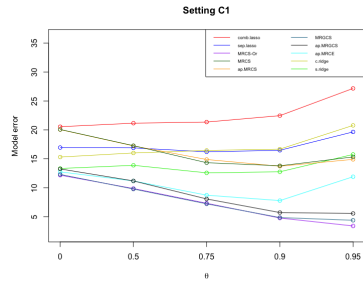
(d) Setting B1



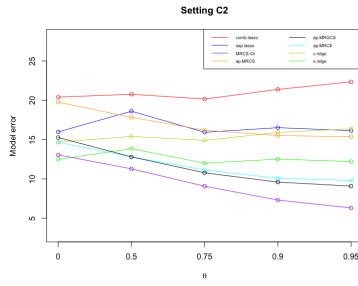
(e) Setting B2



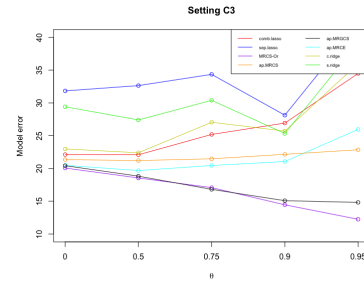
(f) Setting B3



(g) Setting C1



(h) Setting c2



(i) Setting A3

Figure I.44: Model error plots for each setting in Section 8.1.

References

- [1] Breiman, L. and Friedman, J. H. (1997). Predicting multivariate responses in multiple linear regression. *Journal of the Royal Statistical Society Series B: Statistical Methodology* **59**(1), 3–54.
- [2] Bühlmann, P. and Van De Geer, S. (2011). *Statistics for high-dimensional data: methods, theory and applications*. Springer Science & Business Media.
- [3] Chang, L. and Welsh, A. (2023). Robust multivariate lasso regression with covariance estimation. *Journal of Computational and Graphical Statistics* **32**(3), 961–973.
- [4] Friedman, J., Hastie, T., and Tibshirani, R. (2008). Sparse inverse covariance estimation with the graphical lasso. *Biostatistics* **9**(3), 432–441.
- [5] Izenman, A. J. (1975). Reduced-rank regression for the multivariate linear model. *Journal of multivariate analysis* **5**(2), 248–264.
- [6] Lee, W. and Liu, Y. (2012). Simultaneous multiple response regression and inverse covariance matrix estimation via penalized gaussian maximum likelihood. *Journal of multivariate analysis* **111**, 241–255.
- [7] Navon, A. and Rosset, S. (2020). Capturing between-tasks covariance and similarities using multivariate linear mixed models. *Electronic Journal of Statistics* **14**(2), 3821 – 3844.
- [8] Negahban, S. N., Ravikumar, P., Wainwright, M. J., and Yu, B. (2012). A Unified Framework for High-Dimensional Analysis of M -Estimators with Decomposable Regularizers. *Statistical Science* **27**(4), 538 – 557.
- [9] Price, B. S. and Sherwood, B. (2018). A cluster elastic net for multivariate regression. *Journal of Machine Learning Research* **18**(232), 1–39.
- [10] Reinsel, G. C., Velu, R. P., and Chen, K. (2022). *Multivariate Reduced-Rank Regression: Theory, Methods and Applications*. Springer, New York, NY.
- [11] Rothman, A. J. (2022). *MRCE: Multivariate Regression with Covariance Estimation*. R package version 2.4.
- [12] Rothman, A. J., Levina, E., and Zhu, J. (2010). Sparse multivariate regression with covariance estimation. *Journal of Computational and Graphical Statistics* **19**(4), 947–962.
- [13] Tan, K. M., Sun, Q., and Witten, D. (2023). Sparse reduced rank huber regression in high dimensions. *Journal of the American Statistical Association* **118**(544), 2383–2393.
- [14] Wang, J. (2015). Joint estimation of sparse multivariate regression and conditional graphical models. *Statistica Sinica* **25**(3), 831–851.

- [15] Yu, G. and Bien, J. (2019). Estimating the error variance in a high-dimensional linear model. *Biometrika* **106**(3), 533–546.
- [16] Yuan, M. and Lin, Y. (2007). Model selection and estimation in the gaussian graphical model. *Biometrika* **94**(1), 19–35.
- [17] Zhu, Y. (2020). A convex optimization formulation for multivariate regression. *Advances in Neural Information Processing Systems* **33**, 17652–17661.
- [18] Zou, H. (2006). The adaptive lasso and its oracle properties. *Journal of the American statistical association* **101**(476), 1418–1429.